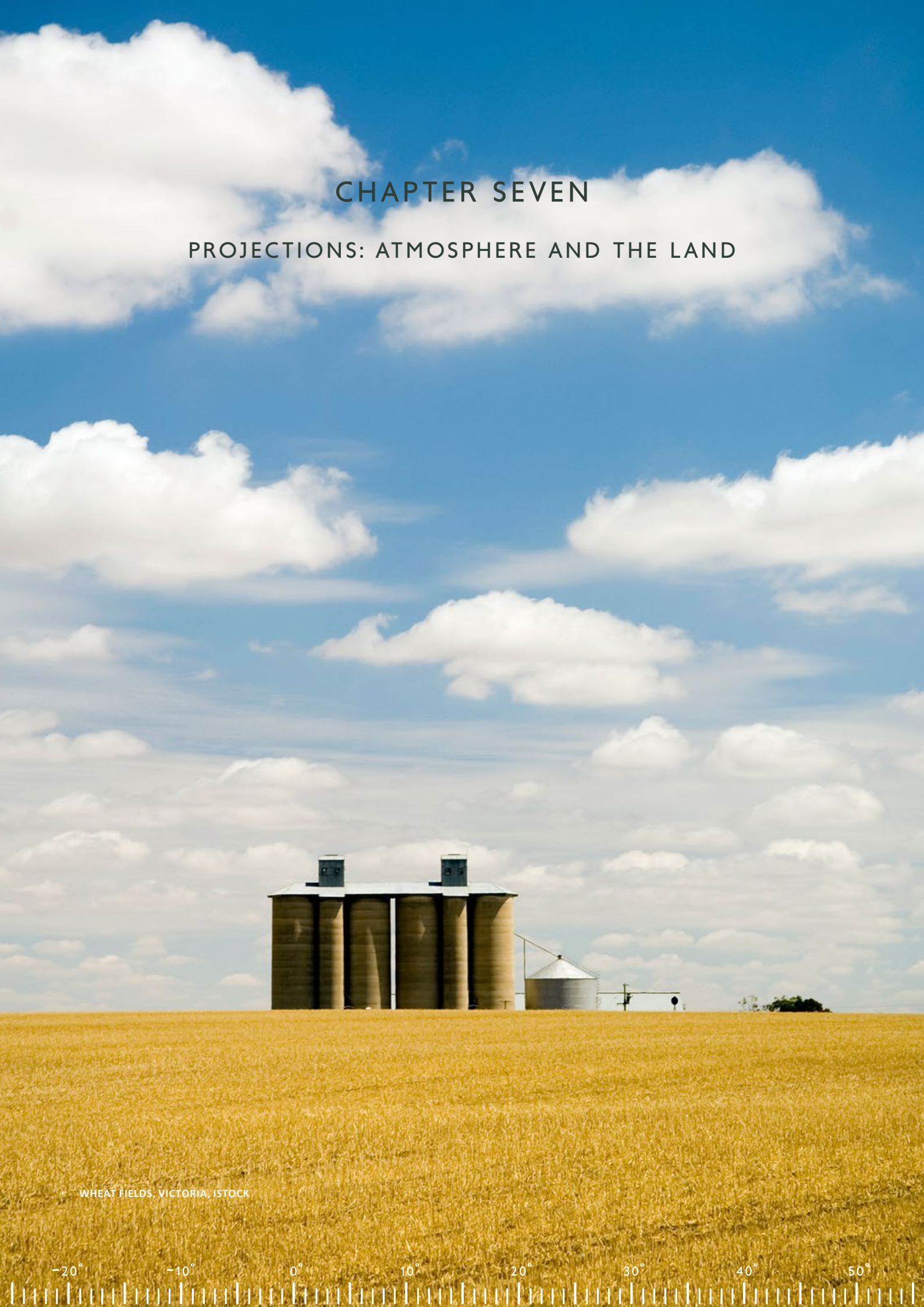


CHAPTER SEVEN

PROJECTIONS: ATMOSPHERE AND THE LAND



WHEAT FIELDS, VICTORIA, ISTOCK

-20° -10° 0° 10° 20° 30° 40° 50°

CHAPTER 7 PROJECTIONS: ATMOSPHERE AND THE LAND

This chapter presents projected changes to Australia's climate based on the results of the CMIP5 models and other relevant information. For changes to mean temperature, rainfall, wind speed, solar radiation, relative humidity and potential evapotranspiration (PE), ranges of regional average change are presented based on 10-90th percentiles of the empirical distribution of the CMIP5 models using the approach described in the previous chapter. Changes are presented for 20 year time slices centred on 2030 and 2090 relative to the simulated climate of 1986–2005 and for selected RCPs (usually RCP2.6, RCP4.5 and RCP8.5). The changes can then be applied to observed climate data for use in impact assessments.

Aspects of projected changes to extremes for temperature (hot days and frosts), rainfall (heavy rainfall events and droughts) and winds are also examined, along with changes to runoff, soil moisture and fire weather derived from offline calculations. Observed changes in these variables are discussed only where these are relevant to assessment of the projections, as the main discussion of trends in observed atmospheric variables is in Section 4.2. For the atmospheric and terrestrial variables, the primary focus in this Report is on area average results for the four large super-clusters: Southern Australia, Northern Australia, Eastern Australia and the Rangelands. Some results are also given at the cluster level, but more detailed results for clusters are available in the Cluster Reports.

7.1 SURFACE TEMPERATURE

This Section presents projections for air temperature near the surface (nominally at 2 m height), followed by changes for seasonal and annual average daily mean, maximum and minimum temperatures, concluding with annual and 20-year extremes.

AUSTRALIA WILL WARM SUBSTANTIALLY DURING THE 21ST CENTURY

There is *very high confidence* in continued increases of mean, daily minimum and daily maximum temperatures throughout this century for all regions in Australia. The magnitude of the warming later in the century is strongly dependent on the emission scenario.

Warming will be large compared to natural variability in the near future (2030) (*high confidence*), and very large compared to natural variability late in the century (2090) under RCP8.5 (*very high confidence*). By 2030, Australian annual average temperature is projected to increase by 0.6-1.3 °C above the climate of 1986–2005 under RCP4.5 with little difference between RCPs. The projected temperature range by 2090 shows larger differences between RCPs, with 0.6 to 1.7 °C for RCP2.6, 1.4 to 2.7 °C for RCP4.5 and 2.8 to 5.1 °C for RCP8.5.

Mean warming is projected to be greater than average in inland Australia, and less in coastal areas, particularly in southern coastal areas in winter.

7.1.1 AVERAGE TEMPERATURE

Figure 7.1 shows simulated temperature change from 1910 to 2090 (see Box 6.2.2 for guidance on reading these plots). The figure includes the median and range of the change averaged over Australia from all models under both historical forcing and three future scenarios. Future yearly values from a representative CMIP5 model show similar variability to that in the observations. In this, and similar plots for the various cluster regions, the observational data usually lie within the spread of the model values, indicating consistency between the real-world and modelled series. The median temperatures from CMIP5 models also match closely the observed climatology for the 1986–2005 base period (Section 5.2.1).

Similar to the change in global mean temperature shown in Figure 3.5.1, the median Australian warming (Figure 7.1.1) increases steadily in the RCP8.5 scenario. The range of change broadens into the future because of both the range of global warming from the models and the range of local sensitivity to that warming, according to the interpretation presented in Section 6.2 and by Watterson and Whetton (2013). For the RCP4.5 scenario the median warming plateaus after around 2060. The RCP2.6 warming peaks earlier, around 2045. These warmings mirror those projected globally (Chapter 3) and thus represent the regional expression of global warming. They are also similar to the previous projections for Australia (CSIRO and BOM, 2007) (see further discussion below and in Appendix A).

-20° -10° 0° 10° 20° 30° 40° 50°

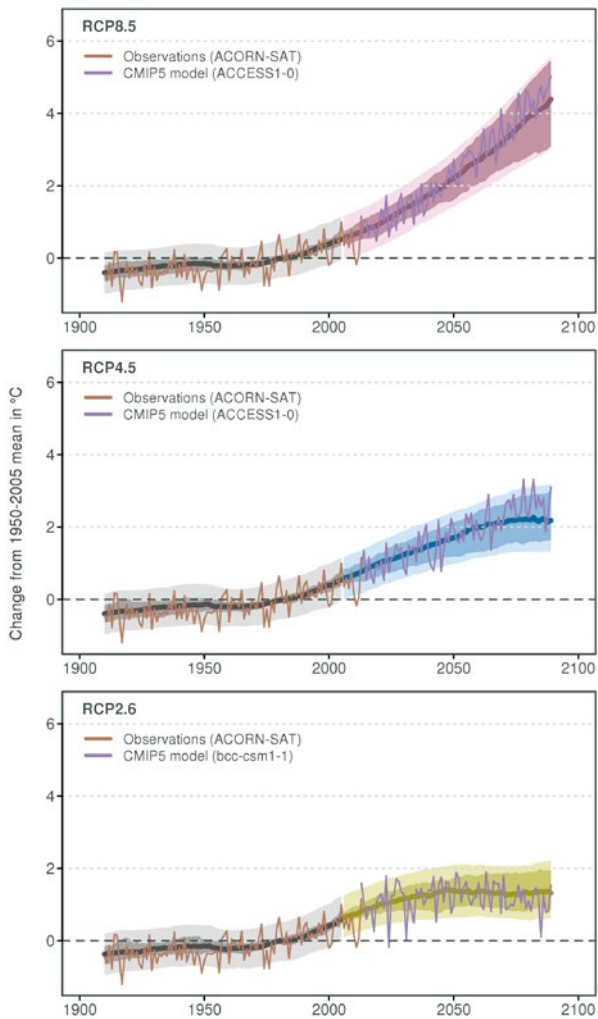


FIGURE 7.1: TIME SERIES FOR AUSTRALIAN AVERAGE TEMPERATURE FOR 1910–2090 AS SIMULATED IN CMIP5, RELATIVE TO THE 1950–2005 MEAN. THE CENTRAL LINE IS THE MEDIAN VALUE, AND THE SHADING IS THE 10TH AND 90TH PERCENTILE RANGE OF 20-YEAR RUNNING MEANS (INNER) AND SINGLE YEAR VALUES (OUTER). THE GREY SHADING INDICATES THE PERIOD OF THE HISTORICAL SIMULATION, WHILE THREE FUTURE SCENARIOS ARE SHOWN WITH COLOUR-CODED SHADING: RCP8.5 (PURPLE), RCP4.5 (BLUE) AND RCP2.6 (GREEN). ACORN-SAT OBSERVATIONS ARE SHOWN IN BROWN AND A SERIES FROM A TYPICAL MODEL ARE SHOWN INTO THE FUTURE IN LIGHT PURPLE (SEE BOX 6.2.2 FOR MORE EXPLANATION OF PLOT).

Figure 7.1.2 shows the range of mean warming for 2090 (the period 2080–2099) relative to 1986–2005 in each season, with results for the daily maximum and minimum also shown (the annual results are shown later). Overall the median warming is similar in each season and for each quantity. The warming is largest in spring for RCP8.5, and smallest in winter in the RCP2.6 case.

Spatial variation in the warming is evident from the regional values for RCP8.5 shown in Figure 7.1.3 (see Table 2.2 for description). Median projected temperature increases are typically 4 °C by 2090, while those in the north-east and far south are 3 °C or less. The climatological annual temperatures for the base period 1986–2005 averaged over each region are also shown. Generally similar changes occur for the maximum and minimum temperatures (not shown). However, increases in daily maximum temperature are around 0.5 °C greater than those for minimum temperature in the southern regions.

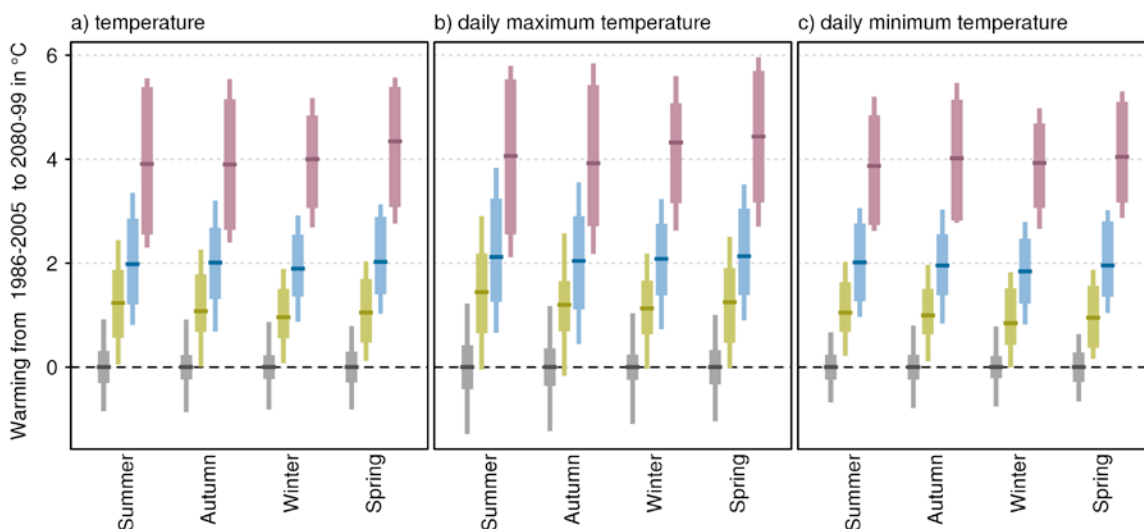


FIGURE 7.1.2: MEDIAN AND 10TH TO 90TH PERCENTILE RANGE OF PROJECTED AUSTRALIAN SEASONAL TEMPERATURE CHANGE FOR 2080–2099 RELATIVE TO THE 1986–2005 PERIOD (GREY BAR) FOR RCP2.6 (GREEN), RCP4.5 (BLUE) AND RCP8.5 (PURPLE). FINE LINES SHOW THE RANGE OF INDIVIDUAL YEARS AND SOLID BARS FOR TWENTY YEAR RUNNING MEANS FOR (A) MEAN TEMPERATURE, (B) DAILY MAXIMUM TEMPERATURE, AND (C) DAILY MINIMUM TEMPERATURE.



Table 7.1.1 presents medians and ranges averaged over Australia and four super-cluster regions for four cases. For 2030, the Australian average warming range is 0.6 to 1.3 °C (10th and 90th percentile) under RCP4.5 (and differs little for other scenarios). Later in the century, the scenario choice has a large effect on the projected warming. The projected Australian average temperature ranges for 2090 are 0.6 to 1.7 °C for RCP2.6, 1.4 to 2.7 °C for RCP4.5 and 2.8 to 5.1 °C for RCP8.5. Warming ranges in the super-clusters are similar, with slighter greater warming in the predominantly inland Rangelands (e.g. 2.9 to 5.3 °C in 2090 for RCP8.5), and slightly less warming in Southern Australia (e.g. 2.7 to 4.2 °C in 2090 for RCP8.5).

The spatial variation in the warming, on the scale resolved by the models, is evident from the median warming calculated using the ‘pattern scaling’ approach of the 2007 projections for a 1-degree common grid of points over Australia. Figure 7.1.4 presents results for each season under

RCP8.5. The median estimate for mean warming in the interior is some 20 % larger than the best estimate of the global mean value, which is 3.7 °C for this case. Warming is lower along most coasts, particularly in the south in the winter. In Appendix A, Figure A1 shows that there is little difference in the CMIP5 results relative to those inferred from CMIP3, although the warming in the north-west in the warmer seasons was greater in the earlier projections.

As for the cluster averages in Figure 7.1.3, there is a considerable range of possible warming at locations, determined using the scaling approach and shown in the maps of Figure A1, even for a single scenario. Much of the range relates to the range in global warming (Section 3.6). Some of the local range, and its seasonal variation, is associated with the influence of changes in atmospheric circulation and rainfall and hence with the external drivers of those changes (see Watterson (2012), Section 3.6, and Box 7.1).

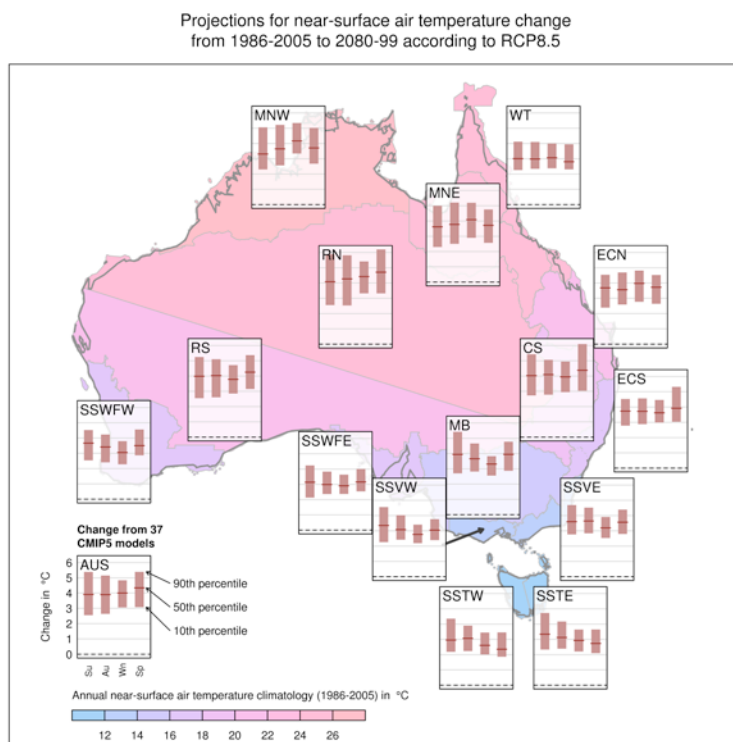


FIGURE 7.1.3: MEDIAN AND 10TH TO 90TH PERCENTILE RANGE OF PROJECTED CHANGE IN SEASONAL TEMPERATURE FROM 37 CMIP5 GCMS FOR 2080–2099 RELATIVE TO 1986–2005 FOR RCP8.5 FOR 20-YEAR MEANS. THE CHARTS FOR 15 REGIONS OVERLIE A MAP WITH EACH REGION COLOURED TO INDICATE ITS BASE CLIMATE AVERAGE (SEE SCALE). THE AUSTRALIAN AVERAGE RESULT IS IN THE BOTTOM LEFT.

TABLE 7.1.1: MEDIAN AND 10TH TO 90TH PERCENTILE RANGE OF PROJECTED TEMPERATURE CHANGE (IN °C) FOR AUSTRALIA, AND FOUR SUPER-CLUSTER REGIONS, RELATIVE TO THE 1986–2005 PERIOD. FOUR FUTURE CASES ARE GIVEN, WITH 2030 INDICATING THE PERIOD 2020–2039, AND 2090, BEING 2080–2099, FOR THREE RCPS.

	2030 RCP4.5	2090 RCP2.6	2090 RCP4.5	2090 RCP8.5
AUSTRALIA	0.9 (0.6 to 1.3)	1.0 (0.6 to 1.7)	1.9 (1.4 to 2.7)	4.1 (2.8 to 5.1)
NORTHERN AUSTRALIA	0.9 (0.6 to 1.3)	0.9 (0.5 to 1.6)	1.7 (1.3 to 2.6)	3.7 (2.7 to 4.9)
RANGELANDS	1.0 (0.6 to 1.4)	1.1 (0.6 to 1.8)	2.1 (1.5 to 2.9)	4.3 (2.9 to 5.3)
EASTERN AUSTRALIA	0.9 (0.6 to 1.2)	1.0 (0.6 to 1.6)	1.9 (1.3 to 2.6)	3.9 (2.8 to 5)
SOUTHERN AUSTRALIA	0.8 (0.5 to 1)	0.9 (0.5 to 1.4)	1.7 (1.2 to 2.1)	3.5 (2.7 to 4.2)



The temperatures for 2090 under RCP8.5 are shown in panel (b), using the same colours. A deep red area, indicating a very warm average, extends over a larger part of the continent in 2090. Blue, cooler areas have contracted. These changes are evident also from the shifts in the highlighted contours. The previous positions of the three are indicated by dashed lines. There is a southward movement across the interior of typically 8 ° latitude (about 900 km). The 15 °C line has retreated to the highlands of the south-east and southern Tasmania. Temperature analogues of the climate can be related to the original position of the new contour.

Adding the projected change from coarse model outputs to a detailed base temperature map is a simple form of downscaling (as discussed further in Chapter 6.3). More detail in the changes themselves, particularly on the coast, may be available from downscaled results on a fine grid. The coastal land is likely to be more strongly affected by maritime influences, which could mean slightly lower temperatures than shown in Figure 7.1.6(b).

In summary, continued increases in mean, daily maximum and daily minimum temperatures are projected for Australia with very *high confidence*, taking into account the strong agreement on the direction and magnitude amongst GCMs, downscaling results and the robust understanding of the driving mechanisms of warming. The magnitude of the warming later in the century is strongly dependent on the emission scenario. These warmings will be large compared to natural variability in the near future (2030) (*high confidence*), and very large compared to natural variability late in the century (2090) under RCP8.5 (*very high confidence*). Mean warming is projected to be greater than average in inland Australia, and less in coastal areas, particularly in southern coastal areas in winter.

7.1.2 EXTREME TEMPERATURE

MORE FREQUENT AND HOTTER HOT DAYS AND FEWER FROST DAYS ARE PROJECTED

Projected warming will result in more frequent and hotter hot days and warmer cold extremes (*very high confidence*) and reduced frost (*high confidence*).

Hot days are projected to occur more frequently. For example, in Perth, the average number of days per year above 35 °C or above 40 °C by 2090 is projected to be 50 % greater than present under RCP4.5. The number of days above 35 °C in Adelaide also increases by about 50 % by late in the century, while the number of days above 40 °C more than doubles.

Locations where frost occurs only a few times a year under current conditions are projected to become nearly frost-free by 2030. Under RCP8.5 coastal areas are projected to be free of frost by 2090 while frost is still projected to occur inland.

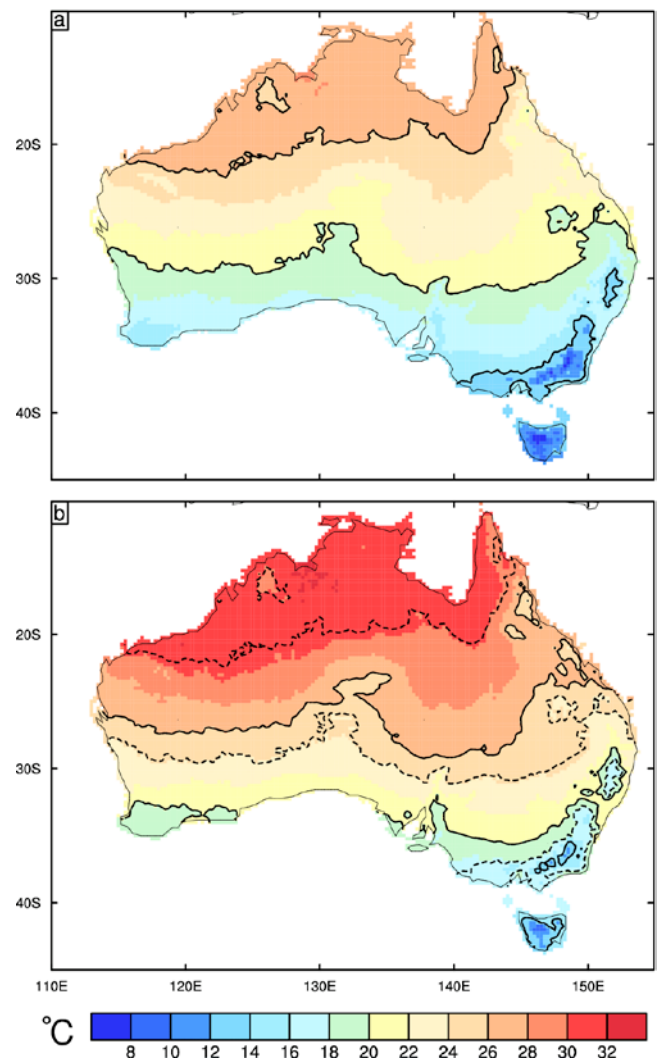


FIGURE 7.1.6: ANNUAL MEAN TEMPERATURE (IN °C), FOR THE PRESENT CLIMATE (A), AND FOR LATE 21ST CENTURY (B). THE FUTURE CASE IS CALCULATED BY ADDING THE MEDIAN (P50) WARMING FROM 1986–2005 TO 2080–2099 UNDER RCP8.5 TO THE MEAN TEMPERATURE OF THE PRESENT CLIMATE. IN EACH PANEL THE 14 °C, 20 °C, AND 26 °C CONTOURS ARE SHOWN WITH SOLID BLACK LINES. IN (B) THE SAME CONTOURS FROM THE ORIGINAL CLIMATE ARE PLOTTED AS DOTTED LINES. TO PROVIDE THE clearest DEPICTION OF THE SHIFTS IN CONTOURS, THE LONGER PERIOD 1950–2008 BOM DATASET IS USED FOR THE PRESENT CLIMATE, ON A 0.25° GRID.

Climate impacts of temperature are often felt through extremes, which are quantified here through the indices described by Karl *et al.* (1999). The extreme temperature indices have been calculated using daily data from the 24 CMIP5 models for which these values could be obtained, and the focus here is on the annual extremes. The Australian average for changes by 2090 under two RCPs is shown in Figure 7.1.7 (a). The changes for the ‘hottest day of the year’ are similar to those for the annual mean of daily maximum (and also for the average summer daily maximum increase (not shown)), as seen in Figure 7.1.2. For example, this means hot days would be around 3-5 degrees warmer in 2090 under RCP8.5. To examine changes in very rare daily maximum temperatures, extreme value theory was used to infer 1-in-20 year return values. The Generalised Extreme Value distribution was fitted to the annual maximum temperature at each location for the 20-year period centred on 2090, and the expected 20-year extreme was calculated and compared to that for 1986-2005. Again, the Australian average changes by a similar amount to the annual value, while the contrast between the scenarios is maintained. The panel in Figure 7.1.7(b) gives the increase in number of days per year that fall within ‘warm spells’, defined as six or more days above the 90th percentile value for daily temperatures over 1961 – 1990. This warm spell metric increases dramatically by 2090, with RCP8.5 showing more than 100 additional warm spell days each year.

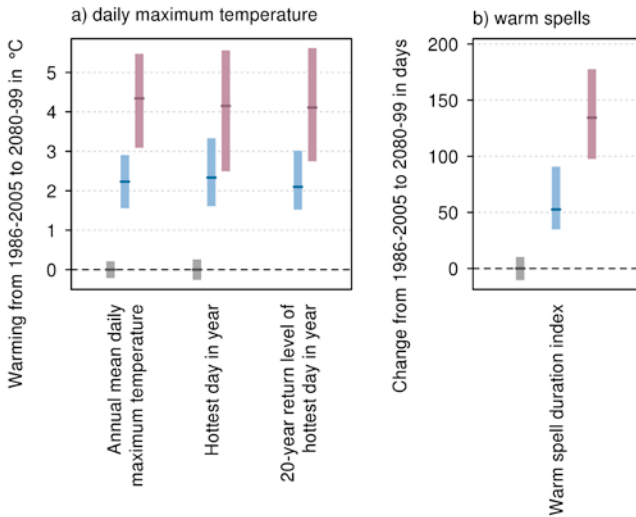


FIGURE 7.1.7: (A) MEDIAN AND 10TH TO 90TH PERCENTILE RANGE OF PROJECTED CHANGE IN MEAN AND EXTREME DAILY MAXIMUM TEMPERATURE AVERAGED OVER AUSTRALIA FOR 2080–2099 RELATIVE TO THE 1986–2005 PERIOD (GREY BAR), FOR RCP4.5 (BLUE) AND RCP8.5 (PURPLE). CHANGES IN DAILY MAXIMUM TEMPERATURES ARE SHOWN FOR ANNUAL MEAN (LEFT), HOTTEST DAY OF THE YEAR (CENTRE), AND 20-YEAR RETURN LEVEL (RIGHT). (B) CHANGES IN NUMBER OF DAYS PER YEAR WITHIN WARM SPELLS (DEFINED AS PERIODS OF 6 OR MORE CONSECUTIVE DAYS ABOVE THE 90TH PERCENTILE OF DAILY TEMPERATURES FOR THE 1961–1990 PERIOD).

Projections for daily maximum near-surface air temperature change from 1986-2005 to 2080-99 according to RCP8.5 for both the annual mean and annual extremes

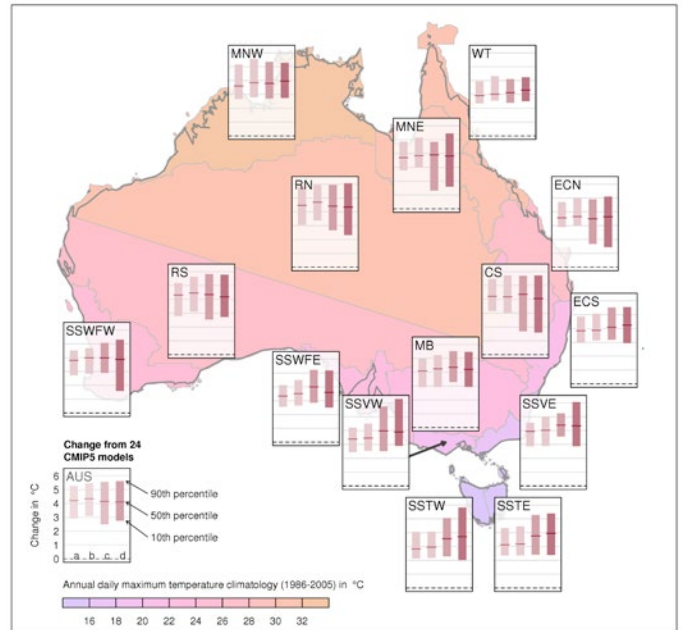


FIGURE 7.1.8: MEDIAN AND 10TH TO 90TH PERCENTILE RANGE OF PROJECTED CHANGE IN DAILY MAXIMUM TEMPERATURE IN SUB-CLUSTERS FOR 2080–2099 RELATIVE TO 1986–2005 FOR RCP8.5. SHOWN IN EACH BOX FROM LEFT TO RIGHT IS (A) THE ANNUAL DAILY MEAN FOR THE LARGER SET OF 37 MODELS, (B) THE ANNUAL DAILY MEAN, (C) THE ANNUAL DAILY MAXIMUM, AND THE (D) 20 YEAR RETURN LEVEL OF ANNUAL DAILY MAXIMUM TEMPERATURE FROM A CONSISTENT SUBSET OF 24 MODELS. THE AUSTRALIAN AVERAGE RESULT IS SHOWN AT BOTTOM LEFT.

Figure 7.1.8 and Figure 7.1.9 show the regional results for extreme temperatures under the RCP8.5 scenario for daily maxima and minima, respectively. In both figures, for each region the median and ranges of the annual mean determined from the full set of CMIP5 models (the first bar) are similar to that from the subset of 24 models (the second bar from the left). As with the mean temperatures, there is some variation around the continent. In Figure 7.1.8, in the warmer regions, there is little difference between changes in the magnitude of annual extremes when compared to changes in 1-in-20 year extremes. The increases in the annual and 1-in-20 year maximums are a little higher than for the means in the southern coastal regions. This seems consistent with the effect of hot winds from the interior providing an even greater temperature contrast to those from across the ocean under the warmer climates, as examined by Watterson *et al.* (2008). Smaller simulated warming of the Southern Ocean may account for a less pronounced temperature rise in cool extremes experienced in southern regions (Figure 7.1.9). Moreover, there tends to be reduced cloud cover in winter (as evidenced by seasonal changes in solar radiation and humidity, Sections 7.4 and 7.5), which can lead to relatively cool minima.



Projections for daily minimum near-surface air temperature change from 1986-2005 to 2080-99 according to RCP8.5 for both the annual mean and annual extremes

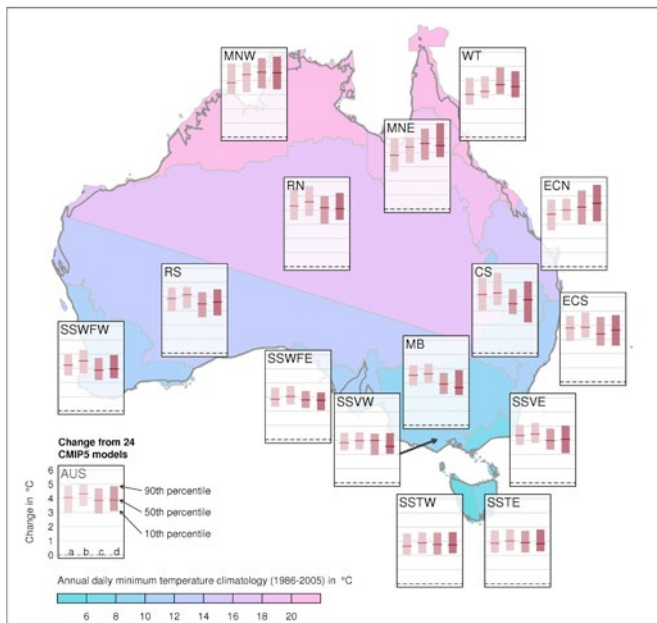


FIGURE 7.1.9: MEDIAN AND 10TH TO 90TH PERCENTILE RANGE OF PROJECTED CHANGE IN DAILY MINIMUM TEMPERATURE IN SUB-CLUSTERS FOR 2080–2099 RELATIVE TO 1986–2005 FOR RCP8.5. SHOWN IN EACH BOX FROM LEFT TO RIGHT IS (A) THE ANNUAL MEAN FOR THE LARGER SET OF 36 MODELS, (B) THE ANNUAL MEAN, (C) THE ANNUAL MINIMUM, AND (D) THE 20 YEAR RETURN LEVEL OF ANNUAL DAILY MINIMUM TEMPERATURE FROM A CONSISTENT SUBSET OF 24 MODELS. THE AUSTRALIAN AVERAGE RESULT IS SHOWN AT BOTTOM LEFT.

Maximum temperatures over 40 °C (Table 7.1.2) also occur in most years at most sites by 2090, and could become normal for a summer day in Alice Springs and Wilcannia.

Changes in the frequency of surface frost have significant implications for agriculture and the environment. Assessing frost occurrence directly from global model output is not reliable, in part because of varying biases in land surface temperatures. However, an indication of future changes in frost can be obtained using a similar approach to that used for hot days. For most regions, the rise in the low extreme temperature (Figure 7.1.9) is similar to that for the means for the winter season (not shown). Therefore, adding the average seasonal change in daily minimum temperatures to an observational record of daily minimum temperatures provides a plausible representation of the series of minimums for the future. On frosty mornings, when the land surface temperature is below 0 °C, the air temperature is typically 2 °C warmer (see the Bureau of Meteorology web pages on potential frost occurrence). This temperature thus provides a suitable criterion to represent the potential for frost to occur, based on the usual (air) temperature data. Table 7.1.3 presents the average annual number of potential frost days calculated using this approach for representative sites (omitting those with zero values). Locations where frost occurs only a few times a year at present are likely by 2030 to be nearly frost free on average. Coastal mainland cities will be frost free on average by 2090 under RCP8.5. Inland locations, even Alice Springs, will retain some frost days. The actual occurrence of frost will depend on many local factors. Downscaling can be used to provide more detailed information (e.g. see Murray Basin cluster report), however assessment of available (regionally restricted) results did not show changes substantially different from those presented here.

In summary, strong model agreement and the understanding of the physical mechanisms of warming indicate more frequent and hotter hot days and warmer cold extremes (*very high confidence*) and reduced frost (*high confidence*).

Given the similarity of the rises in extreme high daily maximum temperatures and those in the mean daily maximum temperature, an estimate of actual daily maximum temperatures in a future climate can be made by adding the average projected changes for daily maximums to observational values – the scaling factor method (Chapter 6). This has been done using seasonal changes (medians and 10th/90th percentiles) for the region in which the location falls (see Figure 7.1.8), although this approach may not account for local effects. If ‘hot’ days are defined using a simple threshold, then tallies of these are readily made. Table 7.1.2 presents the results for 15 cities and regional centres. This calculation does not take into account any change to heat island effects in the future. The results from the recent 30 years (1981–2010 or ‘1995’) for the 35 °C threshold tend to be a little higher than those given in the CSIRO and BOM, (2007) report (Table 5.2) for 1971–2000. Projected numbers are given for the four future cases included in Table 7.1.1 (i.e. 2030 under RCP4.5, and 2090 under RCP2.6, RCP4.5 and RCP8.5, based on model changes for 2020–2039 and 2080–2099 relative to 1986–2005). In 2030 under RCP4.5, the numbers increase considerably, particularly in the northern centres and at some inland sites with larger warming, e.g. Canberra (airport). The increases for the other scenarios are similar in this period (not shown). Numbers of days above 35 °C in the period centred on 2090 are mostly similar to those in 2030 for RCP2.6, but numbers increase further for the other two scenarios.

For example, in Perth, the number of days above 35 °C or above 40 °C by 2090 is 50 % greater than the period centred on 1995 under RCP4.5. The number of days above 35 °C in Adelaide also increases by about 50 % by 2090, whereas the number of days above 40 °C more than doubles.

TABLE 7.1.2: CURRENT (FOR THE 30-YEAR PERIOD 1981–2010) AVERAGE NUMBER OF DAYS PER YEAR WITH MAXIMUM TEMPERATURE ABOVE 35 °C (TOP) AND 40 °C (BOTTOM) FOR VARIOUS LOCATIONS BASED ON ACORN-SAT (TREWIN, 2013). ESTIMATES FOR THE FUTURE ARE CALCULATED USING THE MEDIAN CMIP5 WARMING OF MAXIMUM TEMPERATURES FOR 2030 AND 2090, AND WITHIN BRACKETS THE 10TH AND 90TH PERCENTILE CMIP5 WARMING FOR THESE PERIODS, APPLIED TO THE 30-YEAR ACORN-SAT STATION SERIES. (LOCATION LEGEND: 1 CBD, 2 AIRPORT, 3 AMBERLEY RAAF BASE (INLAND FROM BRISBANE), 4 BATTERY POINT, 5 OBSERVATORY HILL, THE ROCKS).

THRESHOLD 35 °C	1995	2030 RCP4.5	2090 RCP2.6	2090 RCP4.5	2090 RCP8.5
ADELAIDE ¹	20	26 (24 to 29)	28 (24 to 31)	32 (29 to 38)	47 (38 to 57)
ALICE SPRINGS ²	94	113 (104 to 122)	119 (104 to 132)	133 (115 to 152)	168 (145 to 193)
AMBERLEY ³	12	18 (15 to 22)	18 (14 to 30)	27 (21 to 42)	55 (37 to 80)
BROOME ²	56	87 (72 to 111)	95 (70 to 154)	133 (94 to 204)	231 (173 to 282)
CAIRNS ²	3	5.5 (4.4 to 7.9)	5.5 (4.4 to 14)	11 (7.4 to 22)	48 (24 to 105)
CANBERRA ²	7.1	12 (9.4 to 14)	13 (10 to 16)	17 (13 to 23)	29 (22 to 39)
DARWIN ²	11	43 (25 to 74)	52 (24 to 118)	111 (54 to 211)	265 (180 to 322)
DUBBO ²	22	31 (26 to 37)	34 (26 to 43)	44 (36 to 54)	65 (49 to 85)
HOBART ⁴	1.6	2.0 (1.9 to 2.1)	2.0 (1.8 to 2.5)	2.6 (2.0 to 3.1)	4.2 (3.2 to 6.3)
MELBOURNE	11	13 (12 to 15)	14 (12 to 17)	16 (15 to 20)	24 (19 to 32)
MILDURA ²	33	42 (37 to 46)	44 (39 to 50)	52 (45 to 61)	73 (60 to 85)
PERTH ²	28	36 (33 to 39)	37 (33 to 42)	43 (37 to 52)	63 (50 to 72)
ST. GEORGE ²	40	54 (48 to 62)	58 (47 to 69)	70 (59 to 87)	101 (79 to 127)
SYDNEY ⁵	3.1	4.3 (4.0 to 5.0)	4.5 (3.9 to 5.8)	6.0 (4.9 to 8.2)	11 (8.2 to 15)
WILCANNIA	47	57 (53 to 62)	60 (54 to 66)	67 (59 to 75)	87 (72 to 100)

THRESHOLD 40 °C	1995	2030 RCP4.5	2090 RCP2.6	2090 RCP4.5	2090 RCP8.5
ADELAIDE ¹	3.7	5.9 (4.7 to 7.2)	6.5 (5.2 to 8.5)	9.0 (6.8 to 12)	16 (12 to 22)
ALICE SPRINGS ²	17	31 (24 to 40)	37 (24 to 51)	49 (33 to 70)	83 (58 to 114)
AMBERLEY ³	0.8	1.2 (1.1 to 1.6)	1.2 (1.1 to 2.5)	2.1 (1.5 to 3.9)	6.0 (2.9 to 11)
BROOME ²	4.1	7.2 (6.0 to 9.3)	7.7 (5.7 to 13)	11 (7.7 to 22)	30 (17 to 61)
CAIRNS ²	0	0.1 (0.1 to 0.2)	0.1 (0.1 to 0.3)	0.3 (0.2 to 0.4)	0.7 (0.5 to 2.0)
CANBERRA ²	0.3	0.6 (0.4 to 0.8)	0.7 (0.5 to 1.3)	1.4 (0.8 to 2.8)	4.8 (2.3 to 7.5)
DARWIN ²	0	0.0 (0.0 to 0.0)	0.0 (0.0 to 0.0)	0.0 (0.0 to 0.2)	1.3 (0.2 to 11)
DUBBO ²	2.5	3.9 (3.2 to 5.6)	5.0 (3.2 to 8.0)	7.8 (5.1 to 12)	17 (9.9 to 26)
HOBART ⁴	0.1	0.2 (0.2 to 0.4)	0.2 (0.1 to 0.4)	0.4 (0.2 to 0.5)	0.9 (0.5 to 1.4)
MELBOURNE	1.6	2.4 (2.1 to 3.0)	2.7 (2.3 to 3.7)	3.6 (2.8 to 4.9)	6.8 (4.6 to 11)
MILDURA ²	7.2	10 (8.8 to 12)	11 (9.4 to 14)	15 (12 to 20)	27 (19 to 35)
PERTH ²	4	6.7 (5.4 to 7.5)	6.9 (5.6 to 9.0)	9.7 (6.9 to 13)	20 (12 to 25)
ST. GEORGE ²	5.1	8.2 (6.3 to 11)	10 (6.1 to 16)	15 (11 to 23)	31 (20 to 49)
SYDNEY ⁵	0.3	0.5 (0.5 to 0.8)	0.7 (0.5 to 0.9)	0.9 (0.8 to 1.3)	2.0 (1.3 to 3.3)
WILCANNIA ¹	11	16 (14 to 20)	18 (15 to 25)	23 (18 to 31)	40 (27 to 53)



TABLE 7.1.3: CURRENT (FOR THE 30-YEAR PERIOD 1981–2010) AVERAGE NUMBER OF POTENTIAL FROST DAYS PER YEAR FOR VARIOUS LOCATIONS BASED ON ACORN-SAT (TREWIN, 2013). ESTIMATES FOR THE FUTURE ARE CALCULATED USING THE MEDIAN CMIP5 WARMING OF MINIMUM TEMPERATURES FOR 2030 AND 2090, AND WITHIN BRACKETS THE 10TH AND 90TH PERCENTILE CMIP5 WARMING FOR THESE PERIODS, APPLIED TO THE 30-YEAR ACORN-SAT STATION SERIES. THE CRITERION USED FOR POTENTIAL FROST IS 2 °C. (LOCATION LEGEND: 1 CBD, 2 AIRPORT, 3 AMBERLEY RAAF BASE (INLAND FROM BRISBANE), 4 BATTERY POINT).

	1995	2030 RCP4.5	2090 RCP2.6	2090 RCP4.5	2090 RCP8.5
ADELAIDE ¹	1.1	0.5 (0.8 to 0.4)	0.4 (0.8 to 0.3)	0.2 (0.4 to 0.1)	0.0 (0.0 to 0.0)
ALICE SPRINGS ²	33	24 (28 to 19)	24 (30 to 17)	13 (20 to 8.4)	2.1 (6.0 to 0.8)
AMBERLEY ³	22	16 (18 to 14)	17 (20 to 12)	11 (14 to 7.4)	3.1 (6.8 to 0.7)
CANBERRA ²	91	81 (87 to 76)	80 (87 to 71)	68 (75 to 61)	43 (52 to 35)
DUBBO ²	39	30 (34 to 27)	31 (35 to 22)	21 (26 to 13)	6.0 (10 to 2.4)
HOBART ⁴	9.1	5.8 (6.9 to 3.7)	5.3 (7.7 to 2.3)	2.1 (4.1 to 1.1)	0.3 (0.6 to 0.1)
MELBOURNE	0.9	0.6 (0.8 to 0.4)	0.5 (0.7 to 0.2)	0.2 (0.3 to 0.1)	0.0 (0.0 to 0.0)
MILDURA ²	19	14 (16 to 12)	13 (16 to 9.4)	9.0 (11 to 6.7)	3.0 (4.9 to 1.2)
PERTH ²	3.4	2.1 (2.5 to 1.4)	1.9 (2.5 to 1.0)	0.9 (1.3 to 0.7)	0.1 (0.4 to 0.0)
ST. GEORGE ²	17	12 (15 to 11)	13 (15 to 8.7)	8.3 (11 to 5.5)	1.5 (3.5 to 0.5)
WILCANNIA	20	14 (17 to 11)	14 (16 to 9.7)	9.4 (12 to 6.3)	2.4 (4.4 to 1.0)

7.2 RAINFALL

This section considers changes to average rainfall conditions, as well as indices of extreme rainfall, drought occurrence and snow. The evidence considered is based mainly on CMIP5 GCM results, but various downscaled data sets are also considered. As part of considering the plausible processes driving the simulated rainfall changes, the section also considers changes to some patterns of atmospheric circulation.

7.2.1 PROJECTED MEAN RAINFALL CHANGE

COOL-SEASON RAINFALL IS PROJECTED TO DECLINE IN SOUTHERN AUSTRALIA; CHANGES ARE UNCERTAIN ELSEWHERE

Southern Australia: Cool season (winter and spring) rainfall is projected to decrease (*high confidence*), though little change or increases in Tasmania in winter are projected (*medium confidence*). The winter decline may be as great as 50 % in south-western Australia in the highest emission scenario (RCP8.5) by 2090. The direction of change in summer and autumn rainfall in southern Australia cannot be reliably projected, but there is *medium confidence* in a decrease in south-western Victoria in autumn and in western Tasmania in summer.

Eastern Australia: There is *high confidence* that in the near future (2030), natural variability will predominate over trends due to greenhouse gas emissions. For late in the century (2090), there is *medium confidence* in a winter rainfall decrease.

Northern Australia and northern inland areas:

There is *high confidence* that in the near future (2030) natural variability will predominate over trends due to greenhouse gas emissions. There is *low confidence* in the direction of future rainfall change for late in the century (2090), but substantial changes to wet-season and annual rainfall cannot be ruled out.

There is a range of dominant drivers of change in the different regions of Australia, and projected changes to some of these are well understood and robust among models (see also Section 4.2). For example, one consistent finding is that an increase in pressure in the sub-tropics, poleward shifts in the storm tracks, expansion of the Hadley Cell and positive trends in the Southern Annular Mode are leading to a general drying of the sub-tropics and southern continental Australia - especially in winter. Other changes, including those in the tropics are less consistent in theory and models. Therefore, this Report focuses primarily on rainfall changes and the reasons behind them for sub-regions of Australia rather than the nation as a whole.

GCM-BASED RAINFALL PROJECTIONS

Global climate models can resolve rainfall changes due to shifts in atmospheric circulation, storm tracks and extra-tropical cyclones as well as integrate the results of changes to thermodynamic processes to create projections of rainfall change. Global climate models vary in their simulation of circulation change and other processes over Australia, and this implies a range of projected changes in rainfall. The report focuses on the range between models as a measure of the uncertainty in the response in atmospheric circulation and rainfall processes, rather than on a single model or the multi-model mean.

To give a broad overview of the rainfall projections from CMIP5, Figure 7.2.1 gives the model simulated annual rainfall for 1910 to 2090 for each of the Northern Australian (NA), Southern Australian (SA), Eastern Australian (EA) and Rangelands (R) super-clusters. Table 7.2.1 gives results in numerical form for 2030 (RCP4.5) and 2090 (RCP2.6, RCP4.5 and RCP8.5). The table also indicates levels of agreement amongst models on increase, decrease etc, using the categories defined in Section 6.4.

It is immediately clear from the time series (Figure 7.2.1) that natural variability of rainfall remains significant compared to any climate change signal out to 2090. Indeed, under the RCP2.6 and RCP4.5 scenarios it is difficult to detect any marked change in many cases. This is particularly the case in the Australia wide average results (not shown). This is in marked contrast to the results for temperature reported in the previous section.

Nevertheless, under RCP8.5 there is an emerging drying trend clearly evident in Southern and Eastern Australia, and in Southern Australia this is also evident under the lower RCPs. This is in line with the global-scale patterns of rainfall decrease in the mid-latitudes and is consistent with theory, knowledge of climate dynamics and previous model results (e.g. CSIRO and BOM, 2007). The expanding uncertainty with time that is visible in all cases under RCP8.5, and to a lesser extent under the lower RCPs, is indicative of the fact that there are differing forced responses for at least some models, even in cases where the model median indicates little change. As indicated in Table 7.2.1 there is medium agreement amongst models on a substantial annual decrease in Eastern and Southern Australia, whereas in the Rangelands and Northern Australia there is low agreement on the direction of change.

By 2090, the projected changes are larger for the higher emission scenario, consistent with the understanding of climate forcings. The magnitude of the ranges of projected change in rainfall in 2030 relative to 1995 (under RCP4.5) are around -10 % to little change in Southern Australia, and -10 to +5 % in the other regions (see Table 7.2.1). In 2090 under RCP8.5 the projected rainfall changes -25 to +5 % in Southern Australia, around -25 to +10 % in Eastern Australia, around -30 to +20 % in the Rangelands and -25 to +25 % for Northern Australia. Changes are generally much more moderate in 2090 under RCP2.6.



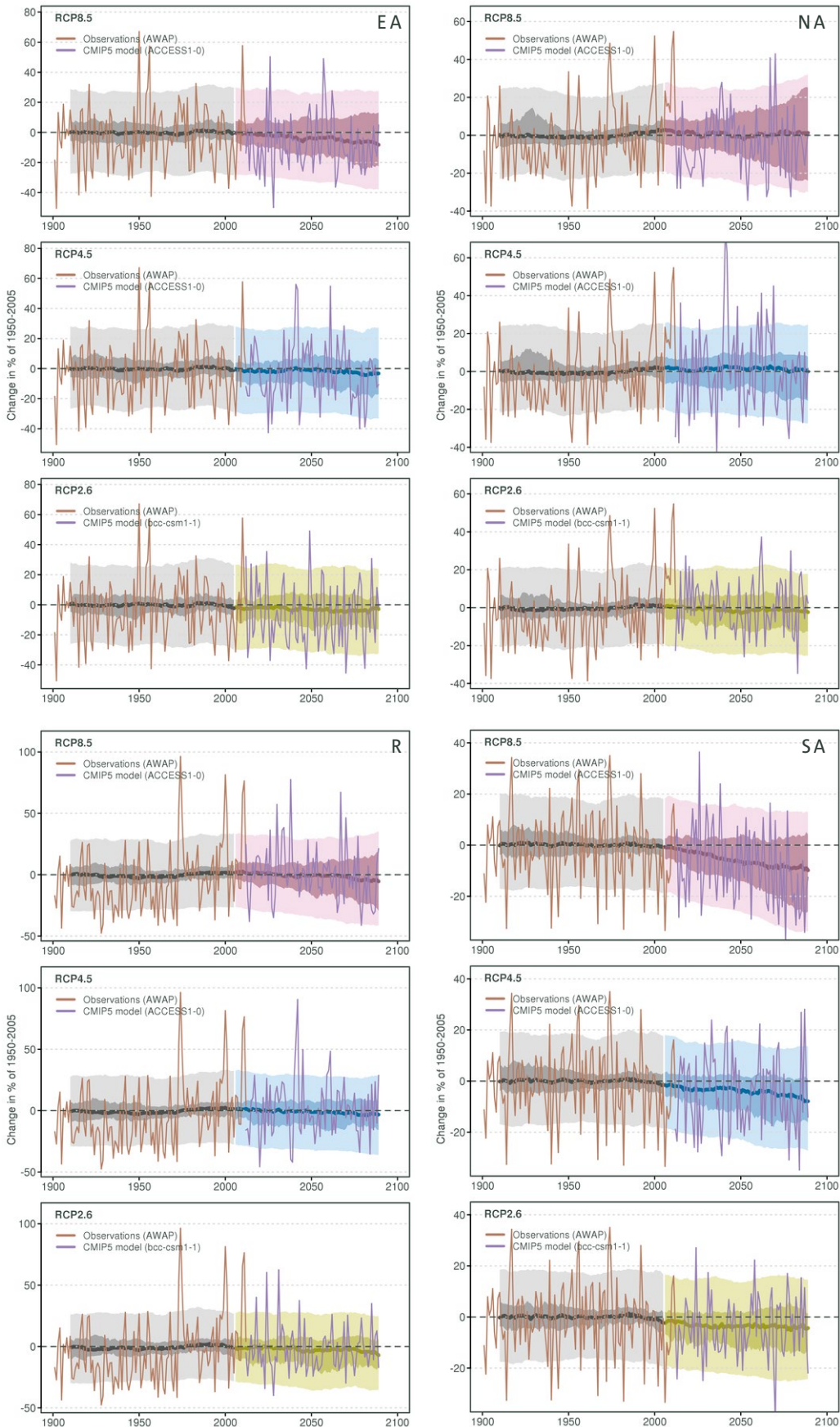


FIGURE 7.2.1: RAINFALL FOR 1910–2090 AS SIMULATED IN CMIP5 FOR EACH OF THE EASTERN AUSTRALIAN (EA; TOP LEFT), NORTHERN AUSTRALIAN (NA; TOP RIGHT), RANGELANDS (R; BOTTOM LEFT) AND SOUTHERN AUSTRALIAN (SA; BOTTOM RIGHT) SUPER-CLUSTERS. THE CENTRAL LINE IS THE MEDIAN VALUE, AND THE SHADING IS THE 10TH AND 90TH PERCENTILE RANGE OF 20-YEAR MEANS (INNER) AND SINGLE YEAR VALUES (OUTER). THE GREY SHADING INDICATES THE PERIOD OF THE HISTORICAL SIMULATION, WHILE THREE FUTURE SCENARIOS ARE SHOWN WITH COLOUR-CODED SHADING: PURPLE RCP8.5, BLUE RCP4.5 AND GREEN RCP2.6. AWAP OBSERVATIONS ARE SHOWN IN BROWN AND A SERIES FROM A TYPICAL MODEL ARE SHOWN INTO THE FUTURE IN LIGHT PURPLE (SEE BOX 6.2.2 FOR MORE EXPLANATION OF PLOT).

TABLE 7.2.1: MEDIAN AND 10TH TO 90TH PERCENTILE RANGE OF PROJECTED RAINFALL CHANGE (PERCENT) FOR NORTHERN AUSTRALIA, EASTERN AUSTRALIA, RANGELANDS AND SOUTHERN AUSTRALIA SUPER-CLUSTERS (COMPARED TO 1986–2005 BASELINE). MODEL AGREEMENT ON PROJECTED CHANGES IS SHOWN FOR 2090 AND RCP8.5 (WITH ‘MEDIUM’ BEING MORE THAN 60% OF MODELS, ‘HIGH’ MORE THAN 75%, ‘VERY HIGH’ MORE THAN 90%, AND ‘SUBSTANTIAL’ A CHANGE OUTSIDE THE 10 TO 90% RANGE OF MODEL NATURAL VARIABILITY).

SEASON	2030 RCP4.5	2090 RCP2.6	2090 RCP4.5	2090 RCP8.5	MODEL AGREEMENT 2090 RCP8.5 (PERCENTAGES SHOW FRACTION OF MODELS)
RAINFALL CHANGE IN NORTHERN AUSTRALIA (%)					
ANNUAL	0 (-9 to +4)	-4 (-12 to +3)	-1 (-14 to +6)	0 (-26 to +23)	<i>Low agreement in direction of change</i> (51% decrease), but substantial decrease (37%) & increase (32%) possible.
DJF	-1 (-8 to +8)	-2 (-16 to +4)	-1 (-18 to +8)	+2 (-24 to +18)	<i>Low agreement in direction of change</i> (56% increase), but substantial increase (42%) & decrease (29%) possible.
MAM	0 (-17 to +7)	-4 (-18 to +11)	-2 (-17 to +12)	-2 (-30 to +26)	<i>Medium agreement in little change</i> (37% of models), but substantial decrease (33%) and increase (31%) possible.
JJA	-5 (-26 to +16)	-8 (-41 to +16)	-14 (-35 to +20)	-15 (-48 to +46)	<i>Medium agreement in decrease</i> (67%).
SON	-4 (-26 to +20)	-7 (-32 to +13)	-7 (-32 to +27)	-13 (-44 to +44)	<i>Medium agreement in decrease</i> (64%).
RAINFALL CHANGE IN EASTERN AUSTRALIA (%)					
ANNUAL	-1 (-13 to +5)	-4 (-19 to +6)	-7 (-16 to +6)	-10 (-25 to +12)	<i>Medium agreement in substantial decrease</i> (52%), but substantial increase possible (21%).
DJF	-2 (-12 to +13)	-6 (-20 to +13)	-2 (-15 to +13)	+4 (-16 to +28)	<i>Medium agreement in little change</i> (61%), but substantial increase (27%) and decrease (13%) possible.
MAM	-4 (-22 to +13)	-8 (-25 to +15)	-7 (-28 to +18)	-8 (-33 to +26)	<i>Medium agreement in little change</i> (55%), but substantial decrease (28%) & increase (17%) possible.
JJA	-3 (-19 to +9)	-4 (-24 to +9)	-10 (-25 to +8)	-16 (-40 to +7)	<i>Medium agreement in substantial decrease</i> (53%).
SON	-2 (-18 to +11)	-3 (-26 to +11)	-10 (-27 to +9)	-16 (-41 to +8)	<i>Medium agreement in substantial decrease</i> (57%).
RAINFALL CHANGE IN RANGELANDS (%)					
ANNUAL	-2 (-11 to +6)	-6 (-21 to +3)	-5 (-15 to +7)	-4 (-32 to +18)	<i>Low agreement in direction of change</i> (59% decrease), but substantial decrease (41%) and increase (22%) possible.
DJF	-1 (-16 to +7)	-6 (-22 to +8)	-2 (-16 to +10)	+3 (-22 to +25)	<i>Low agreement in direction of change</i> (52% increase), but substantial decrease (36%) and increase (33%) possible.
MAM	+0 (-23 to +21)	-6 (-26 to +18)	0 (-23 to +27)	+9 (-42 to +32)	<i>Medium agreement in little change</i> (54%), but substantial increase (28%) and decrease (19%) possible.
JJA	-7 (-20 to +14)	-4 (-31 to +12)	-11 (-34 to +7)	-20 (-50 to +18)	<i>Medium agreement in substantial decrease</i> (61%), but substantial increase possible (14%).
SON	-3 (-21 to +19)	-5 (-32 to +15)	-10 (-26 to +11)	-11 (-50 to +23)	<i>Medium agreement in decrease</i> (68%).
RAINFALL CHANGE IN SOUTHERN AUSTRALIA (%)					
ANNUAL	-4 (-9 to +2)	-3 (-15 to +3)	-7 (-16 to +2)	-8 (-26 to +4)	<i>Medium agreement in substantial decrease</i> (69%)
DJF	-1 (-17 to +9)	-5 (-22 to +6)	-2 (-13 to +8)	+1 (-13 to +16)	<i>High agreement in little change</i> (71%), but substantial increase (18%) & decrease (11%) possible.
MAM	-2 (-18 to +8)	-5 (-17 to +11)	-2 (-19 to +10)	-1 (-25 to +13)	<i>Medium agreement in little change</i> (57%), but substantial decrease (28%) & increase (15%) possible.
JJA	-4 (-12 to +3)	-3 (-9 to +4)	-9 (-19 to +2)	-17 (-32 to -2)	<i>High agreement in substantial decrease</i> (80%).
SON	-4 (-13 to +5)	-5 (-23 to +4)	-10 (-23 to +1)	-18 (-44 to -3)	<i>High agreement in substantial decrease</i> (79%).

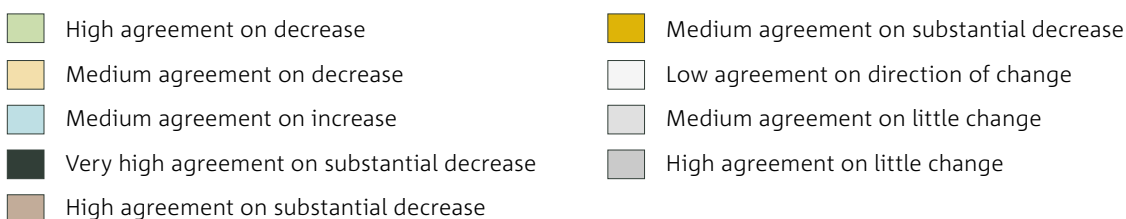


Figure 7.2.2 shows the seasonal variation in the projected rainfall changes for 2030 and 2090 under three emission scenarios, with additional seasonal information in Table 7.2.1. Figure 7.2.2 also contrasts the projected changes with natural variability (with ‘substantial’ changes exceeding natural variability). In all seasons in 2030 under RCP4.5 ranges of change show mostly small differences from the ranges expected from natural variability, and thus represent mostly little change, although a tendency to decrease is present in winter and spring, particularly in Southern Australia (-10 to +5 %). By 2090, winter and spring decreases

are clearly evident throughout Australia under RCP8.5 and also in Southern Australian under RCP4.5. The magnitude of these changes is around -40 % to little change in Southern Australia, and -40 % to +10 % in Eastern Australia and -50 % to +20 % in the Rangelands. Under RCP4.5, the 2090 changes are generally about half as large. The decreases in southern areas also become evident as early as 2050 under RCP8.5 (not shown). By contrast, under RCP4.5 and RCP8.5 in 2090, there is medium to high agreement on little change throughout Australia in autumn, and in Southern Australia and Eastern Australia in summer, but still with some models showing large changes. In the Rangelands and Northern Australia there is low agreement on the direction of summer rainfall change under RCP8.5 with the changes spanning a large range (around -25 to +25 %). Decreases are projected in spring and winter, but rainfall amounts are low in these seasons, particularly winter, so results are not discussed quantitatively.

To illustrate finer spatial variations in projected rainfall change, this Report presents seasonal changes for each of the 15 sub-clusters (Figure 7.2.3 and 7.2.4). To highlight the contrast between areas of projected increase and decrease in rainfall, RCP8.5 and 2090 was chosen as this maximises signal to noise. Figure 7.2.3 show ranges of model results contrasted to natural variability, whereas agreement amongst models on simulated changes is summarised in Figure 7.2.4. The figures show that the Southern and Eastern Australia winter drying is present in all the southern clusters including the southern Rangelands, but is absent in Tasmania where there is a tendency amongst the models for little change or an increase in winter rainfall. This borderline between mainland Australia and Tasmania is consistent with the relative position and projected change in the mean atmospheric circulation. The simulated tendency for spring decrease is present in all clusters except the northern Rangelands and the Top End. All clusters show medium agreement on little change in autumn with only some Queensland clusters showing a slight tendency to decrease. The summer signal is mixed in all areas, except for decrease in western Tasmania. In many of the southern and eastern areas, the range of projected summer change is not much larger than that expected due to natural variability, with the consequence that the result can be characterised there as ‘high agreement on little change’, although a tendency to increase over New South Wales can be noted.

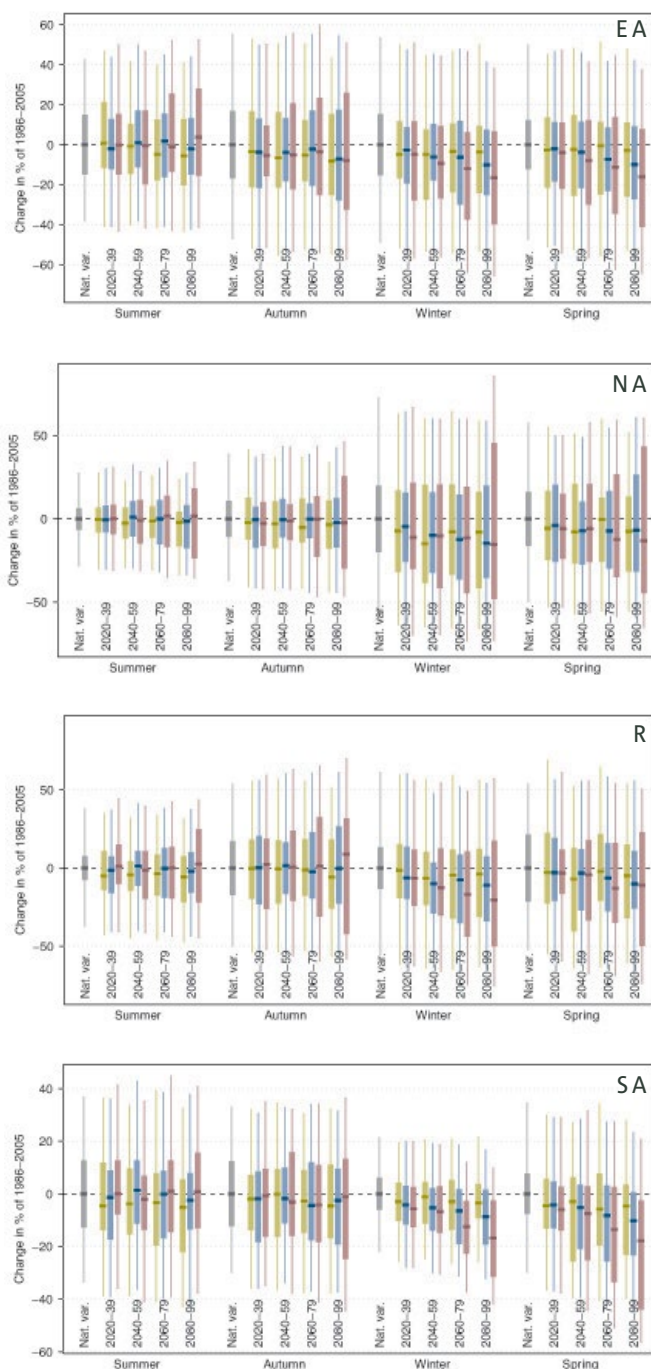
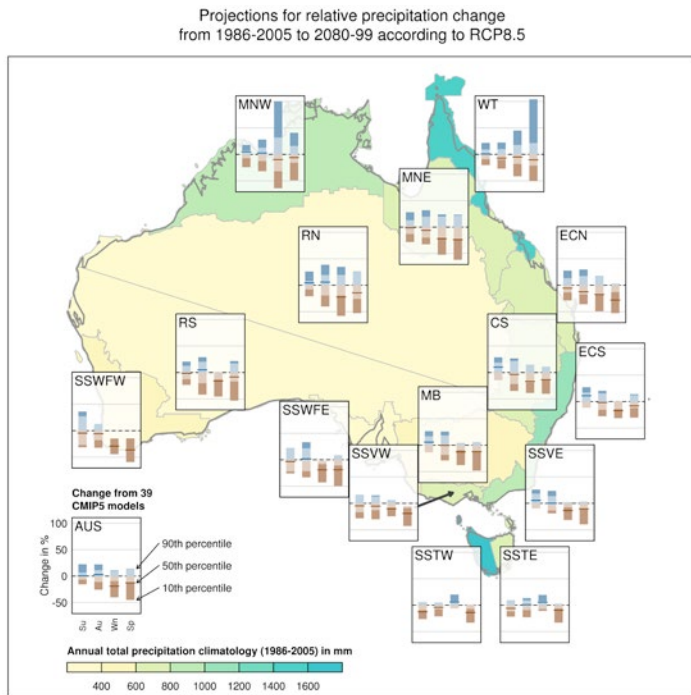


FIGURE 7.2.2: MEDIAN AND 10TH TO 90TH PERCENTILE RANGE OF PROJECTED SEASONAL RAINFALL PERCENT DIFFERENCE FOR FOUR FUTURE TWENTY YEAR PERIODS RELATIVE TO THE 1986–2005 PERIOD (GREY BAR) FOR RCP2.6 (GREEN), RCP4.5 (BLUE) AND RCP8.5 (PURPLE). FINE LINES SHOW THE RANGE OF INDIVIDUAL YEARS AND SOLID BARS FOR TWENTY YEAR RUNNING MEANS. RESULTS ARE SHOWN FOR EASTERN AUSTRALIAN (EA), NORTHERN AUSTRALIAN (NA), RANGELANDS (R) AND SOUTHERN AUSTRALIAN (SA) SUPER-CLUSTERS.



The magnitude of the simulated changes varies substantially between regions, seasons and by model. In this RCP8.5 2090 case changes approach 50 % at the ends of the model range for some regions and seasons (e.g. up to 50 % rainfall reduction in winter and spring in south-western WA). For the tropical clusters, it should be noted, however, that the large spread for the winter season can be explained by the fact that these are relative changes and winter has very low levels of rainfall (i.e. even small absolute changes will result in large percentage changes). In general, the magnitude of the projected change scales down for earlier dates and lower RCPs. An exception is rainfall change over NSW, where the direction of the change under RCP2.6 in summer is opposite to what it is under the other RCPs (not shown). This result is likely to be due to the greater impact of ozone recovery versus increasing greenhouse gas concentrations in the RCP2.6 scenario. As shown by Eyring *et al.* (2013), this scenario leads to a contrary response in the Southern Annular Mode (SAM) compared to the others (implying a westerly anomaly over south-eastern Australia in this season and less rainfall) (Hendon *et al.* 2007).

FIGURE 7.2.3: MEDIAN AND 10TH TO 90TH PERCENTILE RANGE OF PROJECTED SEASONAL RAINFALL CHANGES IN SUB-CLUSTERS FOR 39 CMIP5 GCMS FOR 2080–2099 RELATIVE TO 1986–2005 FOR RCP8.5 (IN PERCENT). BLUE INDICATES INCREASE AND BROWN DECREASE (SEE KEY). THE PALER PORTION OF THE BAR IS THE 10TH TO 90TH PERCENTILE RANGE EXPECTED FROM NATURAL VARIABILITY AND THE DARKER PORTIONS ARE WHERE THE CHANGES ARE LARGER THAN THE 10TH AND 90TH PERCENTILE EXPECTED FROM NATURAL VARIABILITY. THE AUSTRALIAN AVERAGE RESULT IS IN THE BOTTOM LEFT. NOTE THE CHOICE OF A HIGH FORCING CASE (2090 AND RCP8.5) WHICH WAS MADE SO THAT REGIONAL DIFFERENCES COULD BE MORE CLEARLY ILLUSTRATED. FOR QUANTITATIVE CLUSTER PROJECTION INFORMATION FOR OTHER RCPs AND FOR 2030, SEE RELEVANT CLUSTER REPORT.

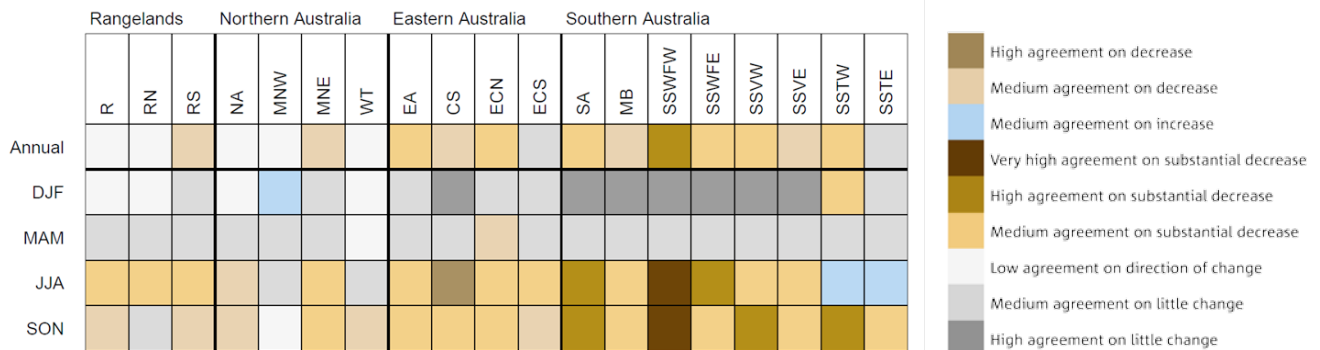


FIGURE 7.2.4: CLUSTER AND SUB-CLUSTER ANALYSIS OF AGREEMENT AMONGST CMIP5 MODELS ON MAGNITUDE AND DIRECTION OF SIMULATED RAINFALL CHANGE IN 2090 UNDER RCP8.5 ('MEDIUM' IS MORE THAN 60 % OF MODELS, 'HIGH' MORE THAN 75 %, 'VERY HIGH' MORE THAN 90%, AND 'SUBSTANTIAL' REPRESENTS A CHANGE OUTSIDE THE 10 TO 90 % RANGE OF MODEL NATURAL VARIABILITY).



In addition to the ranges of rainfall change presented above by region, ranges of rainfall change have also been prepared at the individual grid point level. This uses the same method of producing gridded percentiles of the projected change as was applied in the CSIRO and BOM, (2007) projections (Section 6.2). Maps of the 10th, 50th and 90th percentiles of seasonal rainfall change are shown in Figure 7.2.5 for a case with a global warming of 3.7 °C

(the RCP8.5 2090 mid case – see Chapter 5). Percentiles at the grid point level allow finer spatial details in projected change to be considered. These gridded projected changes can also be used in combination with a high resolution observed baseline to consider projected future climate change in absolute terms. When the 10th percentile annual rainfall change is applied (the driest case) rainfall contours can shift hundreds of kilometres coastward compared to

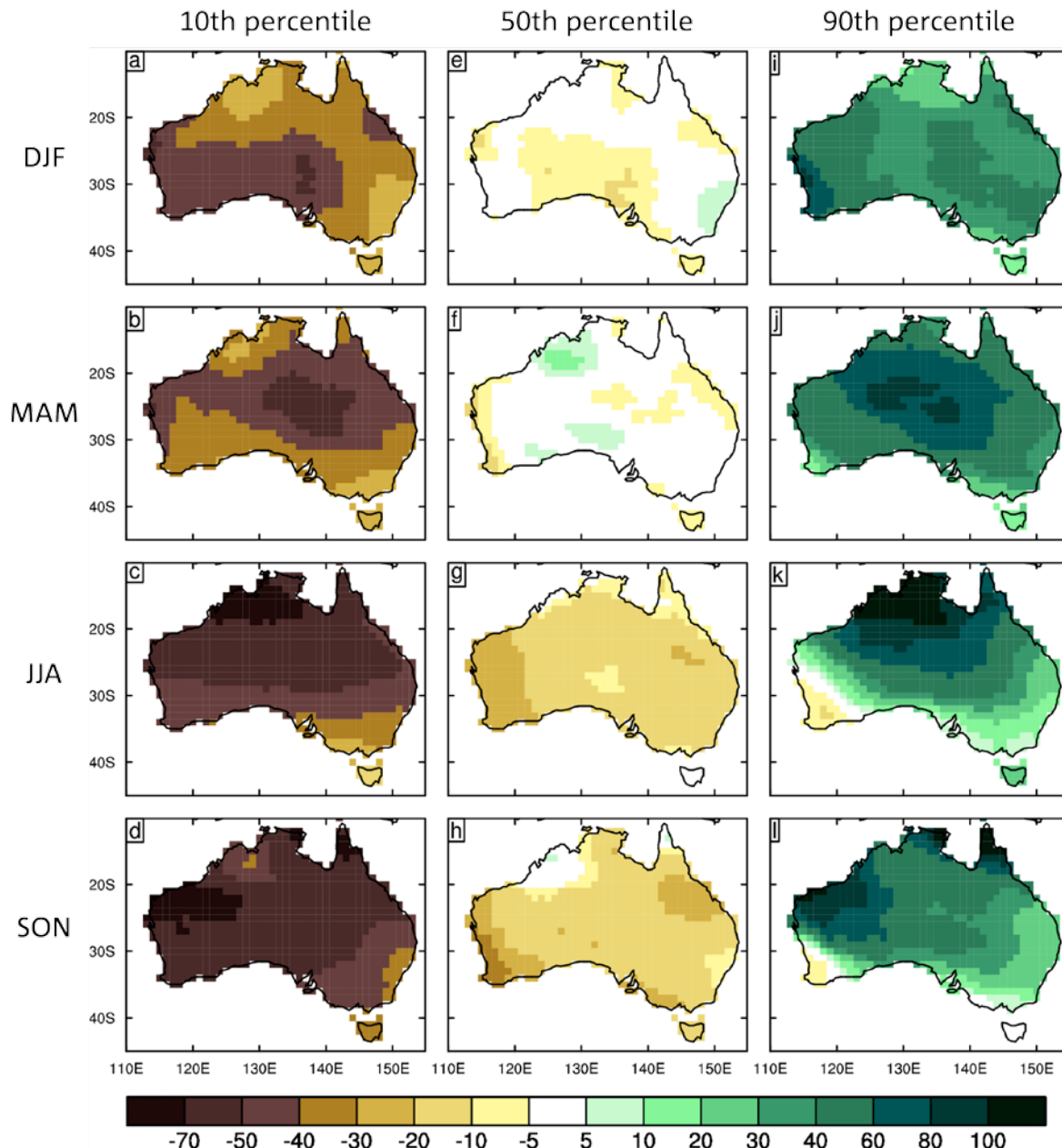


FIGURE 7.2.5: GRIDDED 10TH, 50TH AND 90TH PERCENTILE SEASONAL RAINFALL CHANGES FROM CMIP5, 2090 RCP8.5 (METHOD OF CSIRO AND BOM, 2007).

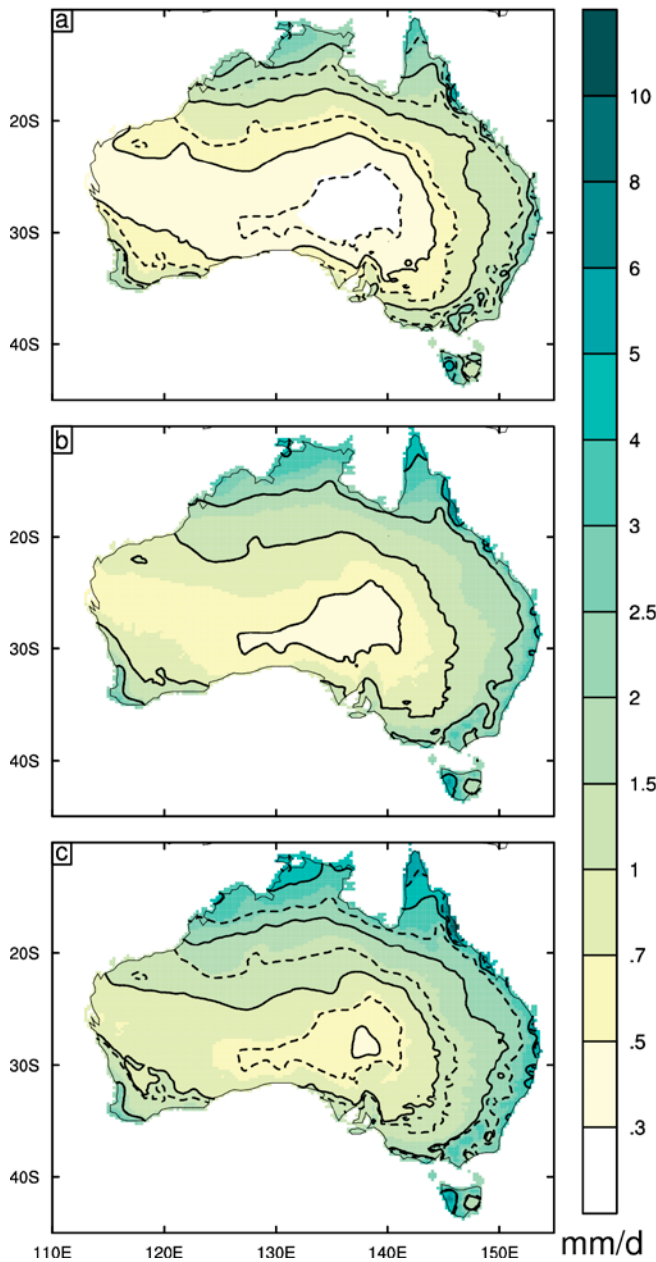


FIGURE 7.2.6: ANNUAL MEAN RAINFALL (AS A RATE IN MM/DAY), FOR THE PRESENT CLIMATE (B), AND FOR DRIER CONDITIONS (A) OR WETTER CONDITIONS (C). THE PRESENT IS USING A BOM DATA SET FOR 1958–2001, ON A 0.25 GRID. THE DRIER/WETTER IS USING THE 10TH AND 90TH PERCENTILE FACTOR FOR % CHANGE AT 2090, UNDER RCP8.5. IN EACH PANEL THE 0.5 MM/DAY, 1 MM/DAY, 2 MM/DAY AND 4 MM/DAY CONTOURS ARE PLOTTED WITH SOLID BLACK LINES. IN (A) AND (C) THE SAME CONTOURS FROM THE ORIGINAL CLIMATE (B) ARE PLOTTED AS DOTTED LINES.

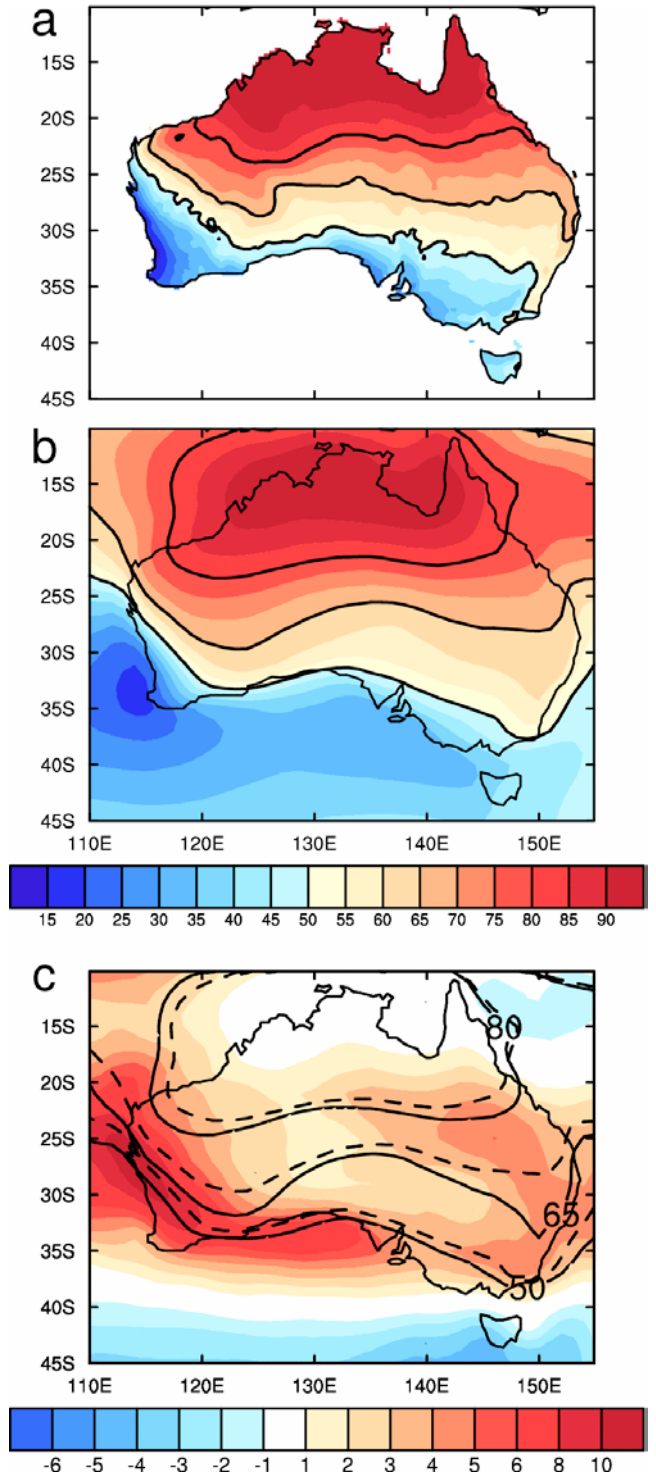


FIGURE 7.2.7: PERCENTAGE OF ANNUAL RAIN THAT FALLS IN THE WARMER SIX MONTHS FROM: (A) BOM 1900–2008, AND (B) CMIP5 40-MODEL MEAN, FOR 1986–2005 (SHOWING 50 %, 65 % AND 80 % CONTOUR LINES). NOTE ALSO THE OBSERVATIONAL DATA SET DOES NOT EXTEND OVER THE OCEAN AREAS IN (A)). (C) CHANGE IN PERCENTAGE OF RAIN IN THE WARMER SIX MONTHS, FROM THE MEAN CHANGES FOR 2080–2099 UNDER RCP8.5, COMPARED TO 1986–2005. THE 50 %, 65 % AND 80 % CONTOUR LINES FROM THE BASE CLIMATE ARE SHOWN AS DASHED LINES, WITH THOSE FOR THE 2080–2099 CLIMATE SHOWN AS SOLID LINES.



present, whereas with the 90th percentile projection (the wettest case) rainfall contours shift a similar distance in the opposite direction (Figure 7.2.6).

Finally, the tendency for winter rainfall decrease combined with a lack of clear change in summer rainfall, implies a projected southward shift of the summer-dominated rainfall zone. This shift is illustrated in Figure 7.2.7. Under an RCP8.5 2090 case, the multi-model mean indicates a southward expansion of the boundary between the summer and winter rainfall zones, which especially affects southern and south-western parts of Australia.

DOWNSCALED CMIP5 RESULTS

This Section examines the projected rainfall changes using two downscaling methods (CCAM and SDM – see Section 6.3) applied to a subset of CMIP5 models. The focus is on differences in the projected changes consistently produced by downscaling compared to the GCMs, either as a difference in the magnitude of change compared to the host models, or a regional difference in the direction of change. We use up to 22 simulations from SDM (all models that provided suitable inputs) and six CCAM simulations

(chosen for their performance over Australia and the globe). Figure 7.2.8 compares the projected rainfall change for Australia from GCMs and the equivalent from downscaling for a common set of five models. It is notable that these five models tend towards rainfall increase in northern Australia.

Downscaling has the potential to show more regional detail in projected changes, especially where finer resolution is a benefit in simulating important fine-scale processes or topographic effects (see Chapter 6.3.5). Where this can be demonstrated, this is termed ‘added value’ in the climate change signal. In these results there are plausible differences between the rainfall projection in eastern and western Tasmania in CCAM in summer, as was found in the Climate Futures for Tasmania project (Grose *et al.* 2013). There is also an indication of difference between east and west Tasmania in winter, especially in the SDM results. There is also a greater projected rainfall decline in western Victoria in autumn in SDM results than the host models (not shown), which is more in line with recent trends. There are some indications of a different projection in the Eastern Seaboard compared to west of the Great Dividing Ranges in summer, but the results are not clear and consistent so remain an ongoing research topic.

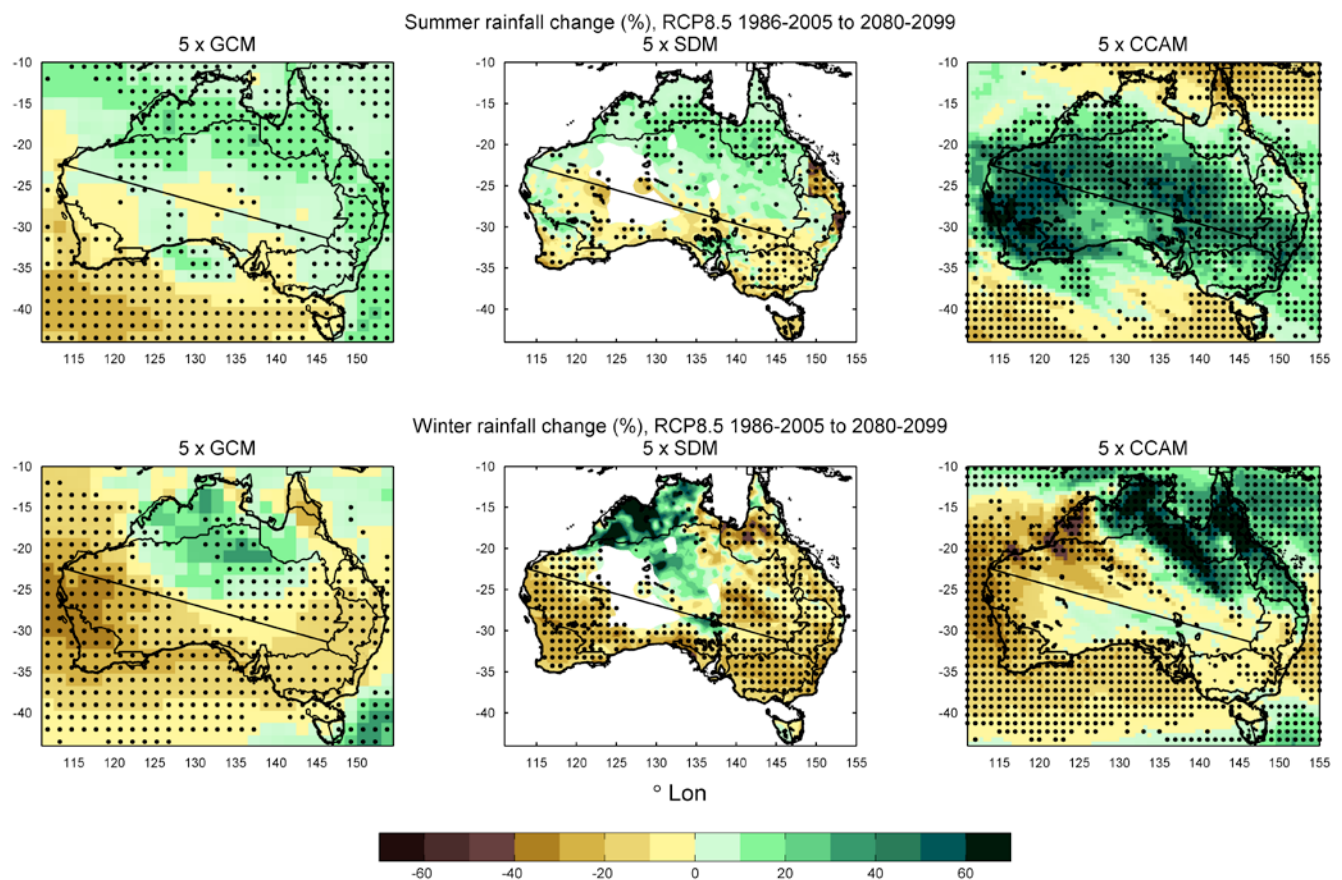


FIGURE 7.2.8: PROJECTED CHANGE IN MEAN RAINFALL FOR RCP8.5 1986–2005 TO 2080–2099 FOR: (TOP ROW) SUMMER AND (BOTTOM ROW) WINTER, IN: (LEFT) FIVE GLOBAL CLIMATE MODELS (GCMs): ACCESS-1.0, CNRM-CM5, MPI-ESM-LR, CCSM4, NORESM1-M, (MIDDLE) BUREAU OF METEOROLOGY STATISTICAL DOWNSCALING USING THE SAME FIVE GCMs AS INPUT, AND (RIGHT) CCAM DYNAMICAL DOWNSCALING ALSO USING THE SAME FIVE GCMs AS INPUT. STIPPLING SHOWS WHERE AT LEAST FOUR OUT OF FIVE SIMULATIONS AGREE ON THE DIRECTION OF CHANGE.

There are other cases where the downscaling produces a different projection to the global climate model but there is not a clear and intuitive link to the resolution of surface effects such as topography. In these instances, the downscaled projection can't be considered a superior projection for a physically plausible reason. However, the results may represent another plausible projection, that could be combined with GCM projections and therefore widen the range of projected change. These cases include a wetter future for many regions of southern and western Australia in summer, shown in both downscaling methods, primarily CCAM (Figure 7.2.8).

There are also cases where downscaling can produce different results from the host model due to the nature of the method or model used. These differences are an unavoidable result of the process and provide important context for interpreting the results. The Bureau of Meteorology statistical downscaling method uses a distinct set of predictors for different climate regions and this can produce regional differences with artificial sharp boundaries, such as in East Coast South and East Coast North in summer (Figure 7.2.8b). Dynamical downscaling such as CCAM can produce different patterns of change at the wider scale since it uses a new atmospheric model with its own model components for simulating the atmosphere.

In these circumstances it is not clear that wider-scale changes from CCAM should be trusted any more than those from the GCM.

In balancing this potential for 'added value' in the regional climate change signal but also the potential for different results due to the method used, this Report examines the regionally-averaged results for downscaling (Figure 7.2.9 and Figure 7.2.10).

Figure 7.2.9 shows projected rainfall changes from 22 of the CMIP5 GCMs downscaled using the SDM compared to the original GCM results for the same set of models. The range of projected changes is very similar to the GCM-based projected ranges in most sub-regions and seasons, but there are some potentially important differences in coastal eastern Australia, namely a markedly stronger decrease in south-western Victoria in summer and autumn, and spring increase as opposed to decrease in south-east Queensland. Differences in the magnitude of changes in eastern Tasmania compared to western Tasmania can be seen in some seasons such as winter. Notably all these differences are in regions with fine-scale and potentially strong topographical influences which would not be well represented in the GCMs. The SDM projects a summer decrease in the clusters on the east coast compared to the slight increase in GCMs however the magnitude of this

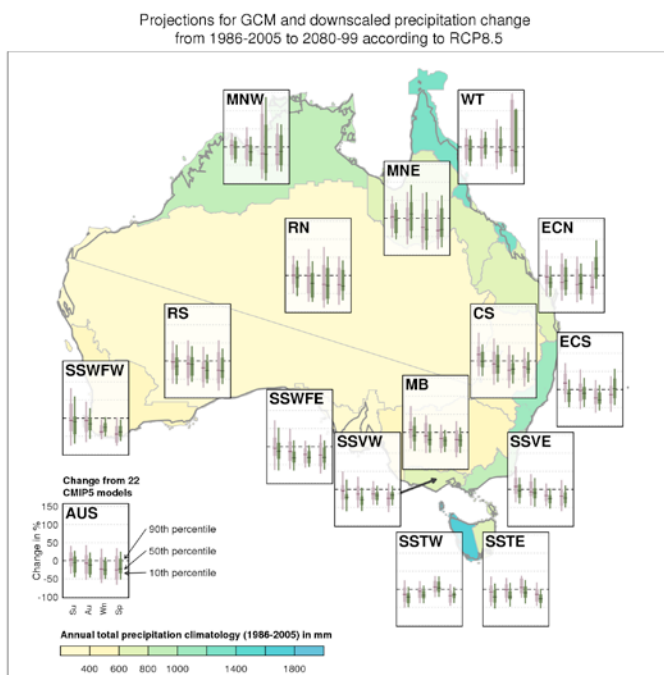


FIGURE 7.2.9: MEDIAN AND 10TH TO 90TH PERCENTILE PROJECTED CHANGES TO RAINFALL IN SUB-CLUSTERS FOR 22 CMIP5 GCMs, AND FOR THE SAME 22 MODELS DOWNSCALED USING THE BOM-SDM DOWNSCALING SYSTEM, FOR 2080–2099 RELATIVE TO 1986–2005 FOR RCP8.5. FINE LINES SHOW THE RANGE OF INDIVIDUAL YEARS AND SOLID BARS FOR TWENTY YEAR RUNNING MEANS. EACH PAIR OF BARS HAS THE CHANGES FROM THE GCMs ON THE LEFT (PURPLE) AND THE CHANGES FROM THE DOWNSCALING ON THE RIGHT (GREEN), EACH AVERAGED OVER THE REGION.

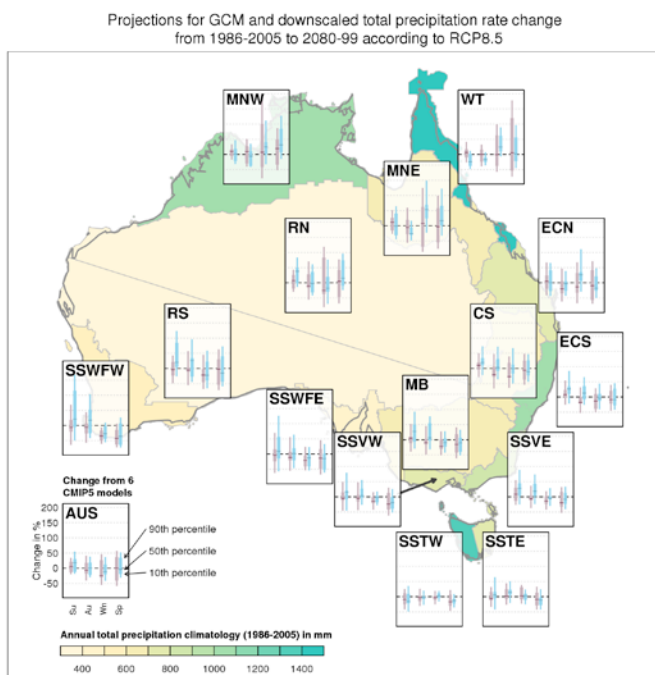


FIGURE 7.2.10: MEDIAN AND 10TH TO 90TH PERCENTILE PROJECTED CHANGES IN RAINFALL IN SUB-CLUSTERS FOR 6 CMIP5 GCMs, AND FOR THE SAME 6 MODELS DOWNSCALED USING THE CCAM DYNAMICAL DOWNSCALING MODEL FOR 2080–2099 RELATIVE TO 1986–2005 FOR RCP8.5. FINE LINES SHOW THE RANGE OF INDIVIDUAL YEARS AND SOLID BARS FOR TWENTY YEAR RUNNING MEANS. EACH PAIR OF BARS HAS THE CHANGES FROM THE GCMs ON THE LEFT (PURPLE) AND THE CHANGES FROM THE DOWNSCALING ON THE RIGHT (BLUE), EACH AVERAGED OVER THE REGION.



change is influenced by the artificial boundaries between regions in this area (see Figure 7.2.8, centre panels).

The case for ‘added value’ in downscaling compared to host models is strengthened if different downscaling methods agree on a particular change and its difference from the host models. However, many of these differences between downscaling and GCM results from the SDM results are not also found in the CCAM downscaled results (Figure 7.2.10). Differences between CCAM and the host GCMs are most evident in the tropics, with the strong indication of summer rainfall decline in wet tropical Queensland (as opposed to a mixed result in the GCMs). Proportional changes in the tropical dry season are less significant in absolute terms. The CCAM comparison is small (six models), and further analysis of these results combined with those from further downscaling, will be needed to properly assess likely rainfall changes in these key coastal regions.

Due to the effect of enhanced resolution of the atmosphere and the additional surface details, downscaled results may show a climate change signal that is different and more physically plausible than that from the host model. This indicates the potential for ‘added value’ in the downscaling and thus may give reason to use this over the GCM alone. However, the lack of consistency between downscaled results in many cases here indicates there are some unresolved questions about what is driving the changes and where the downscaling results provide unambiguous added value. A different direction of change in eastern compared to western Tasmania in some seasons, and a greater autumn rainfall decline in south-east Australia than GCMs project are the two main cases of potential added value from these projections. The results show that one must keep in mind the range of possible climate change, as projected by the GCMs, when using the downscaled data.

PLAUSIBLE PROCESSES AND CONFIDENCE IN RAINFALL PROJECTIONS

This section discusses the plausible processes which are likely to be associated with the CMIP5-simulated rainfall changes for Australia presented in the previous sections. Drawing upon this, and other relevant information, such as downscaling results, model evaluation, and consistency of historical CMIP5 projections with observed trends (Chapter 5), conclusions are drawn on projected rainfall change with associated confidence levels (see Section 6.4). These statements are also presented systematically, along with their rationale in Table 7.2.2. As this discussion focuses on interpreting the regional response and the confidence in it, the evidence used (and presented in Table 7.2.2) is predominantly for the high forcing case (RCP8.5 and 2090) when this response is most evident. The discussion in this section is organised according to the four super-clusters, but clusters and sub-clusters are explicitly discussed where there are notable exceptions at that level. Some further relevant discussion for specific clusters can be found in the Cluster Reports.

SOUTHERN AUSTRALIA (SOUTHERN FLATLANDS, SOUTHERN SLOPES, MURRAY BASIN)

Mean annual rainfall is projected to decrease in southern Australia as a whole over the course of the century, with this being particularly evident in winter and spring (Table 7.2.1). In all seasons by 2030, ranges of change show mostly small differences from the ranges expected from natural variability, although a tendency to decrease is present in winter and spring. By 2090, winter and spring decreases are strongly evident throughout under RCP8.5 and RCP4.5 (Tables 7.2.1 and 7.2.2). There are various lines of evidence that support this.

The future changes of greatest plausibility are the global increase in temperature, specific humidity and, for the Southern Hemisphere, a southward shift and intensification of the westerlies and expansion of the tropics coinciding in an upward trend in the Southern Annular Mode (SAM), and a shift to higher pressures over the Australian region (IPCC, 2013, see also Section 7.3.2). These pressure changes broadly lead to reduced cool season rainfall, which is a projected continuation of a recent trend.

Many regions within southern Australia have experienced declining cool-season rainfall since the 1970s, particularly in late-autumn and early winter (IOCI, 2002, Timbal, 2009, CSIRO, 2012), driven at least in part by changes to large-scale circulation that are projected to continue in the 21st century. These are the intensification and possibly southerly movement of the subtropical ridge (STR) of high pressure, changes in atmospheric blocking, and a poleward movement of the westerly storm tracks (Frederiksen and Frederiksen, 2005, 2007; CSIRO, 2012, Timbal and Drosdowsky, 2013). These trends are discussed further in Section 4.2 and Section 7.3, but are considered here in the context of rainfall projections. Overall the mean meridional (north-south) circulation (MMC) has been observed to widen, a change that is particularly consistent for the Southern Hemisphere across a range of different measures (Lucas *et al.* 2014) and is linked to surface changes observed such as the strengthening and shift of the STR (Nguyen *et al.* 2013). The relationship is significant across the entire cool season from April to October in south-eastern Australia (Timbal and Drosdowsky, 2013).

GCMs consistently project a future increase of the STR intensity and a further southward shift in the region of summer rainfall dominance (Figure 7.2.11 and see Section 7.3.3). In general GCMs capture many of the broad features of the MMC with accuracy, including having the STR broadly in the correct place and with a correct annual cycle (see Section 5.2). However, they can have a poor depiction of the inter-annual STR-rainfall relationship across southern Australia (Kent *et al.* 2013). These biases can be seen in the seasonal cycle of rainfall (see Figure 7.2.7), which shows that the dominance of summer rainfall extends too far south



in the climate model simulations of the present climate. These biases lower the confidence in the magnitude of the models' regional rainfall projections associated with the circulation changes described above. Also, the link to increased STR intensity is weaker in models than observed in the zonal mean (Timbal and Drosowsky, 2013, Whan *et al.* 2014), so the rainfall decrease associated with these projected circulation changes may be underestimated.

There are some regional exceptions to the general projection of drying. Winter rainfall in Tasmania is

projected to experience little change or to increase due to its southern location where it continues to be influenced by the westerlies as they strengthen and changes to the moisture content of air may also play a role (see Figure 7.2.11). The MMC describes changes across the breadth of Australia, however there are also important changes that differ in the west compared to the east of the Australian region that are important to rainfall change. One such change is projected change to atmospheric blocking and associated weather systems (Pook *et al.* 2012, Risbey *et al.* 2013a,b). These studies show that much of the recent rainfall decline in the south-west and south-east is related

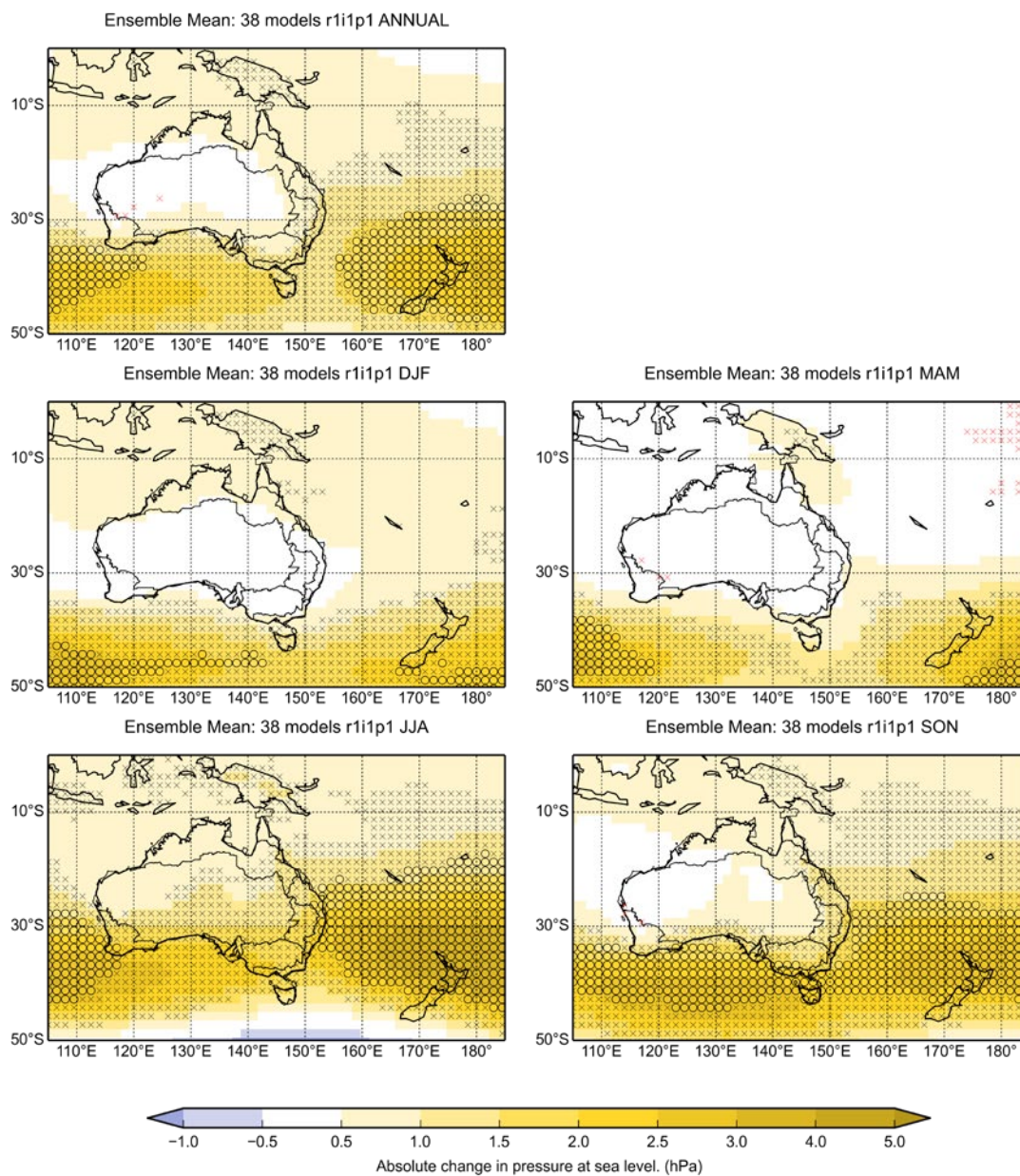


FIGURE 7.2.11: ENSEMBLE MEAN CHANGES IN MEAN SEA LEVEL PRESSURE (IN HPA) UNDER RCP8.5 (PERIOD 2080–99 VERSUS PERIOD 1986–2005) FOR ANNUAL (TOP LEFT) AND THE 4 SEASONS. THE STIPPLING DENOTES MODEL AGREEMENT ON CHANGES GREATER THAN 0.5 HPA (INCREASES OR DECREASES) AT THE LEVEL OF GREATER THAN 90 % (BLACK CIRCLES) OR GREATER THAN 67 % (BLACK CROSSES). THE EQUIVALENT MODEL AGREEMENT ON CHANGES LESS THAN 0.5 HPA (I.E. ESSENTIALLY NO CHANGE) ARE SHOWN IN RED.



to cut-off lows. The variation in rainfall from cut-off lows in turn is driven by longer period shifts in the preferred location and intensity of blocking and the zonally asymmetric circulation. Climate models have difficulty capturing the magnitude and variability of blocking, which is a source of additional uncertainty for rainfall projections for southern Australia.

There is less certainty and more regional variation in the rainfall projections in summer and autumn than for winter and spring (see Table 7.2.2). On average in southern Australia there is at least medium agreement amongst models on little change even under high forcing (2090 and RCP8.5) but the model range indicates that significant changes of either direction are also possible. Regional exceptions in the direction of summer rainfall change include a projected substantial decrease in western Tasmania (*medium confidence* – see Table 7.2.2), which is an expected response to an enhanced easterly regime as SAM shifts to a more positive mode through the century.

There are some regions of complex topography and a diversity of regional climate influences across a relatively small area in southern Australia, including across Tasmania and over the Great Dividing Range. Therefore, downscaling of climate models (see above and Section 6.3) has the potential for producing ‘added value’ in the regional climate change signal for such regions. For example, CCAM projects a rainfall increase in eastern Tasmania in summer and autumn in contrast to the decrease in the west, supporting the results from the Climate Futures for Tasmania project (Grose *et al.* 2013). However these new CCAM projections agree with GCMs for a decrease in spring rainfall in Tasmania which is in contrast to the Climate Futures for Tasmania results. The Bureau SDM (but not CCAM) shows an enhancement of the projected decline in rainfall in south-west Victoria in autumn. This decline is consistent with the observed decline (discussed above) whereas the GCM projections are not (see Section 5.3). Since the SDM more finely resolves the relationship between weather systems and local rainfall for this relatively restricted region, this may be a more physically plausible projection than the GCMs and suggests that the projected cool season decline may have a stronger influence on autumn rainfall than the GCMs results would indicate.

Based on the above considerations, the confidence on projected rainfall change in southern Australia is summarised in Table 7.2.2 for the high forcing case (RCP8.5 and 2090). The high likelihood of a hemispheric circulation response to increasing greenhouse gases resulting in reduced cool season rainfall, along with the consistency between models for projected declines in cool-season (winter and spring) rainfall across southern Australia (and the converse in winter in Tasmania) provide *high confidence* in the cool season rainfall decline across southern Australia (and increase in winter in Tasmania). In general, the direction of change in summer and autumn rainfall

cannot be confidently projected in the region, but there is *medium confidence* in a decrease in south-western Victoria in autumn and in western Tasmania in summer. The cool season rainfall declines are projected to become evident against natural variability as early as 2030 in the Southern and South-western Flatlands and 2050 under RCP4.5 and 8.5 in south-western Victoria.

CENTRAL SLOPES AND EAST COAST

Projections of mean rainfall change in eastern Australia are the most uncertain of any broad region of Australia. Models show a range of projections for mean annual rainfall, from a substantial decrease to a substantial increase. Nevertheless, there is medium agreement in a substantial decrease in rainfall under high forcing (RCP8.5 and 2090) since around half of GCMs show this trend (Table 7.2.1). While the southern Australian climatological features also have an influence in eastern Australia (more particularly in the East Coast sub-cluster and in the inland cluster of Central Slopes), there are several drivers of change in this region that models do not simulate particularly well, such as the rainfall teleconnection to ENSO (Section 5.2.2) and this reduces the level of confidence in projections along with the large model range.

There is a similar level of uncertainty when it comes to seasonal rainfall projections. There is medium agreement amongst the GCMs in substantial rainfall reductions in winter and spring under RCP8.5 and at 2090 (Table 7.2.1 and 7.2.2), and this is the primary factor driving the simulated reduction in annual rainfall. These changes are driven by some physically plausible drivers of change (see below). By contrast, the rainfall projection for summer and autumn is particularly uncertain, with a large model range and numerous processes involved. Changes in all seasons in 2030 are small relative to natural variability (Table 7.2.1).

The projected reduction in winter rainfall over eastern and south-eastern Australia is shown by the GCMs, as well as the SDM. A considerable proportion of the total winter rainfall in the subtropical and temperate regions of eastern Australia is associated with the occurrence of cut-off lows. This proportion rises as the intensity of the rainfall increases, such that a high proportion of the heavy and extreme rainfall events in this region are caused by these systems (Pepler and Rakich, 2010, Dowdy *et al.* 2013b). These low pressure systems are cut off from (i.e. not embedded within) the storm track region that moves with the prevailing westerly wind to the south of the subtropical ridge. Projections based on global climate models suggest that increasing greenhouse gas concentrations towards the end of this century will lead to fewer cut-off lows in the subtropical East Coast region of Australia where these systems are known as East Coast Lows (Dowdy *et al.* 2014). There may also be fewer cut-off lows in the region around Tasmania while noting that the intensity of the systems that do occur could potentially become stronger (Grose

et al. 2012). These results are consistent with an observed trend towards reduced storminess in eastern and southern Australia since 1890 (Alexander *et al.* 2011). Given that these storms are characterised by strong vorticity and baroclinic instability in the upper troposphere (Risbey *et al.* 2009a, Mills *et al.* 2010, Dowdy *et al.* 2013a), changes in their occurrence are likely related to changes in the climatology of a number of related upper-tropospheric phenomena. These phenomena include Rossby waves, atmospheric blocking and a split in the jet-stream over eastern Australia during winter (Freitas and Rao, 2014, Grose *et al.* 2012).

The Great Dividing Range is a topographic feature that may influence regional differences in projected climate change. There could plausibly be a different mean rainfall trend projected for the Eastern Seaboard (East Coast South) compared to inland from the ranges (Central Slopes). Indeed, a tendency for summer increase in Central Slopes contrasts with a decreasing tendency in East Coast North, and the spring decline is stronger in Central slopes than in East Coast South.

The results from the two downscaling techniques show conflicting signals. The SDM results show a rainfall decrease in East Coast South in summer, in contrast to the GCM projected increase, however CCAM results show an even larger rainfall increase than GCMs. CCAM also projects a larger increase than GCMs in both East Coast South and Central Slopes in autumn. CCAM also projects little change in winter rainfall which is in contrast to the GCM results and the SDM. In East Coast North, the SDM projects a rainfall increase in spring which is the opposite of GCMs, however this is not supported by CCAM results. CCAM projects an increase in winter rainfall which is in contrast to GCM results. Results from the forthcoming regional climate change study for the region, the NSW and ACT Regional climate modelling project (NARCLiM) outlined in Evans *et al.* (2014) will also shed light on this issue.

In summary, for the eastern Australian region as a whole under high climate forcing (RCP8.5 and 2090) there is *medium confidence* in a winter rainfall decrease. This relates to the southward retreat and weakening of winter storm systems. There is *high confidence* in this change in the Central Slopes cluster where there is also *medium confidence* in spring decreases (see Central Slopes Cluster Report). There is also *medium confidence* in a winter decrease in East Coast South. Otherwise, there is *low confidence* in projecting the direction of seasonal rainfall change in this region, with strongly contrasting results between both downscaling methods and with the GCMs, particularly in the East Coast cluster. The large uncertainty in this region is likely to be related to the range of rainfall drivers and competing influences on rainfall change. The regional climate change signal in this area is a topic of ongoing research for both global modelling and downscaling. In the near future (2030), there is *high confidence* that natural variability will predominate over trends due to greenhouse gas emissions.

NORTHERN AUSTRALIA

The strong monsoonal climate across tropical Australia has a distinct West-East pattern: north-western Australia is predominantly impacted by the seasonal progression across the equator of the Inter-tropical convergence zone (setting up the background state for the monsoon onset to occur) while north eastern Australia (Gulf region and coastal North-Queensland) has additional impact from the easterly trade wind regime which can bring rainfall even during the monsoon westerly break periods. It therefore makes sense to assess causes and processes for future changes to rainfall across northern Australia with this geographic distinction in mind. Following is a seasonal assessment of the confidence in rainfall projections across tropical Australia. However, since there is only very little climatological rainfall during winter (Jun-Aug is the dry season) across this domain, projected rainfall changes are not very meaningful and are therefore not considered here for this season.

In summer (peak monsoon season), GCM projections for the entire northern Australia region (NA) show low agreement in the direction of change in the high forcing case (2090 and RCP8.5), with both substantial increases and decreases being projected. In 2030, and at 2090 under RCP4.5, there is at least medium agreement amongst models on little change. Notably, the recent wide-spread decadal upward trend (in western parts) and downward trend (in coastal eastern parts) in rainfall is not captured by the models (see Section 5.3.2). Downscaling results are generally very similar (particularly SDM) with some disagreement for CCAM results. Only for the Monsoonal north-west region there is agreement in the GCMs on some increase. In autumn (which includes the transition of the monsoon retreat) GCM projections for the entire NA super-cluster show some agreement on little change under high forcing (RCP8.5 and 2090), although substantial changes are present in a minority of models. SDM and CCAM downscaling show a similar range of results compared to GCMs with some disagreement in the Wet Tropics region. The observed recent upward trend is not captured in the models. In spring (which includes the transition of the monsoon onset), GCM projections for the entire NA super-cluster show some agreement on a decrease under high forcing (RCP8.5 and 2090), with this being more evident in Monsoonal North East. In the near future (2030), there is model agreement on little change. The SDM and CCAM downscaling show very similar changes compared to the GCMs, but the spread in the CCAM downscaling simulations is somewhat smaller.

Changes to rainfall across the Top End of Australia are closely related to two competing processes evolving more strongly under future climate change conditions: (a) increases in atmospheric moisture content due to higher temperatures favours mean rainfall increases



during the wet season; (b) a slowing down of the tropical circulation favours mean rainfall decreases during the wet season. Because both of these processes are simulated with different strength by different models, the resulting projected changes in wet season rainfall carry large uncertainties in either direction. Furthermore, as with the Rangelands, change in the northern warm season can be related to the pattern of equatorial sea surface temperature changes, which differs considerably among the global models (see Section 3.6).

Relevant in the consideration is the observed rainfall trend over the previous forty years in north-west Western Australia. Recent studies have associated this trend with changes to sea surface temperatures either to the north-west (Indian Ocean) (Shi *et al.* 2008) or north-east (Western North Pacific Warm Pool-) of tropical Australia (Li *et al.* 2013). In the latter case, the relationship between the North Pacific Warm Pool and tropical Australia rainfall in the CMIP5 models would be strongly influenced by one of the typical systematic errors seen in current coupled climate models: the “cold tongue” bias in the equatorial Pacific sea surface temperatures. Indeed, most models fail to adequately reproduce the recent rainfall trend in north-west Western Australia (see Section 5.2).

Another consideration in the assessment is the simulation of some of the important processes associated with tropical Australia rainfall during the wet season: the eastward propagation of the MJO (which can trigger the Australian monsoon onset); the diurnal evolution of rainfall and the additional rainfall contributed by tropical cyclones. While CMIP5 models have some skill in capturing these processes, this skill can be low or only seen in a smaller sub-sample of models (see Section 5.2).

In summary (see Table 7.2.2) under high forcing (2090 & RCP8.5) some models show large annual and wet season change, but there is *low confidence* in projecting the direction of that change. Confidence in the projected rainfall changes is low throughout the region in the other seasons (and not relevant in winter when rainfall is very low). In addition to the widely varying direct GCM results, confidence is low because different processes, such as Monsoon onset, MJO and tropical circulation can have different (and opposite in sign) impact on model projected rainfall changes and there is large spread in the skill of models in simulating these processes. Additionally, there is some inconsistency between model results for historical periods and observations. In 2030, the range of projected changes differs little from that expected due to natural variability (*high confidence*).

RANGELANDS

Annually, and in summer and autumn, rainfall averaged across the Rangelands cluster is dominated by similar rain-bringing mechanisms to the northern Australia super-cluster (just discussed) and has similar projected changes from the GCMs. Under high forcing (RCP8.5 and 2090) the change in summer and autumn (and annual) rainfall could be substantial, but confidence in the direction of change is low for similar reasons to those stated for northern Australia.

Changes in winter (and to a lesser extent, spring) are influenced more by southern Australian rainfall processes and projected changes, as discussed above for the Southern Australian super-cluster. This is particularly the case for the southern portion of the cluster (Rangelands South) where rainfall decreases are strongly indicated in winter (associated with the southward retreat the mid-latitude storm systems) and to a lesser extent in spring.

The projections in the Rangelands are not greatly modified by the available downscaling, although the changes in summer simulated by CCAM tend to be more positive. Changes in rainfall associated with tropical cyclones, which can impact parts of the Rangelands, remain uncertain. Changes in all seasons in 2030 are small relative to natural variability (Table 7.2.1). The likely drying in the south, and little change in the north, leads to a likely southward shift across the Rangelands of the dominance of warm season rainfall (Figure 7.2.7).

In summary, decreases in winter rainfall are projected for the south, with *high confidence*, and become evident later in the century, especially under high forcing (2090 and RCP8.5). There is strong model agreement and good understanding of the physical mechanisms driving this change (southward shift of winter storm systems). Decreases are also projected for spring, but with *medium confidence* only. Changes to rainfall in other seasons, and annually, for later in the century are possible and potentially very important for this region, but the direction of change cannot be confidently projected given the spread of model results. In the near future (2030), there is *high confidence* that that natural variability will predominate over trends due to greenhouse gas emissions.

TABLE 7.2.2: SUMMARY OF RATIONALE FOR CONFIDENCE IN REGIONAL AND SUB-REGIONAL RAINFALL CHANGES (NA, EA, R AND SA SUPER-CLUSTERS, AND EXCEPTIONAL SUB-REGIONS), MEDIUM AND HIGH CONFIDENCE IN DECREASE IS INDICATED BY LIGHT AND ORANGE SHADING RESPECTIVELY, MEDIUM CONFIDENCE IN INCREASE WITH BLUE SHADING, MEDIUM CONFIDENCE IN LITTLE CHANGE WITH DARK GREY SHADING AND LOW CONFIDENCE ON THE DIRECTION OF CHANGE WITH LIGHT GREY SHADING. DJF=SUMMER, MAM=AUTUMN, JJA=WINTER, SON=SPRING. WINTER IN NORTHERN AUSTRALIA NOT SHOWN AS IT IS SEASONALLY DRY.

SEASON	SUB-REGIONAL EXCEPTION	2090 RCP85 CMIP5 RANGE OF CHANGE (%)	2090 RCP8.5 CMIP5 MODEL AGREEMENT (PERCENTS ARE FRACTION OF MODELS)	ADDITIONAL EVIDENCE: DOWNSCALING/CONSISTENCY OF OBSERVED TRENDS WITH GCMs	ADDITIONAL EVIDENCE: PLAUSIBLE PROCESSES/MODEL RELIABILITY	AGREEMENT OF MULTIPLE LINES OF EVIDENCE	SUMMARY STATEMENT WITH CONFIDENCE	DO THE GCM RESULTS PROVIDE A RANGE OF CHANGE FOR USE IN APPLICATIONS
SOUTHERN AUSTRALIA								
ANNUAL		-26 to +4	<i>Medium agreement in substantial decrease</i> (69%)	Downscaling generally agrees, obs. trend not inconsistent	Related to cool season circulation change, e.g. well supported southward shift of westerlies, strengthening of subtropical ridge. Relevant GCM processes reasonable	Good	Medium confidence in decrease	Yes
DJF		-13 to +16	<i>High agreement in little change</i> (71%), but also substantial increase (18%) & decrease (11%).	Downscaling generally agrees, obs. trend not inconsistent	Balance of tropical and mid-latitude influences not certain	Good, but process understanding less certain	Medium confidence in little change	Possibly too narrow, less relevant for Western Tasmania
MAM	WESTERN TASMANIA (SSTW)	-26 to +6	<i>Medium agreement in substantial decrease</i> (63%).	Downscaling generally agrees, obs. trend not inconsistent	Region well exposed to SAM-related weakening westerlies Likely difference between east and west Tasmania	Good	Medium confidence in decrease	Yes
		-25 to +13	<i>Medium agreement in little change</i> (57%), but also substantial decrease (28%) & increase (15%).	Statistical downscaled decrease stronger in many subregions. Obs decrease stronger in some regions.	Balance of tropical influences and strength cool season processes uncertain. Statistical downscaling suggests stronger influence of cool season trend than in GCMs.	Some disagreement	Low confidence in direction of change	GCM range may be biased high
	SOUTH-WESTERN VICTORIA (SSVW)	-30 to +15	<i>Medium agreement in little change</i> (52%), but also substantial decrease (35%) & increase (12%).	Downscaling decrease stronger in SW Vic and more consistent with observed drying	Predominance of cool season southward shift of westerlies and increasing intensity of subtropical ridge	Some disagreement	Medium confidence in decrease	GCM range likely to be biased high. SDM downscaling preferable
JJA		-32 to -2	<i>High agreement in substantial decrease</i> (80%).	Downscaling generally agrees, obs. trend not inconsistent	Related to cool season circulation change, e.g. well supported southward shift of westerlies and related storms. Relevant GCM processes reasonable	Good	High confidence in a decrease	Yes, except in Tasmania
	WESTERN TASMANIA (SSTW)	-6 to +20	<i>Medium agreement in increase</i> (64%).	Downscaling generally agrees, obs. trend not inconsistent	Related to strengthening and moistening of westerlies at this latitude (reasonable evidence)	Good	Medium confidence in an increase	Yes
	EASTERN TASMANIA (SSTE)	-11 to +19	<i>Medium agreement in increase</i> (62%).	Downscaling generally agrees, obs. trend not inconsistent	Related to strengthening and moistening of westerlies at this latitude (reasonable evidence)	Good	Medium confidence in increase	Downscaling will better reveal likely east-west contrast
SON		-44 to -3	<i>High agreement in substantial decrease</i> (79%).	Downscaling generally agrees, obs. trend not inconsistent	Related to cool season circulation change, but increasing tropical influences. Shift in IOD would cause drying	Good, but process understanding less certain	High confidence in decrease	Yes



SEASON	SUBREGIONAL EXCEPTION	2090 RCP85 CMIP5 RANGE OF CHANGE (%)	2090, RCP8.5 CMIP5 MODEL AGREEMENT (PERCENTS ARE FRACTION OF MODELS)	ADDITIONAL EVIDENCE: DOWNSCALING/CONSISTENCY OF OBSERVED TRENDS WITH CCMS	ADDITIONAL EVIDENCE: PLAUSIBLE PROCESSES/MODEL RELIABILITY	AGREEMENT OF MULTIPLE LINES OF EVIDENCE	SUMMARY STATEMENT WITH CONFIDENCE	DO THE GCM RESULTS PROVIDE A RELEVANT RANGE OF CHANGE FOR USE IN APPLICATIONS
--------	-----------------------	--------------------------------------	--	---	--	---	-----------------------------------	---

EASTERN AUSTRALIA

ANNUAL		-25 to +12	<i>Med. agreement in substantial decrease</i> (52%), but also substantial increase (2.1%).	Downscaling generally agrees, obs. trend is not strong.	Balance of tropical and mid-latitude influences not certain	Some disagreement	Low confidence in direction of change	Yes
DJF		-16 to +28	<i>Medium agreement in little change</i> (61%), but also substantial increase (27%) & decrease (13%).	Downscaling does not agree, obs. trend is not strong.	GCMs may not adequately represent the influence of Eastern Seaboard topography on the summer trade winds in producing rainfall	Not good agreement	Low confidence in direction of change	Possibly too narrow, with greater positive changes possible
MAM		-33 to +26	<i>Medium agreement in little change</i> (55%), but also substantial decrease (28%) & increase (17%).	Downscaling agrees, obs. trend is not strong.	Projected changes in physical processes are more difficult for 'shoulder seasons' than summer/winter.	Good, but process understanding less certain	Low confidence in direction of change	Yes
JJA		-40 to +7	<i>Medium agreement in substantial decrease</i> (53%).	Downscaling and obs. generally agree.	Related to southward shift of westerlies and fewer East Coast Lows.	Good	Medium confidence in a decrease	Yes
SON		-41 to +8	<i>Medium agreement in substantial decrease</i> (57%).	Downscaling does not agree, obs. trend is not strong.	Projected changes in physical processes are more difficult for 'shoulder seasons' than summer/winter.	Not good agreement	Low confidence in direction of change	Possibly too narrow, with greater positive changes possible
	COASTAL SE QLD (ECN)	-53 to +3	<i>Medium agreement in substantial decrease</i> (64%).	Downscaling does not agree (indicates little change or an increase), obs. trend is not strong.	Projected changes in physical processes are more difficult for 'shoulder seasons' than summer/winter. Projected windspeed increase reduces confidence in rainfall decrease	Not good agreement	Low confidence in direction of change	Possibly too narrow, with greater positive changes possible



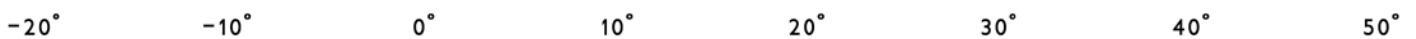
SEASON	SUBREGIONAL EXCEPTION	2090 RCP85 CMIP5 RANGE OF CHANGE (%)	2090 RCP8.5 CMIP5 MODEL AGREEMENT (PERCENTS ARE FRACTION OF MODELS)	ADDITIONAL EVIDENCE: DOWNSCALING/CONSISTENCY OF OBSERVED TRENDS WITH GCMs	ADDITIONAL EVIDENCE: PLAUSIBLE PROCESSES/MODEL RELIABILITY	AGREEMENT OF MULTIPLE LINES OF EVIDENCE	SUMMARY STATEMENT WITH CONFIDENCE	DO THE GCM RESULTS PROVIDE A RANGE OF CHANGE FOR USE IN APPLICATIONS
NORTHERN AUSTRALIA								
ANNUAL		-26 to +23	Low agreement in direction of change (51% decrease), but substantial decrease (37%) & increase (32%) possible.	BOM-SDM Statistical Downscaling generally agrees well; CCAM Downscaling disagrees over Wet Tropics (large decreases).	Competing processes with opposite impact on model projected rainfall changes contribute to uncertainty. May also be sensitive to aerosol forcing. Large model spread in skill of simulating processes involved such as Monsoon onset, MJO and tropical circulation. Also, GCMs may not adequately represent the influence of Eastern Seaboard topography on rainfall.	Some disagreement	Low confidence in direction of change	Yes
DJF		-2.4 to +1.8	Low agreement in direction of change (56% of increase), but substantial increase (42%) & decrease (29%) possible.	BOM-SDM Statistical Downscaling generally agrees – CCAM downscaling disagrees in North-east and Wet Tropics. Observed trend is inconsistent or not captured in many GCMs.	Balance of tropical and mid-latitude influences not certain	Good, but process understanding less certain	Medium confidence in little change	Possibly too narrow, less relevant for Western Tasmania
	MONSOONAL NORTH WEST (MNW)	-2.4 to +1.8	Medium agreement in increase (64%).	Both types of Downscaling generally agree. Observed trend is inconsistent or not captured in many GCMs.	As above.	Some disagreement	Low confidence in direction of change	Yes
MAM		-3.0 to +2.6	Medium agreement in little change (37%), but substantial decrease (33%) and increase (31%) possible.	Both Downscaling generally agree in north-west but disagree in North-east and Wet Tropics.	GCMs vary in their response – some favouring an early, other a late monsoon season retreat – depending on each models circulation changes - contributing to spread either side. Also, GCMs may not adequately represent the influence of Eastern Seaboard topography on rainfall.	Some disagreement	Low confidence in direction of change	GCM range may be biased high
SON		-4.4 to +4.4	Medium agreement in decrease (64%).	BOM-SDM Statistical Downscaling generally agrees. Observed trend is inconsistent in many GCMs.	GCMs vary in their response – some favouring an early, other a late monsoon season retreat – depending on each models circulation changes - contributing to spread either side.	Some disagreement	Low confidence in the direction of change	Yes
	MONSOONAL NORTH EAST (MNE)	-6.2 to +2.4	Medium agreement in substantial decrease (53%), but substantial increase is possible (11%).	CCAM downscaling disagrees. Observed trend is inconsistent in many GCMs.	Changes in surface pressure along North-east coastal regions supports changes to easterly trade regime circulation.	Some disagreement	Low confidence in the direction of change	Yes



SEASON	SUBREGIONAL EXCEPTION	2090 RCP85 CMIP5 RANGE OF CHANGE (%)	2090 RCP8.5 CMIP5 MODEL AGREEMENT (PERCENTS ARE FRACTION OF MODELS)	ADDITIONAL EVIDENCE: DOWNSCALING/CONSISTENCY OF OBSERVED TRENDS WITH GCMS	ADDITIONAL EVIDENCE: PLAUSIBLE PROCESSES/MODEL RELIABILITY	AGREEMENT OF MULTIPLE LINES OF EVIDENCE	SUMMARY STATEMENT WITH CONFIDENCE	DO THE GCM RESULTS PROVIDE A RELEVANT RANGE OF CHANGE FOR USE IN APPLICATIONS
--------	-----------------------	--------------------------------------	---	---	--	---	-----------------------------------	---

RANGELANDS

ANNUAL		-32 to +18	<i>Low agreement in direction of change</i> (59% decrease), but also substantial decrease (41%) and increase (22%)	Observed northern trends not well explained but indicate substantial changes are possible	Influence of low-latitude sea surface temperatures evident in observed ENSO, and variations in long-term trends among models.	Some disagreement	Low confidence in direction of change	Yes
DJF		-22 to +25	<i>Low agreement in direction of change</i> (52% increase), but also substantial decrease (36%) and increase (33%)	As above	As above	As above	Low confidence in direction of change	Yes
MAM		-42 to +32	<i>Medium agreement in little change</i> (54%), but also substantial increase (28%) and decrease (19%)	As above	As above	As above	Low confidence in direction of change	Yes
JJA		-50 to +18	<i>Medium agreement in substantial decrease</i> (61%), but also substantial increase (14%)	See RS discussion below	See RS discussion below	Good for southern rainfall, although will some variation in modelled cool season circulation trends	Medium confidence in a decrease	Yes
	RANGELANDS (RS)	-46 to +1	<i>Medium agreement on substantial decrease</i> (61%)	Observed trends in south partially attributable to forced change, but also indicate substantial changes are possible,	Potential for cool season retreat of westerlies to drive seasonal rainfall trend in south-west and south-east evident from both observations and model trends.	Good for southern rainfall, although will some variation in modelled cool season circulation trends	High confidence in a decrease	Yes
SON		-50 to +23	<i>Medium agreement in decrease</i> (68%)	Observed changes not inconsistent	Influence of IOD-like trends is evident from both observations and models. Also still some potential for cool season circulation changes affecting the south	Good for southern rainfall, although will some variation in modelled cool season circulation trends	Medium confidence in a decrease	Yes



7.2.2 PROJECTED EXTREME RAINFALL CHANGE

EXTREME RAIN EVENTS ARE PROJECTED TO BECOME MORE INTENSE

Extreme rainfall events (wettest day of the year and wettest day in 20 years) are projected to increase in intensity with *high confidence*. Confidence is reduced to *medium confidence* for south-western Western Australia, where the reduction in mean rainfall may be so strong as to significantly weaken this tendency.

As the atmosphere warms, its capacity to hold moisture increases, enhancing the potential for extreme rainfall events and the risk of flooding and erosion events. However, changes in the atmospheric circulation patterns that trigger heavy rainfall events could also change, thereby either enhancing or partially offsetting this effect. Studies of the observed record of extreme rainfall in Australia show some evidence of an increase in rainfall extremes (see Section 4.2.1).

Various studies prior to CMIP5 have noted a tendency for an increase in the intensity and/or the proportion of rainfall in extreme categories, with this being most strongly evident where mean rainfall is projected to increase, but often also evident elsewhere (Alexander and Arblaster, 2009, Rafter and Abbs, 2009). Fine-scale regional modelling based on CMIP3 GCMs shows a tendency for short duration (sub-daily) rainfall to increase more rapidly than longer duration (daily and multi-day) rainfall (Abbs and Rafter, 2009, IPCC, 2012), indicating an increase in extreme rainfall across Australia, but with only *low confidence*.

The CMIP5 results also simulate a strong tendency for an increase in various indices of extreme rainfall in the Australian region. This Report demonstrates this change using the simulated annual maximum daily rainfall, and the estimate (using GEV analysis) of the 20-year return value of the annual maximum. The latter represents changes to rare extremes, which are particularly relevant to studies of flood occurrence. The results shown are from a subset of twenty-one CMIP5 models for which the relevant data were available. Figures 7.2.12 and 7.2.13 show projected changes in the wettest day in 20 years for 2090 alongside those for annual mean and annual wettest day for three RCPs and the four super-cluster regions (Figure 7.2.12) and for RCP8.5 for each of the sub-regions (Figure 7.2.13). These results were calculated point by point and then area-averaged.

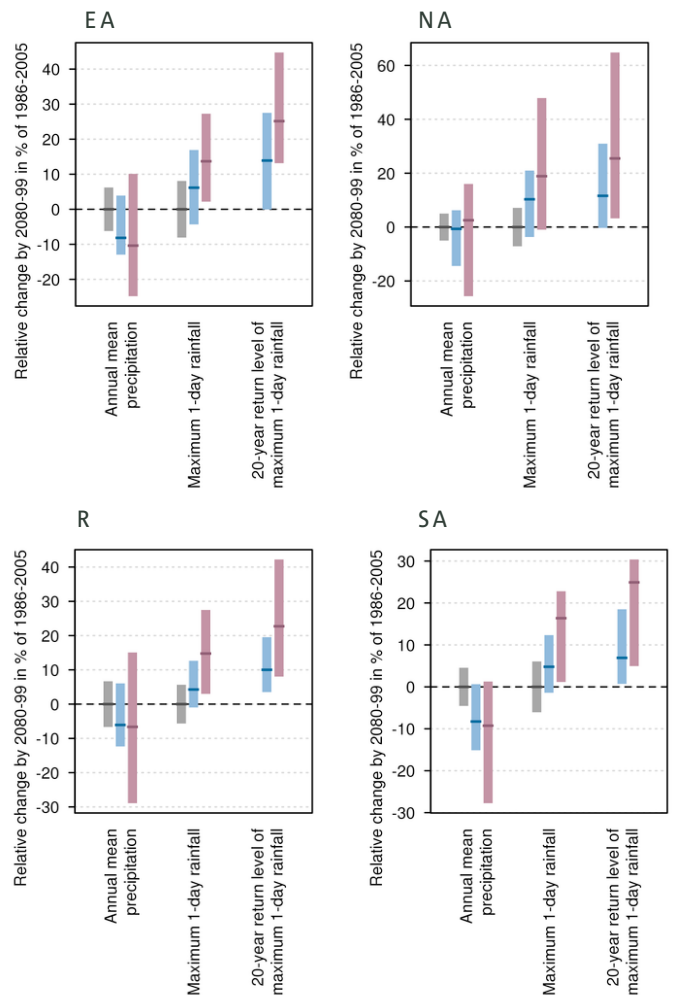


FIGURE 7.2.12: CHANGES TO EXTREME RAINFALL. FOR EACH PANEL FROM LEFT: PROJECTED CHANGE IN 2080–99 FOR ANNUAL MEAN PRECIPITATION, ANNUAL MAXIMUM 1-DAY RAINFALL, AND 20-YEAR RETURN LEVEL OF ANNUAL MAXIMUM 1-DAY RAINFALL IN PERCENT OF THE 1986–2005 AVERAGE. THE HORIZONTAL TICK DENOTES THE MEDIAN AND THE BAR DENOTES THE 10TH TO 90TH PERCENTILES OF THE CMIP5 RESULTS. THE SCENARIOS FROM LEFT TO RIGHT ARE: NATURAL VARIABILITY ONLY (GREY), RCP4.5 (BLUE), AND RCP8.5 (PURPLE). NATURAL VARIABILITY ONLY IS NOT SHOWN FOR THE 20-YEAR RETURN LEVELS. RESULTS ARE SHOWN FOR NORTHERN AUSTRALIAN (NA), EASTERN AUSTRALIAN (EA), RANGELANDS (R) AND SOUTHERN AUSTRALIAN (SA) SUPER-CLUSTERS.



Projections for relative precipitation change from 1986–2005 to 2080–99 according to RCP8.5 for both the annual mean and annual extremes

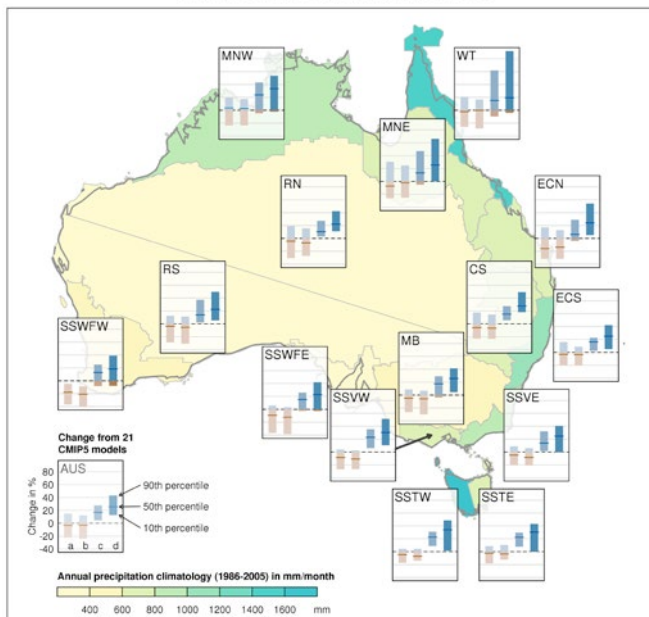


FIGURE 7.2.13: MEDIAN AND 10TH TO 90TH PERCENTILE RANGE OF PROJECTED CHANGE IN DAILY RAINFALL FOR 2080–2099 RELATIVE TO 1986–2005 FOR RCP8.5. SHOWN IN EACH BOX FROM LEFT TO RIGHT IS (A) THE ANNUAL MEAN FOR THE LARGER SET OF 39 MODELS, AS WELL AS (B) THE ANNUAL MEAN RAINFALL, (C) THE ANNUAL WETTEST DAY, AND (D) THE 20 YEAR RETURN LEVEL OF THE ANNUAL WETTEST DAY RAINFALL CALCULATED FROM A CONSISTENT SUBSET OF 21 CMIP5 MODELS. BLUE INDICATES INCREASE AND BROWN DECREASE. THE AUSTRALIAN AVERAGE RESULT IS SHOWN AT BOTTOM LEFT.

The results show a marked tendency for an increase in the annual maximum one day rainfall. This is most evident under high forcing (2090 and RCP8.5), and least evident or absent under RCP2.6 (not shown). The increasing tendency is also present (although small) in 2030 (not shown). The increase under high forcing contrasts markedly with the median change in annual rainfall, which shows little change or a decrease in most cases. Indeed, even in the sub regional analysis (Figure 7.2.13), the median projected change in the annual maximum rainfall is positive in all sub-regions, including sub-regions with a strong decrease in mean rainfall, such as south-west WA.

Projected change in the 20-year return value of the annual maximum rainfall is generally even more consistently positive, and of greater magnitude, than the change in the annual maximum rainfall (Figures 7.2.12 and 7.2.13). Confidence in this result is increased through noting that the full 10th to 90th percentile range of results shows a positive change in many cases. This tendency is more strongly evident in southern Australia and its sub-regions. Increases in the magnitude of this event are around 25 %

under RCP8.5 in 2090. Such increases in the magnitude of 20-year return period events could alternatively be viewed as these events occurring with greater frequency than in the baseline climate.

In summary, the agreement between theoretical expectations, a wealth of previous research and the CMIP5 results means that *high confidence* can be placed in a projection of a future trend toward increases in the intensity of extreme rainfall events (wettest day of the year, on average, and rarer events) throughout most of Australia. Confidence should be reduced to '*medium confidence*' only for south-west WA, where the reduction in mean rainfall may be so strong as to significantly weaken this tendency. It is also important to note that the interpretation of GCM-based extreme rainfall change in quantitative terms is more problematic because of the very large difference in spatial scale between typical extreme rainfall events in the real world and what the GCMs are able to simulate. This means that the magnitude of regional GCM-based extreme rainfall changes are of '*low confidence*' and should be treated as indicative only.

7.2.3 DROUGHT

TIME IN DROUGHT IS PROJECTED TO INCREASE IN SOUTHERN AUSTRALIA, WITH A GREATER FREQUENCY OF SEVERE DROUGHTS

The time in drought is projected to increase over southern Australia with *high confidence*, consistent with the projected decline in mean rainfall. Time in drought is projected to increase with *medium* or *low confidence* in other regions. The nature of droughts is also projected to change with a greater frequency of extreme droughts, and less frequent moderate to severe drought projected for all regions (*medium confidence*).

The previous projections using CMIP3 models (CSIRO and BOM, 2007), indicated that more drought (based on annual rainfall below the 5th percentile) would be likely, and occurring over larger areas, in south-west Australia, Victoria and Tasmanian regions, with little detectable change in the other regions (Hennessy *et al.* 2008). Similar results were also found when the projections were based on analyses of exceptionally low soil moisture (Hennessy *et al.* 2008) and an index involving the ratio between rainfall and potential evapotranspiration (Kirono *et al.* 2011b).

To study how drought might change under increasing greenhouse gases, this Report analyses the Standardised Precipitation Index (SPI, see Box 7.2.1), based on monthly rainfall simulated by CMIP5 GCMs. A brief description about the method used to generate the SPI and to define drought events is provided in Box 7.2.1, which also describes the three measures of drought characteristics reported here, namely drought proportion (or time in drought), frequency, and duration.

Figure 7.2.14 shows the regional average of drought proportion, which is a fraction of the time in drought during each 20 year period for each super-cluster region. The multi-model median indicates a drought proportion of around 35 % (in Rangelands and Northern Australia) to 39 % (in Eastern Australia and Southern Australia) during the 20-year period centred on 1995 (1986-2005), and an increase of roughly 5 to 20 % in the future, depending on the RCP. The bars representing the uncertainty range are relatively large, but they tend to be above the baseline level (1995) and hence suggest a high model agreement on the increase especially over the Southern Australia region. Other regions show a larger mix of results (i.e. between increase and decrease).

Regarding the drought frequency, which is the number of drought events in a 20 year period, the models indicate a decrease for moderate and severe drought but an increase for extreme drought in the future (Figure 7.2.15). Noteworthy is the high agreement among models and emission scenarios. In general, similar results are found in all four NRM super-cluster regions, but with the uncertainty range indicating an increase through to little change for extreme drought, except in Southern Australia where all models indicate an increase (not shown).

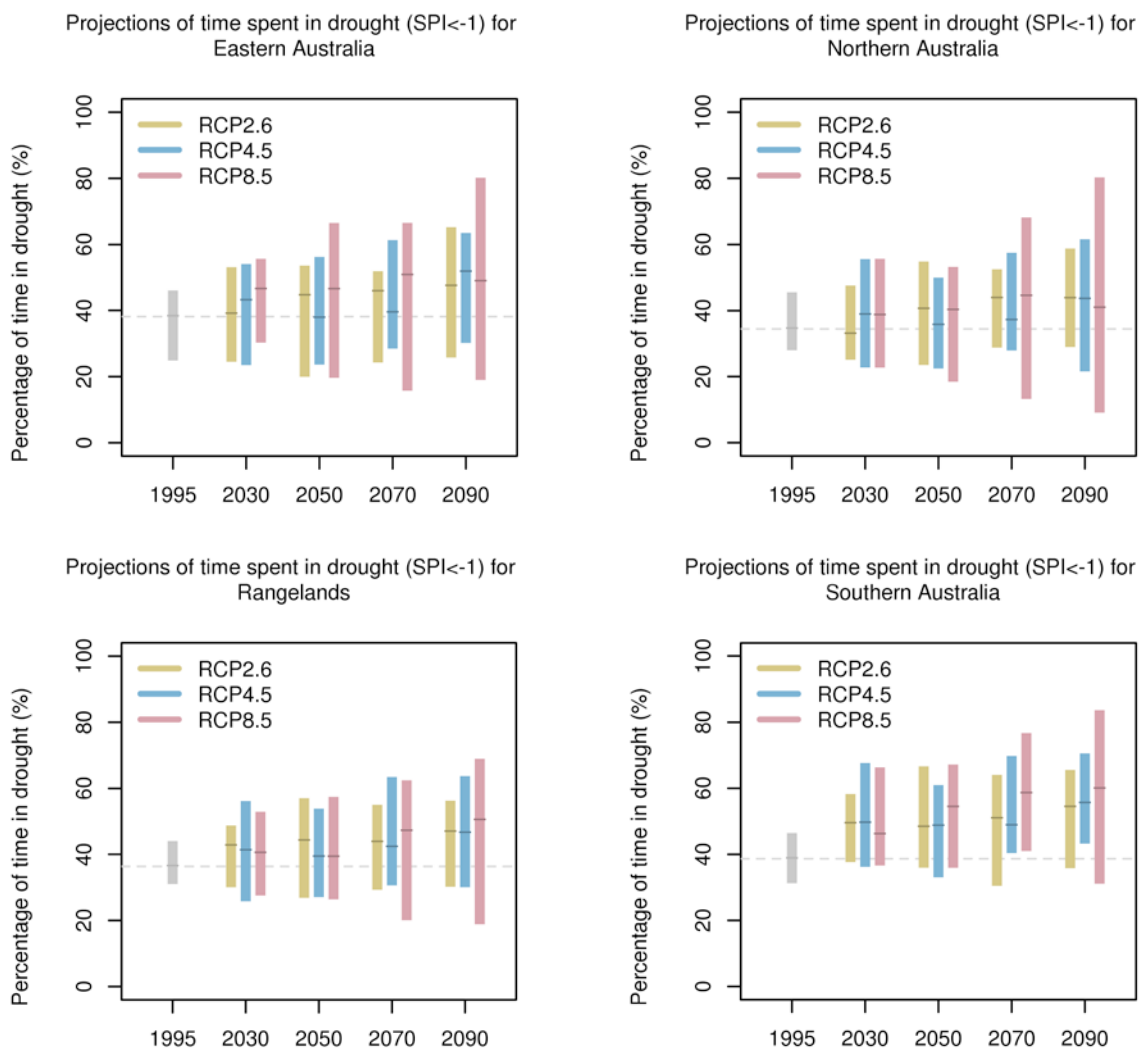


FIGURE 7.2.14: MEDIAN AND 10TH TO 90TH PERCENTILE RANGE IN PROJECTED CHANGE IN PROPORTION OF TIME SPENT IN DROUGHT FOR FIVE 20-YEAR PERIODS. RESULTS ARE SHOWN FOR NATURAL VARIABILITY (GREY), RCP2.6 (GREEN), RCP4.5 (BLUE) AND RCP8.5 (PURPLE) FOR SUPER-CLUSTERS. PROPORTION OF THE TIME IN DROUGHT IS DEFINED AS ANY TIME THE SPI IS CONTINUOUSLY (GREATER THAN OR EQUAL TO 3 MONTHS) NEGATIVE AND REACHES AN INTENSITY OF -1.0 OR LESS AT SOME TIME DURING EACH EVENT (SEE ALSO BOX 7.2.1).



For drought duration, little change is projected in moderate and severe drought but an increase for duration in extreme drought (Figure 7.2.16). For extreme drought, in particular, the multi-model agreement is high, with the largest changes occurring for RCP8.5. Overall, the results for all NRM super-clusters are relatively similar (not shown).

In assessing confidence in these projections, we note that at the global scale the CMIP5 models can reproduce both the observed influence of ENSO on drought over land and the observed global mean aridity trend (Dai, 2013), and that Australia-wide observation-based data always fall within the range of the models' ensemble (Orlowsky and Seneviratne, 2013). The projected increase in time

in drought is consistent with the general tendency for reduced annual rainfall (Section 7.2 and Appendix A), but this tendency is weak in the north. Moreover, there is consistency with the observed increase over the north-east coast, south-east coast and Murray-Darling Basin during 1960-2009 (Gallant *et al.* 2013). The overall increase in the time in drought is also consistent with CMIP3-based studies (Hennessy *et al.* 2008, Kirono *et al.* 2011b). In summary, the drought proportion can be expected with *high confidence* to increase over Southern Australia (and at the cluster level, over SSWF, see Cluster Reports), and with *medium confidence* for the rest of the country except Northern Australia where the increase is with *low confidence*.

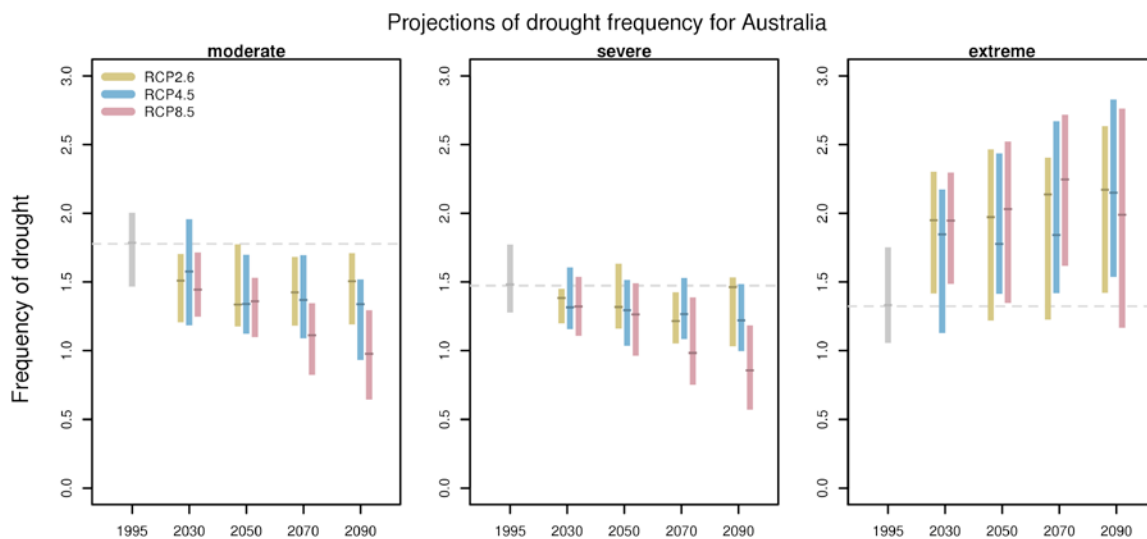


FIGURE 7.2.15: MEDIAN AND 10TH TO 90TH PERCENTILE RANGE OF CHANGE IN AVERAGE DROUGHT FREQUENCY IN AUSTRALIA FOR THREE DROUGHT CATEGORIES AND FOR FIVE 20-YEAR PERIODS. THE DROUGHT FREQUENCY IN A CATEGORY IS THE NUMBER OF EVENTS IN THIS CATEGORY OCCURRING IN THE 20-YEAR PERIOD (SEE ALSO BOX 7.2.1).

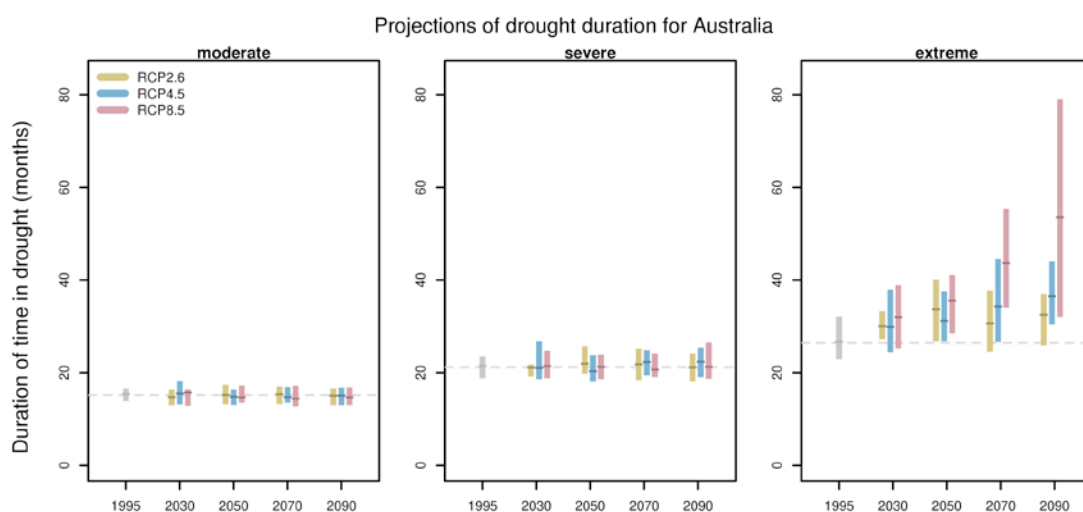


FIGURE 7.2.16: MEDIAN AND 10TH TO 90TH PERCENTILE RANGE OF PROJECTED CHANGE IN THE AVERAGE DURATION OF DROUGHTS IN AUSTRALIA FOR THREE DROUGHT CATEGORIES AND FOR FIVE 20-YEAR PERIODS. DROUGHT DURATION MEASURES THE AVERAGE LENGTH (IN MONTHS) OF A DROUGHT EVENT IN A GIVEN CATEGORY WITHIN A GIVEN 20-YEAR PERIOD (SEE ALSO BOX 7.2.1).

The projections of change to the frequency and duration of drought presented here are consistent with the observed trends as shown in Gallant *et al.* (2013), as well as the indication that ENSO events will intensify as a result of global warming and may cause an intensification of El Niño-driven drying in Australia (Power *et al.* 2013). However, Ault *et al.* (2012) report that CMIP3 and CMIP5 climate models tend to overestimate the magnitude of high frequency fluctuations, and underestimate the risk of future decadal-scale droughts, thus reducing the confidence in projections.

In summary, there is *medium confidence* in less frequent moderate and severe droughts and *medium confidence* in more frequent and longer extreme drought.

Note that this study uses a meteorological drought index which is based on rainfall only. Nicholls (2004) reported the important contribution of temperature (via evaporation) on drought in Australia. Also, see Section 7.7.1 where results demonstrating a decrease in soil moisture due to projected increases in potential evaporation are presented.

BOX 7.2.1: DROUGHT INDEX AND DEFINITION

Drought in general means acute water shortage. The primary cause of any drought is a lack of rainfall over an extended period of time, usually a season or more, resulting in a water shortage for some activities, groups, or sectors. The response of different entities (*e.g.* agricultural and hydrological systems) to water shortage conditions can vary substantially as a function of time scales and other socio-environmental conditions. As such, drought can be experienced and defined in many ways using various indices, which can be classified into meteorological, agricultural, and hydrological drought (Dai, 2011).

Different drought indices give different results so may result in somewhat different change patterns, especially on small scales (Seneviratne, 2012), and drought projections can be dependent on the choice of drought index (Burke and Brown, 2008, Taylor *et al.* 2013). Thus, any drought projection needs to be interpreted cautiously in the context of the drought index being used.

The standardized precipitation index (SPI, McKee *et al.* 1993, Lloyd-Hughes and Saunders, 2002) used in this Report, is based solely on rainfall. It is calculated by fitting a probability density function to the frequency distribution of a long-term (*i.e.* 1900–2005 for this Report) series of rainfall values, summed over the timescale of interest. In this Report, monthly data are used and the timescale of interest is 12 months, which is considered as the time required for water deficit conditions to affect various agricultural and hydrological systems (*e.g.* Szalai and Szinell, 2000, Zargar *et al.* 2011). Thus, each monthly value is the total rainfall for the previous 12 months. Subsequently, the probability distribution is transformed to a standardized normal

distribution. Negative SPI values are indicative of dryness while positive values are indicative of wetness. In addition, the SPI over 1900–2005 has a mean of zero and standard deviation of one, due to the normalisation. Table B7.2.1 provides the classification system to define drought intensities. In this case, a drought event occurs any time the SPI is continuously (greater than or equal to 3 months) negative and reaches an intensity of -1.0 or less at some time during each event (See Figure B7.2.1). The drought begins when the SPI first falls below zero and ends with the first positive value of SPI following a value of -1.0 or less (McKee *et al.* 1993).

This Report describes characteristic of drought for each of the five time periods: 1995 (1986–2005); 2030 (2020–2039); 2050 (2040–2059); 2070 (2060–2079); and 2090 (2080–2099). The characteristics of drought are represented by three measures. The first is drought proportion, which is calculated as the fraction of the time (20-years period) in drought. The second is drought frequency, which is defined as the number of droughts in a given 20-year period. The third, drought duration, measures the average length (in months) of a drought event for the selected period.

TABLE B7.2.1: DROUGHT CATEGORY BASED ON STANDARDISED PRECIPITATION INDEX (MCKEE ET AL. 1993, LLOYD-HUGHES AND SAUNDERS, 2002, DAI, 2011).

SPI VALUE	DROUGHT CATEGORY
0 to -0.99	Near normal
-1.00 to -1.49	Moderate
-1.50 to -1.99	Severe
-2 or less	Extreme



BOX 7.2.1 DROUGHT INDEX AND DEFINITION

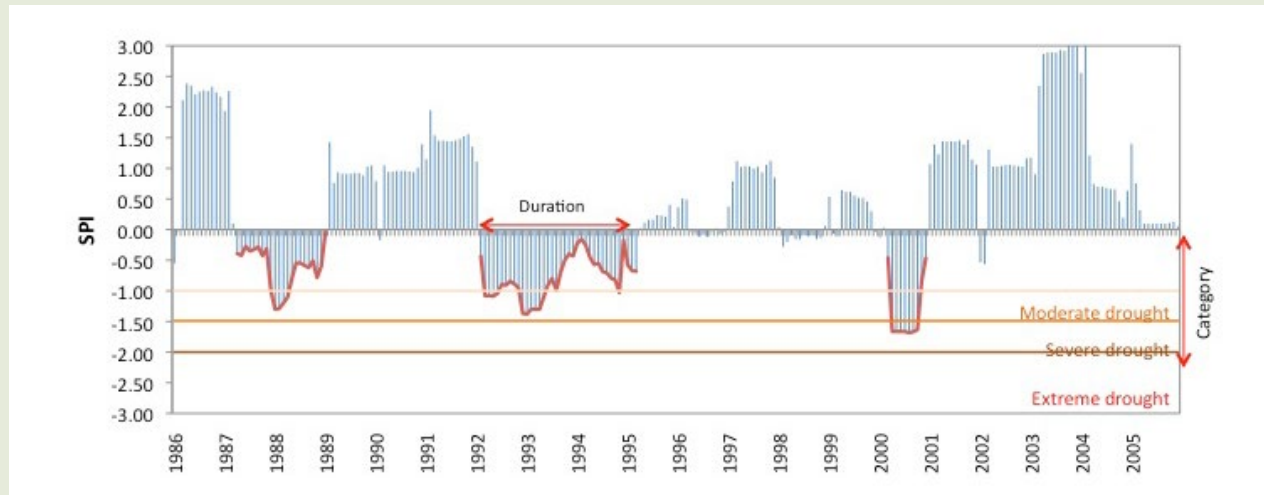


FIGURE B7.2.1: ILLUSTRATION OF A STANDARDISED PRECIPITATION INDEX (SPI) TIME SERIES AND THE ASSOCIATED DROUGHTS (RED-SOLID LINES) FOR A LOCATION WITHIN A 20-YEAR PERIOD. IN THIS EXAMPLE, THE SITE EXPERIENCES: (I) A DROUGHT PROPORTION OF 29 %; (II) TWO MODERATE DROUGHTS (WITH AN AVERAGE DURATION OF 30 MONTHS); AND (III) ONE SEVERE DROUGHT (WITH A DURATION OF 10 MONTHS).

7.2.4 SNOW

SNOWFALL IN THE AUSTRALIAN ALPS IS PROJECTED TO DECREASE, ESPECIALLY AT LOW ELEVATIONS

There is *very high confidence* that as warming progresses there will be a decrease in snowfall, an increase in snowmelt and thus reduced snow cover. These trends will be large compared to natural variability and most evident at low elevations.

The spatial resolution of global climate models is too coarse to represent snow-covered areas in the Australian Alps directly. The highest elevation in CMIP5 models for grid boxes in South-Eastern Australia representative of the Australian Alps is between 290m and 940m (most models' highest elevation is between 450m and 650m); hence no CMIP5 model can represent the snow covered Alpine area. Advanced off-line snow models are required to explore projections of snow conditions across the Australian Alps. These methods provide projections of snow depth, area and duration, and integrate changes in snowfall, melt and ablation (Hennessy *et al.* 2008, Hendrikx *et al.* 2013). Such calculations using the latest climate models dataset (CMIP5) are not available yet.

Projected changes in snowfall have been assessed using statistically downscaled CMIP5 climate model results. Accumulated precipitation falling on days where maximum temperature stays below 2 °C has been used to create an annual total of equivalent snowfall. This has been done using the Bureau of Meteorology analogue-based statistical downscaling approach applied to 22 of the CMIP5 models. The annual equivalent snowfall was computed for two locations: a 5 km grid box (148.40W, 35.95S, elevation 1419m) near Cabramurra (NSW) for which a long-term observed record of annual snow accumulation exists (Davis, 2013), and the highest 5 km grid box (148.40W, 36.15S, elevation 1923m). The two locations provide an insight into future changes in snowfall across a range of elevations spanning the area where snow is currently observed.

At these two locations (Figure 7.2.17), simulated snowfall showed a decline in the last 50 years. This observed snowfall decline is a component of the decline in snow accumulation observed at the Cabramurra station (Davis, 2013). The reduction in simulated snowfall is primarily due to warming rather than a decline in precipitation, *i.e.* an increase in the ratio of rain to snow. Davis (2013) also points to warming as being the primary reason for the observed decline in Cabramurra snow depth.

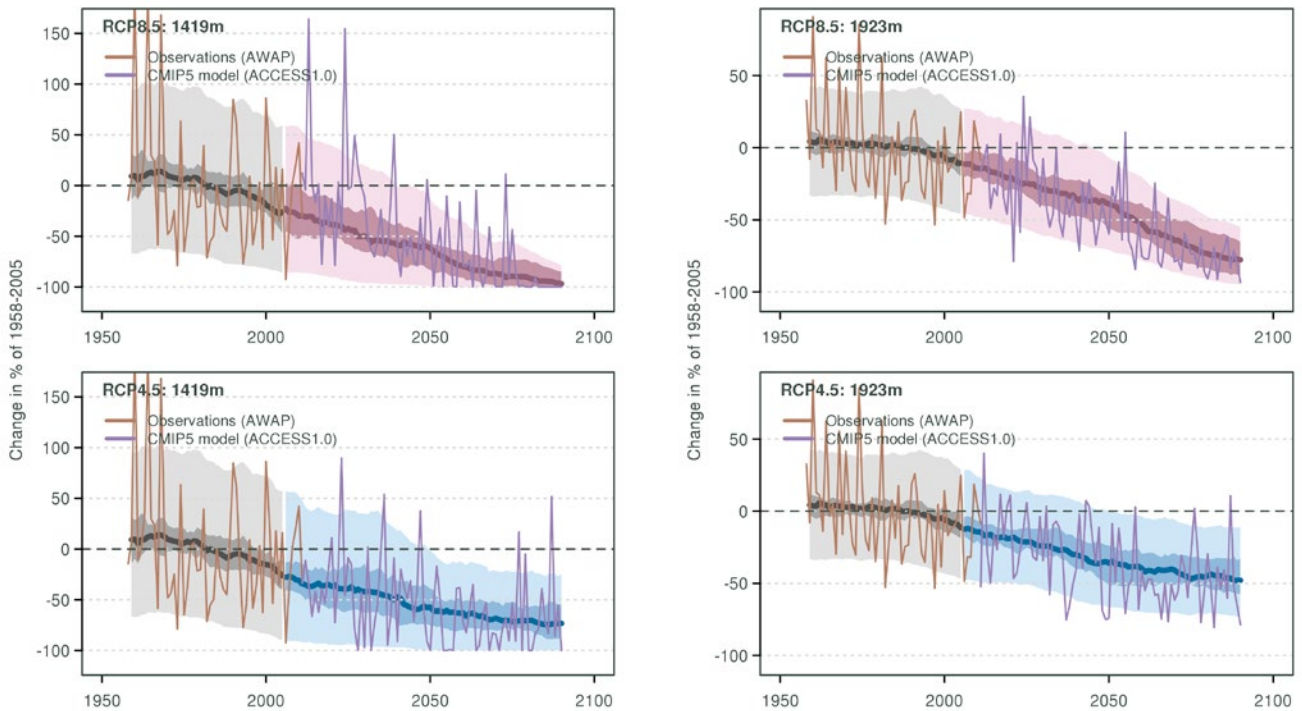


FIGURE 7.2.17: CHANGE IN SNOWFALL FOR TWO LOCATIONS IN THE BUREAU OF METEOROLOGY OPERATIONAL 5-KM GRIDDED OBSERVATIONS CORRESPONDING TO A LOW ELEVATION CONSISTENT WITH THE CURRENT SNOWLINE (LEFT GRAPHS) AND FOR THE HIGHEST ELEVATION IN THE GRIDDED OBSERVATIONS (RIGHT GRAPH). FUTURE PROJECTIONS FROM 2006 ONWARD ARE PROVIDED FOR THE RCP8.5 (TOP GRAPHS) AND RCP4.5 (BOTTOM GRAPH). EACH PANEL SHOWS THE MODEL ENSEMBLE MEDIAN (THICK LINE), THE 10TH TO 90TH PERCENTILE OF ANNUAL SNOWFALL (LIGHT SHADING) AND THE 10TH TO 90TH PERCENTILE OF 20-YEAR MEAN SNOWFALL (DARK SHADING), AWAP OBSERVATIONS (BROWN) AND AN EXAMPLE OF A POSSIBLE FUTURE TIME SERIES (LIGHT PURPLE) FROM A SINGLE MODEL (ACCESS-1.0).

Projections clearly show a continuing reduction in snowfall during the 21st century. The magnitude of decrease depends on the altitude of the region and on the emission scenario (Figure 7.2.17). At the low elevation grid box (1419m), years without snowfall start to be observed from 2030 in some models. By 2090, these years become common with RCP8.5. Figure 7.2.17 displays the result from a single downscaled model (ACCESS 1.0) illustrating how this model depicts interannual variability. It highlights the fact that with RCP4.5, while years without snowfall will become possible, years with normal snowfall (by today's standard) still occur at the end of the 21st century but less frequently. At the high elevation grid box (1923m), the reduction of snowfall is less in percentage terms, averaging about 50 % by 2090 with RCP4.5 and 80 % with RCP8.5.

These projections concern only snowfall, excluding the additional impacts of climate change on snow-melt and ablation. Hence the full picture in terms of snow depth, area and duration is not provided. Such advanced analysis was performed using temperature and precipitation projections from 18 CMIP3 climate models as input to the CSIRO snow model to estimate changes in snow conditions over Victoria for 20-year periods centred on 2020 and 2050, relative to a 20-year period centred on 1990 (Bhend *et al.* 2012). Results were calculated for each climate model for three different IPCC SRES greenhouse gas emissions scenarios: low (B1), medium (A1B) and high (A1FI).

Decreases in maximum snow depth are evident in all these simulations, but there is a wide range of uncertainty due to differences in projections between the 18 climate models

TABLE 7.2.3: SIMULATED ANNUAL-AVERAGE MAXIMUM SNOW-DEPTH (CM) AT FOUR SKI RESORTS FOR 20-YEAR PERIODS CENTRED ON 1990 AND 2050 FOR LOW (B1), MEDIUM (A1B) AND HIGH (A1FI) EMISSION SCENARIOS. THE RANGE OF DEPTHS REPRESENTS THE SPREAD OF RESULTS FROM 18 CMIP3 CLIMATE MODELS. SIMULATED SNOW-DEPTHS HAVE BEEN ROUNDED TO THE NEAREST 5 CM.

SITE	1980-1999	2040-2059		
		LOW EMISSIONS	MED EMISSIONS	HIGH EMISSIONS
FALLS CREEK	150	50-105	30-90	20-80
MT HOTHAM	130	40-95	25-80	15-70
MT BULLER	95	20-60	10-50	5-45
MT BUFFALO	60	10-30	5-25	0-20



(Table 7.2.3). For example, at Falls Creek ski resort, the simulated average maximum depth is 150 cm in the 20-year period centred on 1990. By 2020, the average maximum depth decreases to 80-135 cm for the three different emission scenarios. By 2050, the average maximum depth decreases to 50-105 cm for the low scenario and 20-80 cm for the high scenario. A decline in snow-cover is also simulated. For example, by 2020, the area of Victoria averaging at least 1 day of snow-cover decreases by 10-40 % across the three scenarios. By 2050, the area decreases by 25-55 % for the low scenario and 35-75 % for the high scenario. Across four ski resorts (Falls Creek, Mt Hotham, Mt Buller and Mt Buffalo), by 2020, the average snow season becomes 5-35 days shorter for the three scenarios. By 2050, the average snow season becomes 20-55 days shorter for the low scenario and 30-80 days shorter for the high scenario. Larger changes are likely at lower elevations, such as Mt Baw Baw and Lake Mountain, but projections for these sites were considered to be less robust.

In summary, there is *very high confidence* that as warming progresses there will be very substantial decreases in snowfall, increase in melt and thus reduced snow cover, with these trends being large compared to natural variability, especially under a high emissions scenario.

7.3 WINDS, STORMS AND WEATHER SYSTEMS

7.3.1 MEAN AND EXTREME WINDS

MEAN WIND SPEEDS ARE PROJECTED TO DECREASE IN SOUTHERN MAINLAND AUSTRALIA IN WINTER AND INCREASE IN TASMANIA

By 2030, changes in near-surface wind speeds are projected to be small compared to natural variability (*high confidence*). By 2090, wind speeds are projected to decrease in southern mainland Australia in winter (*high confidence*) and south-eastern mainland Australia in autumn and spring. Winter decreases are not expected to exceed 10 % under RCP8.5. Wind speed is projected to increase in winter in Tasmania. Projected changes in extreme wind speeds are generally similar to those for mean wind.

MEAN WINDS

Wind patterns in Australia are associated with the location and seasonal movement of broad-scale circulation systems, with westerlies south of the subtropical high pressure belt affecting southern Australia in winter, and trade wind south-easterlies to its north, and with monsoonal westerlies over the Top End in summer (Figure 7.3.1). Changes in wind

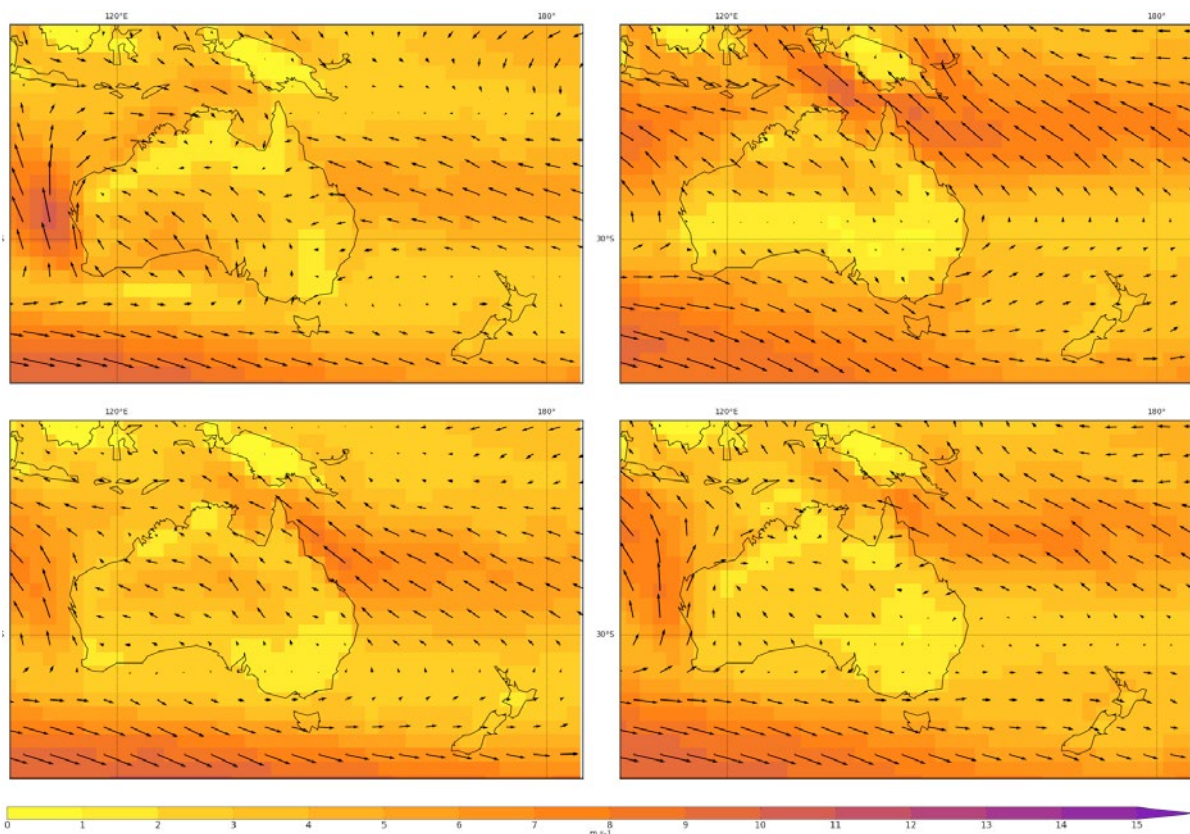


FIGURE 7.3.1: NCEP2 WINDS AVERAGED OVER 1986–2005 FOR SUMMER (DJF), AUTUMN (MAM), WINTER (JJA) AND SPRING (SON). COLOUR SCALE SHOWS WIND SPEED (UNITS ARE M/S) AND VECTOR ARROWS SHOW WIND SPEED AND DIRECTION.

-20° -10° 0° 10° 20° 30° 40° 50°

attributes (e.g. wind speed, direction and extremes) can have large biophysical and societal impacts in both the terrestrial and marine environments. In the terrestrial environment, changes to winds may have potential consequences for the agricultural and energy sectors and building codes. In the marine environment, winds influence waves, currents and coastal sea levels, which in turn affect coastal erosion, sediment transport, inundation and saltwater intrusion into coastal wetlands and aquifers. For example, changes in wind direction and storm-induced wind extremes associated with natural interannual climate cycles affect erosion/accretion patterns along eastern Australian beaches (Harley *et al.* 2010). Wind speeds near the surface undergo strong transition due to frictional effects such as terrain and vegetation (e.g. Troccoli *et al.* 2012, see also Section 4.2). The model-derived surface wind speeds reported in this Section are 10 m above the surface.

Assessment of wind changes in the CMIP5 models involved a smaller set of models than for other variables. This was primarily because wind speed data were not consistently archived by all modelling groups for all time periods required. In addition, inspection of wind speed changes revealed that a small number of models exhibited unusually large increases in some land areas compared to

surrounding areas. Inspection of other model variables suggested that the cause of the wind speed increases were related to large changes in surface roughness across the same small areas of the model. Since these changes were unusual compared to other adjacent regions in the model and compared to the majority of other models assessed, and because these large changes strongly influenced the results of some cluster regions, the particular models concerned were removed from the ensemble. The two models removed were IPSL-CM5A-MR, IPSL-CM5B-LR. This reduced the total number of models assessed for mean winds to 24 models compared with, for example, 39 models for mean rainfall change.

Projected wind speed differences by season in the CMIP5 models are illustrated for the four super-clusters in Figure 7.3.2 for 2030 and 2090 and three RCPs, and for each of the sub-clusters in Figure 7.3.3 for 2090 and RCP8.5. Wind speed differences expected due to natural variability are also indicated in both figures.

In the near future (2030), differences are mostly comparable to those expected due to natural variability, and thus represent little change. This can be seen in Figure 7.3.2 for the super-cluster averages, where these differences are

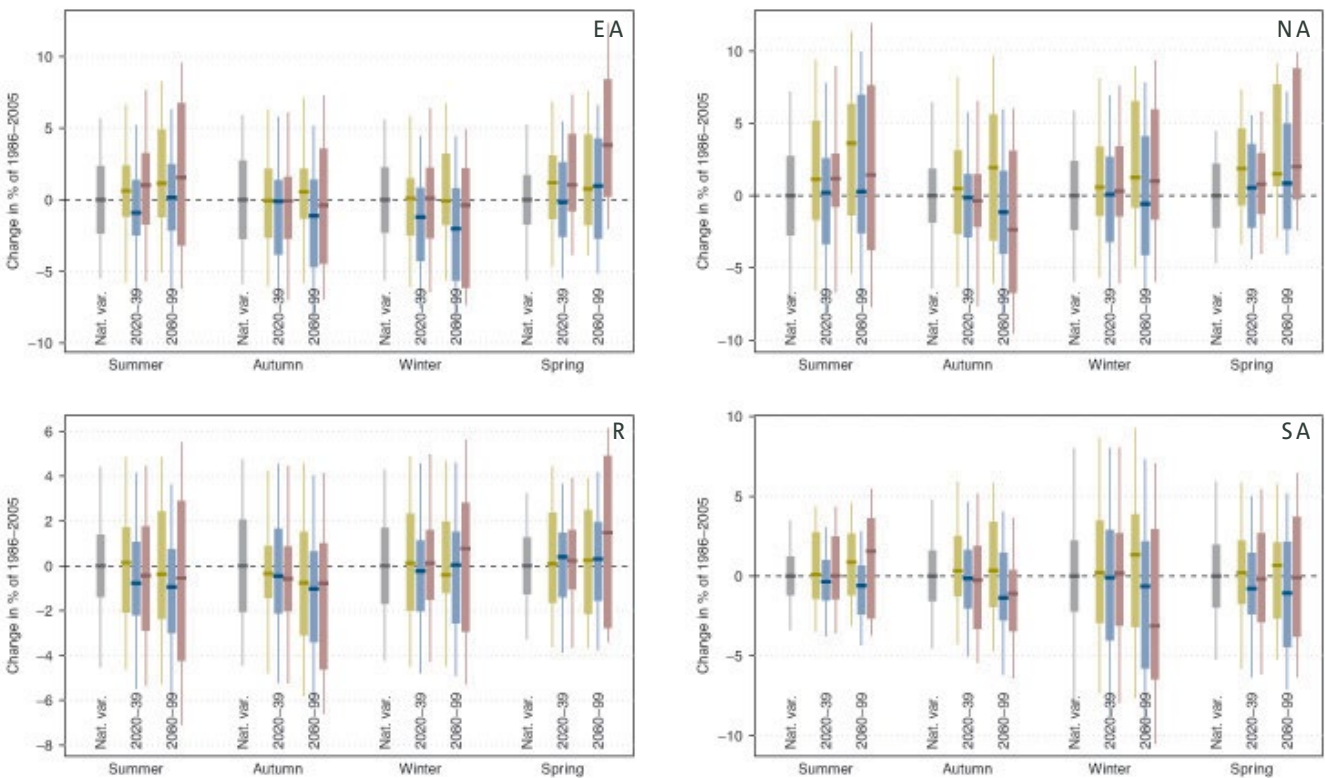


FIGURE 7.3.2: MEDIAN AND 10TH TO 90TH PERCENTILE RANGE OF PROJECTED CHANGE IN SEASONAL WIND SPEED (IN PERCENT) FOR 2020–2039 AND 2080–2099 RELATIVE TO THE 1986–2005 PERIOD (GREY BAR) FOR RCP2.6 (GREEN), RCP4.5 (BLUE) AND RCP8.5 (PURPLE). FINE LINES SHOW THE RANGE OF INDIVIDUAL YEARS AND SOLID BARS FOR TWENTY YEAR RUNNING MEANS. RESULTS ARE SHOWN FOR EASTERN AUSTRALIAN (EA), NORTHERN AUSTRALIAN (NA), RANGELANDS (R) AND SOUTHERN AUSTRALIAN (SA) SUPER-CLUSTERS.



mostly within $\pm 3\%$, although larger ranges are present at the sub-cluster level (not shown). By late in the century (2090) and under RCP8.5, changes become evident in some models, with greatest consistency on spring increases in Eastern Australia and winter decreases in Southern Australia. Changes at this large-scale exceed 5% in some models. This pattern of change is also clear in the sub-cluster results at 2090 and RCP8.5 (Figure 7.3.3) with the north-eastern cluster regions (MNE, WT, ECN, CS and RN), showing spring increase, and the southern mainland sub-cluster regions (CS, ECS, SSWFE and MB) showing winter decreases. The spring increase in the north extends to winter in MNE and WT. In the mainland south-east (SSWFE, SSVW, SSVE and MB), decreases are present in autumn and spring, as well as in winter. However, further south in the Tasmanian regions of SSTW and SSTE, there is a strong tendency for wind speed to increase in winter. Changes in 2090 under RCP8.5 are mostly in the range of $\pm 10\%$ and often less than $\pm 5\%$.

Projections for relative near-surface wind speed change from 1986–2005 to 2080–99 according to RCP8.5

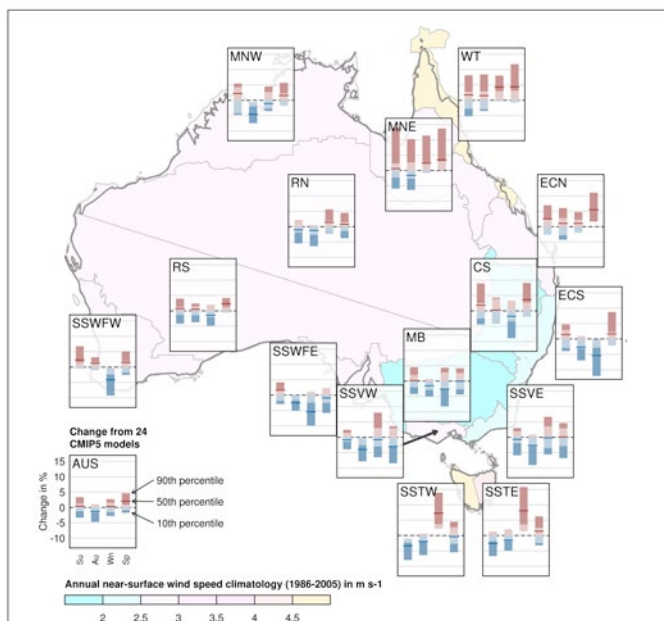


FIGURE 7.3.3: MEDIAN AND 10TH TO 90TH PERCENTILE RANGE OF PROJECTED CHANGE IN SEASONAL 10-M WIND SPEED (PERCENT) ACROSS 24 CMIP5 CLIMATE MODELS FOR EACH SEASON FOR R85 FOR 2080–2099 RELATIVE TO 1986–2005. RED INDICATES INCREASE AND BLUE DECREASE (SEE KEY) AND PALER PORTION OF THE BAR IS THE 10TH TO 90TH PERCENTILE RANGE EXPECTED FROM NATURAL VARIABILITY. THE WIND SPEED CLIMATOLOGY OVER THE 1986–2005 PERIOD IS INDICATED BY THE COLOUR OF THE SHADING ON THE MAP OF AUSTRALIA.

These findings are generally consistent with a previous assessment of wind change in an ensemble of 19 CMIP3 models over the period 2081–2100 relative to 1981–2000 forced by the SRES A1B emissions scenario (McInnes *et al.* 2011). In winter, there was agreement in at least two thirds of models of a general increase in wind speed over the tropical half of mainland Australia north of 30° S, on wind speed decrease between 30 and 40° S and wind speed increase south of 40° S. Overall, these changes were consistent with a projected increase in the trade wind easterlies to the north of 30° S, the southward movement of the subtropical ridge and a strengthening of the mid-latitude westerlies over the Southern Ocean. The seasonal movement of the subtropical ridge southward in summer means that the trade easterlies affect a greater part of the continent during this season (Figure 7.3.1). Future changes to this pattern projected for summer indicate that there was less agreement on the direction of wind speed change between the different models to the north of 30° S, a consistent increase in wind speed over the southern mainland coast and decreases over Tasmania.

In summary, in the near future (2030) changes to mean wind speed are projected to be small compared with natural variability (*high confidence*). However, late in the century under higher RCPs, a pattern of winter wind speed decrease across southern mainland Australia, autumn and spring decrease in south-eastern mainland Australia, and winter increase over Tasmania is projected. These changes are consistent with broad-scale patterns of circulation change and the winter changes are projected with *high confidence*. Earlier studies also pointed to stronger trade winds, but the current results show that tendency primarily in spring. The reason for this spring focus is not clear and this projection is of *low confidence*.

EXTREME WINDS

Extreme winds create hazardous conditions for marine and terrestrial activities and infrastructure. The intensity of extreme winds at the surface is strongly modified by terrain and vegetation, while over the ocean extreme winds lead to high ocean waves which in turn may modify the wind field. GCMs are not able to adequately resolve many small scale meteorological phenomena that contribute to extreme winds such as tropical cyclones, East Coast Lows or thunderstorm downbursts. Therefore, alternative approaches such as downscaling are needed to resolve such systems. This contributes to a general lowering of confidence on extreme wind changes (*e.g.* McInnes *et al.* 2011).

Extreme winds may be characterised by a variety of metrics such as high percentiles or return periods. Here, two extreme wind metrics were calculated; the average of the annual maximum wind speed over the twenty years of data and an estimate of the 20-year return period of the annual maximum calculated using GEV analysis.

Since daily-maximum winds were not available from the CMIP5 archive, extreme wind metrics were evaluated from the daily-averaged wind speed data. Furthermore,

because daily-averaged wind speed was archived in a smaller number of models than daily-averaged zonal and meridional (westerly and northerly) components of wind speed, daily wind speed was recalculated from daily-average wind speed components, so as to make most use of the available the model output. Using the daily averaged wind speed components to produce wind speeds leads to values that are slightly lower than the wind speeds directly output from the model since changes in wind direction through the course of the day tends to reduce the average of the wind speed components. Wind speed values were available for an ensemble of sixteen models, however the two IPSL models were removed for reasons discussed in the previous section leaving only fourteen. Figure 7.3.4 compares the annual changes in the two extremes metrics with changes in the annual mean surface wind. The left-most bar shows the change across the ensemble of 24 models discussed in the previous section while the second bar shows the change just for the 14 models used for the extremes analysis. Comparing these two bars for each sub-cluster region shows that in general, the changes in the average winds across the smaller ensemble are consistent with those from the larger ensemble. The third bar shows the change in the average of the annual maximum wind while the fourth bar shows the 20-year return period wind.

The changes in extreme winds are generally consistent with those seen for mean winds. Across northern Australia there is a tendency for the median wind speed to increase in tropical areas (WT, RN and MNW). Although there is a greater tendency towards an increase in winds in MNE, there is little change in median value. Across south-eastern mainland Australia there is a general tendency towards a decrease across the ensemble in both the annual average and the 20-year wind speed (see results in Figure 7.3.4 for SSWFE, SSVW, MB, ECN, ECS and in CS for the 20-year wind speed only). For SSVE, RS and SSWFW, for annual and 20-year values and CS for annual average only, there is little change in the median value although there is a large spread in the direction and magnitude of change in individual models. Over Tasmania (SSTW and SSTE), median values indicate large increase although again there is a large spread in the direction and magnitude of change in individual models.

The pattern of extreme wind speed change seen here can be compared with the changes reported in McInnes *et al.* (2010) for the CMIP3 model ensemble, although that study characterised extreme winds using the 99th percentile wind speeds (which are less extreme than the annual maximum and 20-year return period values). Changes across the north of the continent consisted mainly of multi-model agreement on small change. Over the southern half of the continent there was multi-model agreement on decreases in extreme winds and over Tasmania, there was multi-model agreement on extreme wind increase, similar to results reported here.

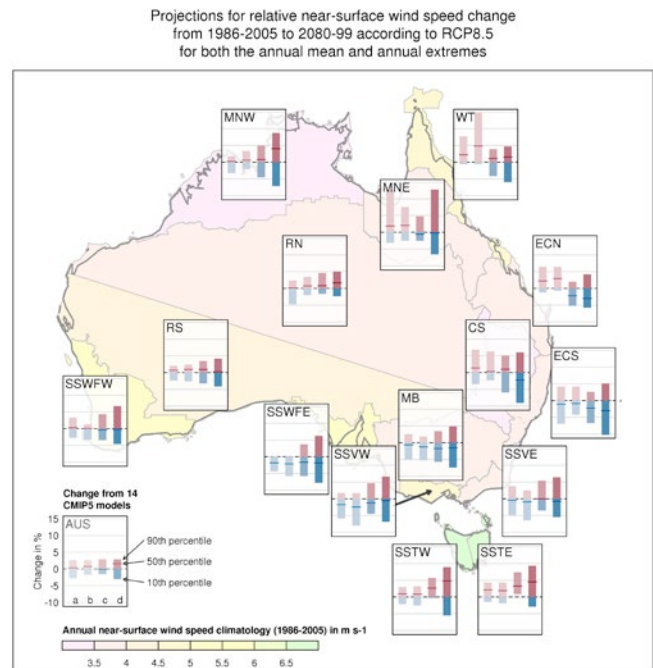


FIGURE 7.3.4: MEDIAN AND 10TH TO 90TH PERCENTILE RANGE OF PROJECTED CHANGE IN ANNUAL MEAN NEAR-SURFACE WIND SPEED IN SUB-CLUSTERS FOR 2080–2099 RELATIVE TO 1986–2005 FOR RCP8.5. SHOWN IN EACH BOX FROM LEFT TO RIGHT IS (A) THE ANNUAL DAILY MEAN NEAR-SURFACE WIND SPEED FOR THE LARGER SET OF 24 MODELS, AS WELL AS (B) THE ANNUAL DAILY MEAN NEAR-SURFACE WIND SPEED, (C) THE ANNUAL WINDIEST DAY, AND (D) THE 20 YEAR RETURN LEVEL OF THE ANNUAL WINDIEST DAY CALCULATED FROM A CONSISTENT SUBSET OF 14 MODELS. RED INDICATES AN INCREASE IN RELATIVE NEAR-SURFACE WIND SPEED AND BLUE A DECREASE.

In summary, changes in extreme winds tend to follow the direction of change indicated for mean winds, with only a few exceptions such as the decrease in extreme winds in the East Coast region during spring. Because of the various shortcomings associated with modelling extremes of near-surface winds, including the inability of models to resolve small scale meteorological systems that contribute to extreme winds such as tropical cyclones, there is generally *low confidence* in wind projections in the tropics. However, there is generally *medium confidence* in decreases in extreme wind speeds over the south of the continent and increases over Tasmania because the changes are consistent with broad-scale changes to circulation in these latitudes and because the scale of the weather systems that are responsible for extreme winds are better characterised by GCMs.

7.3.2 SYNOPTIC SYSTEMS

TROPICAL CYCLONES MAY OCCUR LESS OFTEN, BECOME MORE INTENSE, AND MAY REACH FURTHER SOUTH

Tropical cyclones are projected to become less frequent with a greater proportion of high intensity storms (stronger winds and greater rainfall) (*medium confidence*). A greater proportion of storms may reach south of 25 degrees South (*low confidence*).

MID-LATITUDE WEATHER SYSTEMS ARE PROJECTED SHIFT SOUTH IN WINTER, AND THE TROPICS TO EXPAND SOUTHWARD

The observed intensification of the subtropical ridge and expansion of the Hadley Cell circulation are projected to continue in the 21st century (*high confidence*). Both represent an expansion of the tropics.

In winter, mid-latitude weather systems are projected to shift south and the westerlies are projected to strengthen (*high confidence*). Concurrent and related changes in various measures of mid-latitude circulation are projected, including a more positive Southern Annular Mode, a decrease in the number of deep lows affecting south-west Western Australia and a decrease in the number of fronts in southern Australia.

Synoptic systems are a major cause of severe weather including strong winds and heavy rainfall. It is therefore important to assess how these systems may change in the future. Systems relevant to Australia include tropical cyclones, mid-latitude cyclones and their associated cold fronts.

TROPICAL CYCLONES

Tropical cyclones are phenomena that are a major cause of socio-economic loss and damage for tropical and subtropical Australia. Knutson *et al.* (2010) reviewed the results of a number of studies analysing changes in tropical cyclones by the end of the 21st century. The changes are found to be largely model-dependent but suggest an overall decrease in numbers of tropical cyclones globally. These changes vary between individual ocean basins but the decrease in tropical cyclone activity is most pronounced in the Southern Hemisphere. More recently the IPCC *Fifth Assessment Report* (IPCC, 2013; pg 1220) concludes “it is likely that the global frequency of occurrence of tropical cyclones will either decrease or remain essentially unchanged, concurrent with a likely increase in both global mean tropical cyclone maximum wind speed and precipitation rates. The future influence of climate change on tropical cyclones is likely to vary by region, but the specific characteristics of the changes are not yet well quantified and there is low confidence in region-specific projections of

frequency and intensity.” Most recent global and regional studies are consistent with these findings (*e.g.* Murakami *et al.* 2012, Tory *et al.* 2013b,c, Chattopadhyay and Abbs, 2012). However, Emanuel (2013) downscaled a suite of CMIP5 GCMs, finding an increase in both the frequency and intensity of tropical cyclones in most locations, with the exception of the south-western Pacific region near Australia; it should be noted that these CMIP5 results are found to differ substantially from the application of this downscaling technique to a selection of CMIP3 models.

This Report presents an analysis of projected changes of tropical cyclone frequency and location in the Australian region in CMIP5 models. Although the resolution of the majority of global climate models is coarse, the current generation of GCMs is able to simulate the broad-scale atmospheric conditions associated with tropical cyclone activity and they do produce atmospheric circulations that resemble tropical cyclones with global distributions that generally match the observed tropical cyclone climatology (*e.g.* Camargo *et al.*, 2005). However, they have insufficient temporal and spatial resolution to capture the high wind speeds and other small-scale features associated with observed tropical cyclones.

Three “empirical methods” were used to infer tropical cyclone activity from the large-scale environmental conditions and were applied to the outputs of CMIP5 GCMs. These three schemes are known as the Genesis Potential Index (GPI) (Emanuel and Nolan, 2004), the Murakami modification of the GPI (GPI-M) (Murakami and Wang, 2010) and the Tippett Index (Tippett *et al.* 2011). Two “direct detection” schemes were applied to the outputs from a subset of CMIP5 GCM model outputs: these are the CSIRO Direct Detection (CDD) scheme which is a modified version of the Nguyen and Walsh (2001) detection scheme coupled with the tracking scheme of Hart (2003), and the Okubo-Weiss-Zeta Parameter (OWZP) of Tory *et al.* (2013 a,b,c). Projections from the CDD and OWZP only consider GCMs which reproduced a tropical cyclone climatology with annual tropical cyclone numbers within $\pm 50\%$ of that observed.

These methods were applied to a selection of CMIP5 models to investigate changes in the frequency of tropical cyclones at the end of the 21st century under the RCP8.5 emissions scenario relative to the historical run. The analysis was performed over both the north-east (0-40 °S; 130-170 °E) and north-west (0-40 °S; 90-130 °E) of the continent.

Over both regions, results indicate a general decrease in tropical cyclone genesis (formation) frequency (Figures 7.3.5 and 7.3.6), although the five methods show different results across the different models. Using the direct detection methodologies (OWZP or CDD), a little over a half of projected changes are for a decrease in genesis frequency of between 15 to 35 % in the eastern region whereas in the west, the majority of models (around 85 %) project a decrease. The three empirical techniques assess changes in the main atmospheric conditions known to be



necessary for tropical cyclone formation. About two-thirds of models suggest the conditions for tropical cyclone formation will become less favourable in both regions with about one third of projected changes being for a decrease of between 5 and 30 %. There is *medium confidence* for this projection. Further analysis of the CDD results shows negligible changes in genesis latitude and storm duration for the Australian region; importantly a larger proportion of storms are projected to decay south of 25 °S in the late 21st century. This projected southward movement in the decay location of tropical cyclones is consistent with the observed migration of tropical cyclone activity away from the tropics (Kossin *et al.* 2014).

To enable changes in intensity, size and rainfall to be captured, it is necessary to use some form of downscaling. Downscaling studies of tropical cyclones affecting the Australian and south-west Pacific (Lavender and Walsh, 2011, Abbs and Rafter, 2012, Abbs *et al.* 2014) consistently project an increase in the proportion of high intensity (high windspeed, low minimum pressure) storms, a corresponding decrease in the proportion of mid-range intensity storms and an increase in the rainfall close to the storm centre; in particular the increase is largest in the most intense tropical cyclones. In summary, based on global and regional studies, tropical cyclones are projected to become less frequent with a greater proportion of high intensity storms (stronger winds and greater rainfall) (*medium confidence*); a greater proportion of storms may reach south of 25 degrees south (*low confidence*).

EXTRA-TROPICAL CYCLONES AND STORM TRACKS

The mean transport of energy via the Hadley Cell from the tropics to the subtropical ridge transfers energy away from the tropics. This large-scale climatological feature has impacts on the weather of southern Australia (see Section 4.1.2). Over the last 30 years the Hadley Cell has been expanding poleward (Lucas *et al.* 2012), although not all climate models capture the magnitude of this trend (Nguyen *et al.* 2013). CMIP3 climate model simulations generally indicate a poleward expansion of the Hadley circulation of a further 1 to 2 ° of latitude (approximately 100 to 200 km) by the end of the 21st century, and an associated expansion of the subtropical dry zone (Previdi and Liepert, 2007). In response to the Hadley circulation broadening, climate models project an increase in the subtropical ridge intensity over the 21st century in the vicinity of Australia and a southward movement of its mean position (Kent *et al.* 2013; see also Figure 7.2.11). These projected changes are likely to contribute to reductions in storminess and rainfall over southern Australia. However, it is important to note that most CMIP3 climate models failed to adequately reproduce the correlation between the subtropical ridge intensity and south-eastern Australian rainfall which lowers the confidence in GCM rainfall projections for southern Australia (Kent *et al.* 2013).

The number of extra-tropical cyclones impacting Australia is expected to decline, as indicated by the changes projected in the large-scale climate features described

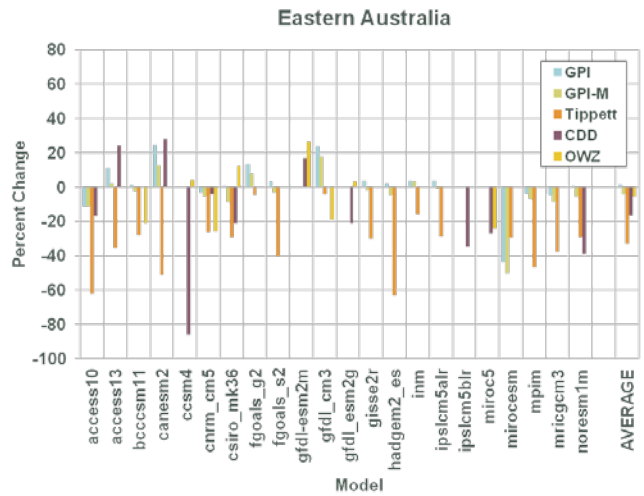


FIGURE 7.3.5: PROJECTED PERCENTAGE CHANGE IN THE FREQUENCY OF TROPICAL CYCLONE FORMATION FOR EASTERN AUSTRALIA (0-40°S; 130 °E -170 °E) FOR 22 CMIP5 CLIMATE MODELS, BASED ON FIVE METHODS (SEE TEXT FOR DEFINITIONS), FOR 2080–2099 RELATIVE TO 1980–1999 FOR RCP8.5.

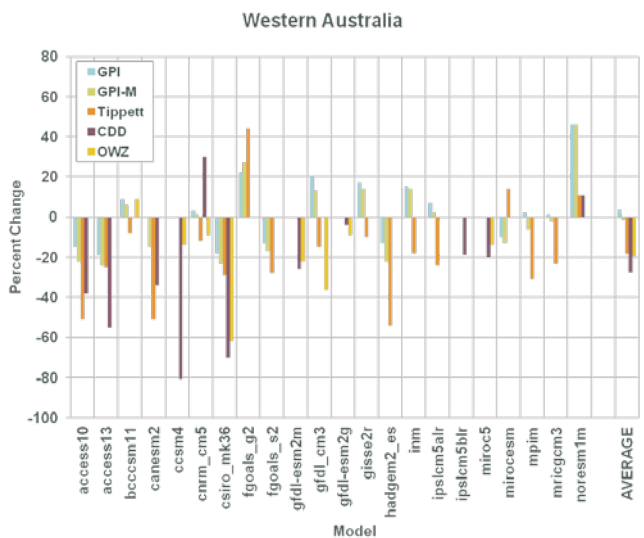


FIGURE 7.3.6: AS FOR FIG 7.3.5 FOR WESTERN AUSTRALIA (0-40 °S; 90-130 °E).

above. A decrease in the number of winter deep low pressure systems impacting south-west Western Australia is projected through this century by a number of CMIP3 models under the A2 scenario (Hope *et al.* 2006). That study showed fewer weather disturbances. This aligns with the atmosphere in the region becoming increasingly stable through this century as shown by Frederiksen *et al.* (2011). There is a projected decrease in the number of fronts across most models in the south and an associated decrease in frontal rainfall, particularly in the south-west by 2090 (Catto *et al.* 2013). In summer, the results are less clear, as the interactions between frontal systems and the continent



are markedly different due to a stronger thermal contrast between the land and the ocean. For example, Hasson *et al.* (2009) found that intense frontal systems affecting south-eastern Australia associated with extreme winds and dangerous fire weather will increase strongly by end of the 21st century although this increase is strongly dependent on the emission scenario considered for the projections. Cut-off lows are also important rain-bearing low pressure systems across southern and eastern Australia (Risbey *et al.* 2009a, Pook *et al.* 2012). In CCAM and an example CMIP3 model these are projected to decline (Grose *et al.* 2012).

In eastern Australia, cut-off lows are often termed East Coast Lows and are very important for rainfall (Pepler and Rakich, 2010, Dowdy *et al.* 2013b). These and other types of cut-off lows in Australia are influenced by blocking in the Tasman Sea (Pook *et al.* 2013). Throughout the 21st century, climate models project a continuation of the decreasing trend in East Coast Low occurrence that has been observed over the last 30 years (Dowdy *et al.* 2013c, Dowdy *et al.* 2014). The projected trend results in an approximately 30 % reduction in East Coast Low formation in the late 21st century compared to the late 20th century. The changes in intensity of cut-off lows have been investigated for Tasmania in CCAM downscaling of CMIP3 models and there is some indication that the most severe cut-off lows could increase in their severity (Grose *et al.* 2012).

In summary, mid-latitude weather systems are projected to shift south and the westerlies are projected to strengthen (*high confidence*). Concurrent and related changes in various measures of mid-latitude circulation are projected, including an increase in the Southern Annular Mode, a decrease in the number of deep lows affecting south-west Western Australia and a decrease in the number of fronts in southern Australia.

7.4 SOLAR RADIATION

MORE SUNSHINE IN WINTER AND SPRING

There is *high confidence* in little change in solar radiation over Australia in the near future (2030). Late in the century (2090), there is *medium confidence* in an increase in winter and spring in southern Australia. The increases in southern Australia may exceed 10 % by 2090 under RCP8.5.

Changes in solar radiation would have impacts on many sectors including agriculture and livestock, health, ecosystems and energy. The CMIP5 simulations indicate that, as in the case of rainfall, natural variability in solar radiation remains large compared to the greenhouse gas induced climate signal over time (Figure 7.4.1). Annual results (not shown) indicate generally little change in Northern Australia and Rangelands, whereas increases are

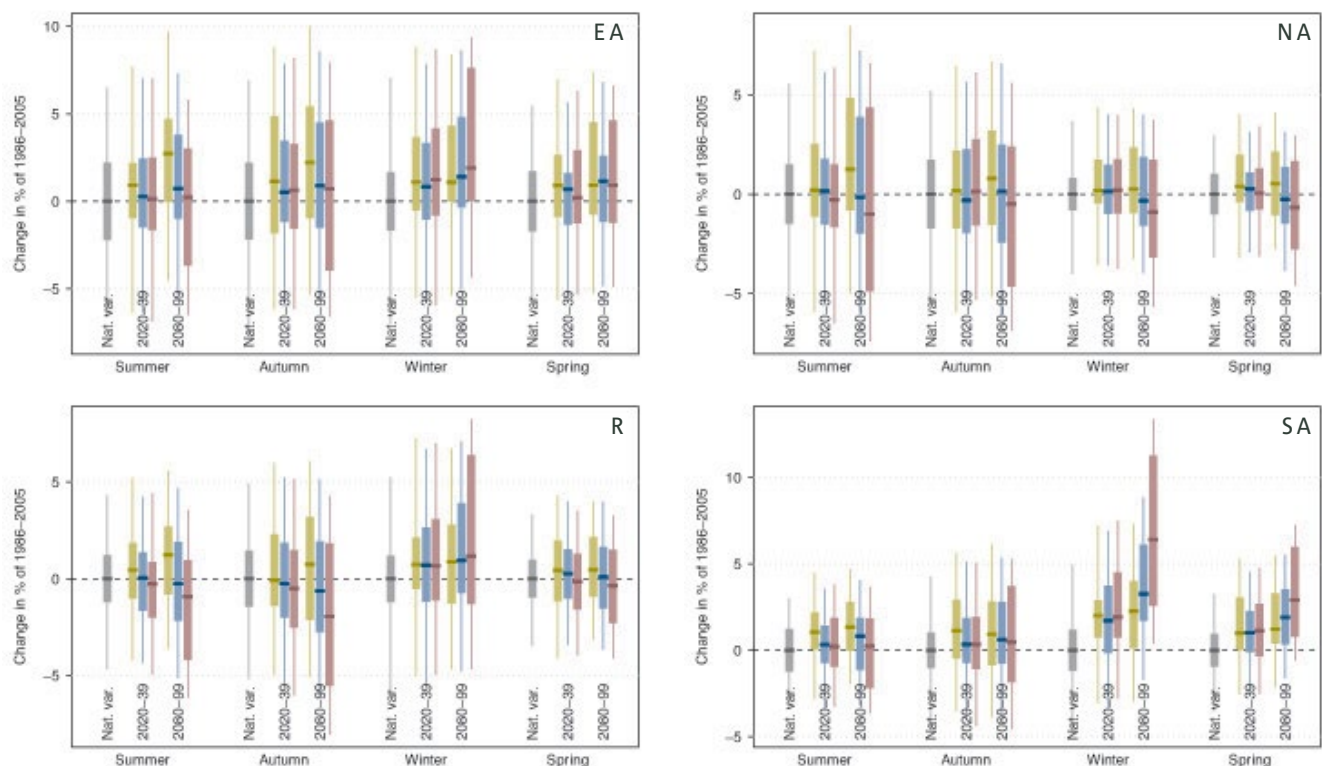


FIGURE 7.4.1: MEDIAN AND 10TH TO 90TH PERCENTILE RANGE OF PROJECTED SEASONAL SOLAR RADIATION CHANGE FOR 2020–2039 AND 2080–2099 RELATIVE TO THE 1986–2005 PERIOD (GREY BAR) FOR RCP2.6 (GREEN), RCP4.5 (BLUE) AND RCP8.5 (PURPLE) FOR FOUR SUPER-CLUSTER REGIONS. FINE LINES SHOW THE RANGE OF INDIVIDUAL YEARS AND SOLID BARS FOR TWENTY YEAR RUNNING MEANS.

-20° -10° 0° 10° 20° 30° 40° 50°

evident in Southern and Eastern Australia, consistent with previous projections (CSIRO and BOM, 2007). The increases for Southern Australia are generally less than 3 % even by 2090 under RCP8.5. The results by season (Figure 7.4.1) show that the southern Australian increase is primarily in winter and spring. For other regions, the signal is mixed although the median values indicate a small increase in Eastern Australia and Rangelands, and a small decrease in Northern Australia. In summer and autumn in 2090, the median values indicate a small increase in all regions for RCP2.6 scenario, and no-change or small decrease for RCP4.5 and RCP8.5, although changes outside that expected due to natural variability are simulated by some models. In general, the pattern of the change is the opposite to that of rainfall (Section 7.2).

Projections for relative surface downwelling shortwave radiation change from 1986-2005 to 2080-99 according to RCP8.5

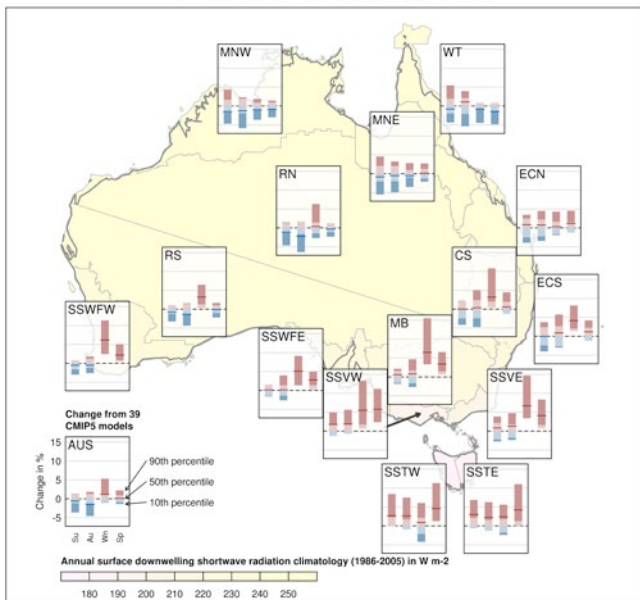


FIGURE 7.4.2: MEDIAN AND 10TH TO 90TH PERCENTILE RANGE OF PROJECTED CHANGES IN SEASONAL SOLAR RADIATION FOR 2080–2099, RELATIVE TO 1986–2005, FOR RCP8.5 FOR 20-YEAR MEANS IN SUB-CLUSTERS. RED INDICATES INCREASE AND BLUE DECREASE (SEE KEY) AND PALER PORTION OF THE BAR IS THE 10TH TO 90TH PERCENTILE RANGE EXPECTED FROM NATURAL VARIABILITY. THE SOLAR RADIATION CLIMATOLOGY OVER THE 1986–2005 PERIOD IS INDICATED BY THE COLOUR OF THE SHADING ON THE MAP OF AUSTRALIA.

Examining finer spatial variations in projected solar radiation change (Figure 7.4.2), it can be seen that the increases in winter and spring under high forcing (2090 and RCP8.5) are present in all the southern regions, whereas a decrease is evident over the Monsoonal North. The summer and autumn signal is mixed in almost all southern regions, except for increases in Tasmania and south-west Victoria. Again, the direction of changes in radiation is in general negatively related to changes in rainfall (Section 7.2), since less/more rainfall often means more/less radiation. A further comparison also reveals that overall the projected change in radiation is the opposite to that of the cloud condensed water content, a measure of the mass of water in cloud in a specified amount of dry air (not shown).

To a large extent, these new projections are consistent with the previous ones (CSIRO and BOM, 2007), particularly for summer and autumn, and the increase for winter and spring. Compared to CMIP3, CMIP5 generally suggests a larger decrease and a lesser increase over the north (See Appendix A).

In summary, annual radiation observations in Australia show a high year to year variability with no significant long-term change (only a very weak increase) during the latter half of the 20th century (Chapter 4). Such high variability remains strong compared to the greenhouse gas induced climate change signal out to 2100. On a seasonal basis, there are variations in magnitude of changes for the near future and late in the century and across regions. Overall, the new projected changes are consistent with the observed trends and with the 2007 projections. However, an Australian wide model evaluation suggests that not all models can reproduce the climatology of solar radiation reasonably well (Chapter 5), while a global study has shown that as with CMIP3, CMIP5 models underestimate the observed trends in some regions in the world due to an underestimation of aerosol direct radiative forcing and/or a deficient aerosol emission inventories (Allen *et al.* 2013). Nevertheless, there is *high confidence* in little change in solar radiation over Australia in the near future (2030). Late in the century (2090), there is *medium confidence* in a small increase in winter and spring in southern Australia.

7.5 HUMIDITY

LOWER RELATIVE HUMIDITY

Relative humidity is projected to decline in inland regions and where rainfall is projected to decline. By 2030, the decreases are relatively small (*high confidence*). By 2090, there is *high confidence* that humidity will decrease in winter and spring as well as annually, and there is *medium confidence* in declining relative humidity in summer and autumn.

Water vapour (humidity), at the surface, has a role in many hydrometeorological and ecological processes (*e.g.* hydrology, atmospheric heat transport, cloud formation, human comfort and plant transpiration).

Unlike other atmospheric variables, humidity can be measured in different ways. Relative humidity and specific humidity are the common ones, describing the degree of saturation of the air and the amount of water in the air, respectively. Through the Clausius-Clapeyron relation, if relative humidity is constant then specific humidity increases close to exponentially with temperature. Another common measure is the dewpoint temperature which is the temperature to which the air needs to be cooled to allow condensation to occur. The closer the dew point temperature is to the current air temperature, the higher the relative humidity of the air. Chapter 4 describes historical humidity variability based on the observations in Australia.

The new CMIP5 model results for relative humidity show a tendency for a decrease across Australia and in all seasons. This is large compared to natural variability mainly in winter and spring in southern Australia, and especially at 2090 under RCP8.5 (Figure 7.5.1). The magnitude of changes depends on time frame and RCP, but even under RCP8.5 the seasonal changes are generally not outside the range of +1 to -6 %. In the near future (2030), the corresponding range is +1 to -3 %. Increases are present in some models, especially in summer and autumn and in regions other than southern Australia, but in no case does the model median show increase.

Figure 7.5.2 shows seasonal changes for each of the fifteen sub-regions in 2090 under RCP8.5. It is notable here that the magnitude of the decrease has the potential to be larger in the regions with a large inland component and smaller in the more coastally oriented regions, particularly southern ones, such as southern Victorian and Tasmania.

These results are relatively similar to those of CMIP3 (see Appendix A). They are also consistent with the tendency for relative humidity to decline over land with increasing temperature. This has been noted globally in observations and in CMIP5 results and is related to the land warming faster than the neighbouring ocean. This means that moisture laden air moving from oceans to land encounters warmer land than was previously the case, resulting in reduced relative humidity (Simmons *et al.* 2010, IPCC,

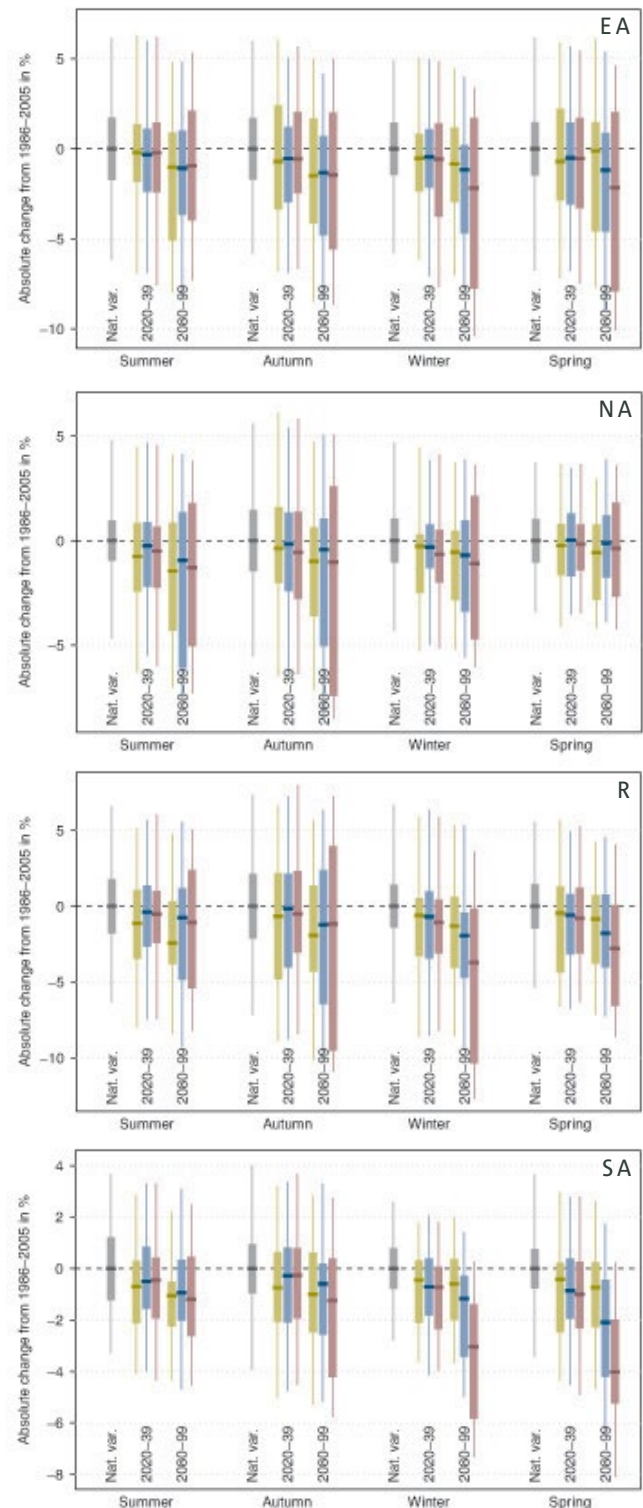


FIGURE 7.5.1: MEDIAN AND 10TH TO 90TH PERCENTILE RANGE OF PROJECTED SEASONAL RELATIVE HUMIDITY CHANGE FOR 2020–2039 AND 2080–2099 RELATIVE TO THE 1986–2005 PERIOD (GREY BAR) FOR RCP2.6 (GREEN), RCP4.5 (BLUE) AND RCP8.5 (PURPLE) FOR FOUR SUPER-CLUSTER REGIONS. FINE LINES SHOW THE RANGE OF INDIVIDUAL YEARS AND SOLID BARS FOR TWENTY YEAR RUNNING MEANS.

2013, Chapter 12). The stronger tendency is for a decrease in southern areas (including coastal areas) in winter and spring, and is clearly related to the simulated reduction in rainfall in those regions and seasons (Section 7.2).

In summary, the pattern of change simulated in CMIP5 is consistent with a general tendency for reduced relative humidity over land and in regions where rainfall is projected to decline. Australia-wide annual humidity observations also show a weak long-term drying – at roughly the same rate as that identified globally (e.g. (Dai, 2006, Simmons *et al.* 2010), although it is unclear whether the Australian observed changes are due to an anthropogenic cause (see Chapter 4). It may also be noted that CMIP3 model results have been shown to simulate climatological means and interannual variability of humidity characteristics well compared to the observations (Willett *et al.* 2010). It is concluded that there is a *high confidence* that humidity will decrease in winter and spring as well as annually, and there is a *medium confidence* of a decline in summer and autumn in 2090. In the near future (2030) the decreases are relatively small (i.e. less than 3 %), thus there is a *high confidence* in modest change in the near future.

7.6 POTENTIAL EVAPOTRANSPIRATION

HIGHER EVAPORATION RATES

There is *high confidence* in increasing potential evapotranspiration (atmospheric moisture demand) closely related to local warming, although there is only *medium confidence* in the magnitude of change.

Evapotranspiration is a collective term for the transfer of water vapour to the atmosphere from both vegetated and unvegetated land surfaces. It is a key component in the water balance of a system such as a landscape, catchment or irrigation region. In practice, actual evapotranspiration is rather difficult to measure and its estimate is often based on information about potential evapotranspiration and soil moisture. Potential evapotranspiration is often regarded as the maximum possible evaporation rate that would occur under given meteorological conditions if water sources were available. It is commonly estimated through pan evaporation, that gives a measure of potential evaporation over a small open water body, or alternatively it is estimated using a formulation which considers meteorological variables affecting evapotranspiration (see McMahon *et al.* (2013) for a detailed practical guide).

Generally, it is expected that potential evapotranspiration will increase with increasing temperatures and an intensifying hydrologic cycle (Huntington, 2006). The previous projections, based on CMIP3 models, of annual potential evapotranspiration indicated increases over Australia (CSIRO and BOM, 2007). The multi-model median estimates in 2070 under the high emission scenario (A1FI) were six percent in the south and west, and ten percent in the north and east.

Those estimates are based on the *Morton model* (Morton, 1983), which has been widely used in Australia including in constructing Australia’s evaporation atlas (BOM, 2001) and in the hydrological impact of climate change on major Sustainable Yields assessment projects in Australia (e.g. Chiew *et al.* 2008). The Morton model requires input of air temperature, relative humidity and downward solar radiation at the surface, but not the wind speed. It parameterises the vapour transfer coefficient which is dependent on atmospheric pressure, but not directly on wind speed. This approach was found to have a small mean annual error (i.e. less than 2.5 % of mean annual rainfall) (Hobbins *et al.* 2001). Also, the method compares favourably with other methods for calculating potential evaporation in rainfall-runoff modelling (Chiew and McMahon, 1991) and is strongly correlated to the pan evaporation observations (Kirono *et al.* 2009). This provides confidence in the use of the Morton method in Australia. When applied to the CMIP3 model data, the Morton model results reproduce the spatial distribution of the observed annual mean and coefficient of variation, but show less skill in reproducing the linear trends (Kirono and Kent, 2011).

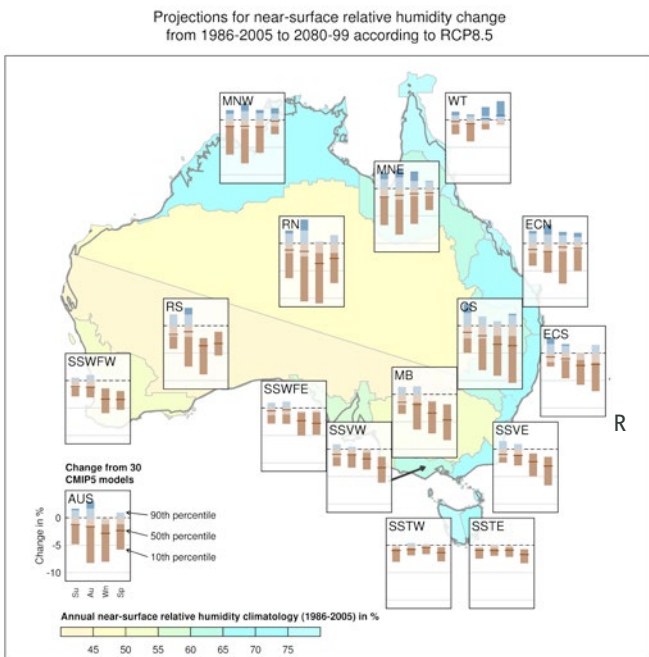


FIGURE 7.5.2: MEDIAN AND 10TH TO 90TH PERCENTILE RANGE OF PROJECTED SEASONAL RELATIVE HUMIDITY CHANGES FROM CMIP5 MODELS FOR 2080–2099 RELATIVE TO 1986–2005 FOR RCP8.5 FOR 20-YEARS MEANS IN SUB-CLUSTERS. THE BARS FOR 15 REGIONS OVERLIE A MAP WITH EACH REGIONS COLOURED TO INDICATE ITS BASE MODEL CLIMATE AVERAGE. BLUE INDICATES INCREASE AND BROWN DECREASE (SEE KEY) AND PALER PORTION OF THE BAR IS THE 10TH TO 90TH PERCENTILE RANGE EXPECTED FROM NATURAL VARIABILITY. THE RELATIVE HUMIDITY CLIMATOLOGY OVER THE 1986–2005 PERIOD IS INDICATED BY THE COLOUR OF THE SHADING ON THE MAP OF AUSTRALIA.



For this Report, potential evapotranspiration is calculated using the Morton model using the CMIP5 model data. There are three types of evaporation generated using the model, i.e. point potential evapotranspiration, areal potential evapotranspiration and actual evapotranspiration. This Report focuses on the areal potential evapotranspiration, which is also known as wet-environment areal evapotranspiration (McMahon *et al.* 2013). Unlike pan evaporation that represents evaporation occurring from a small area of water surface only, areal potential evapotranspiration represents potential evapotranspiration (from soil, vegetation, and water surfaces) that would occur when moisture supply was not limited over a large area (greater than 1km²) (BOM, 2001). The climatology over Australia indicates that both point and areal potential evapotranspiration have similar spatial patterns, but the average areal potential evapotranspiration is lower than the point value (www.bom.gov.au). As in the CMIP3 case, the CMIP5 modelled results reproduce the spatial distribution and annual cycle of the observed climatology (not shown here).

The simulated potential evapotranspiration change for 2030 and 2090 for different emission scenarios (Figure 7.6.1) show a strong tendency for increases throughout Australia in all four seasons. This is also true for annually averaged projections (results not shown). In 2030 the increases are already large compared to natural variability (although

less than 5% in magnitude), and are very marked in 2090 under RCP8.5 (around 10-20% increase seasonally as well as annually). In percentage terms, the largest increase is projected in autumn and winter while the smallest is in summer and spring, although in absolute terms (not shown) the summer changes are the largest. The seasonal changes for each of the 15 sub-regions in 2090 under RCP8.5 (Figure 7.6.2) show a similar pattern at the sub-regional level, although the relative increase in winter is particularly noticeable in the south-east of the continent.

In summary, an increase in areal potential evapotranspiration can be projected with *high confidence*. The increasing trend emerges even in the near future (2030). This increase agrees with theoretical expectations, and is consistent amongst almost all CMIP5 models (and CMIP3 models). However, *medium confidence* is placed on the magnitude of the increase. This is due to there being no clear changes observed in pan evaporation across Australia in data available since 1970 (Section 4.2) (although it is noted that pan evaporation is a different measure to areal evapotranspiration). Also, it has been shown that some CMIP3 GCMs have a tendency to not reproduce the historical linear trends (Kirono and Kent, 2011).

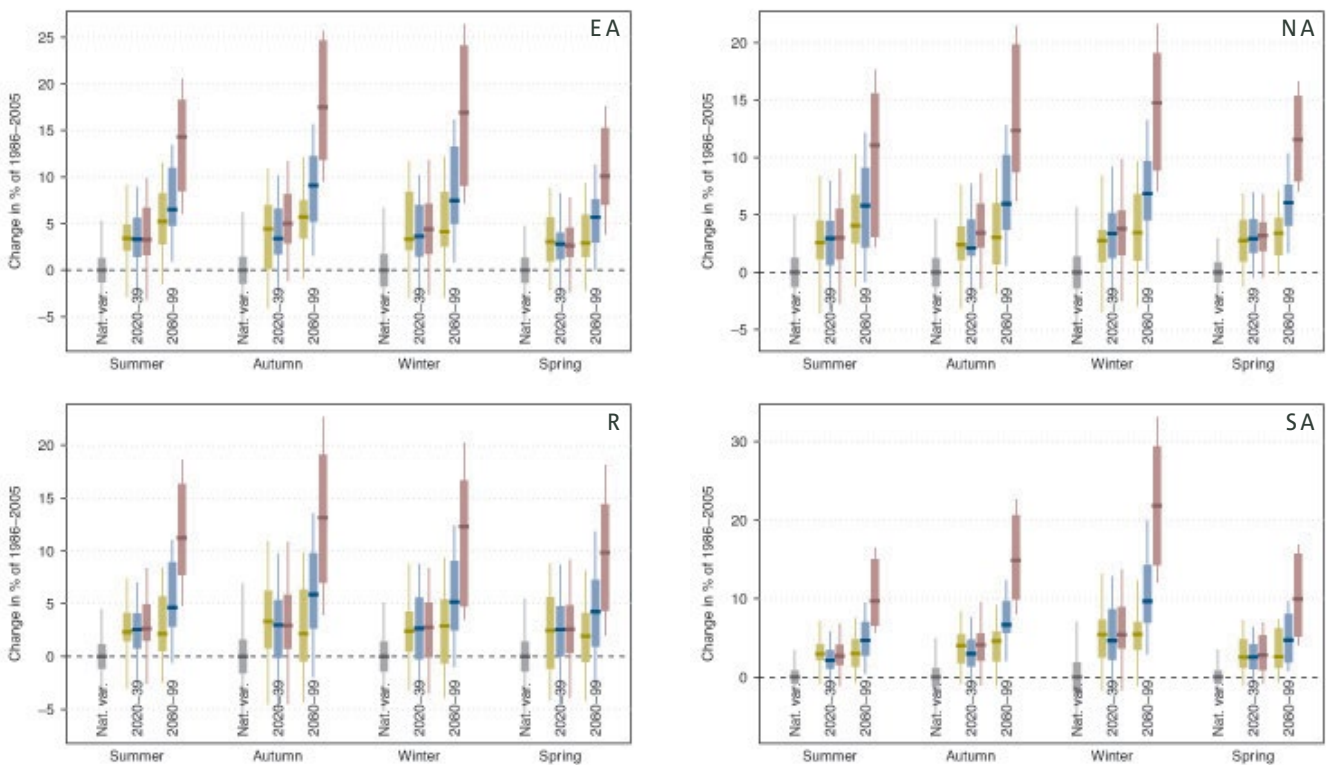


FIGURE 7.6.1: MEDIAN AND 10TH TO 90TH PERCENTILE RANGE OF PROJECTED CHANGE IN SEASONAL POTENTIAL EVAPOTRANSPIRATION FOR 2020–2039 AND 2080–2099 RELATIVE TO THE 1986–2005 PERIOD (GREY BAR) FOR RCP2.6 (GREEN), RCP4.5 (BLUE) AND RCP8.5 (PURPLE) FOR FOUR SUPER-CLUSTER REGIONS. FINE LINES SHOW THE RANGE OF INDIVIDUAL YEARS AND SOLID BARS FOR TWENTY YEAR RUNNING MEANS.

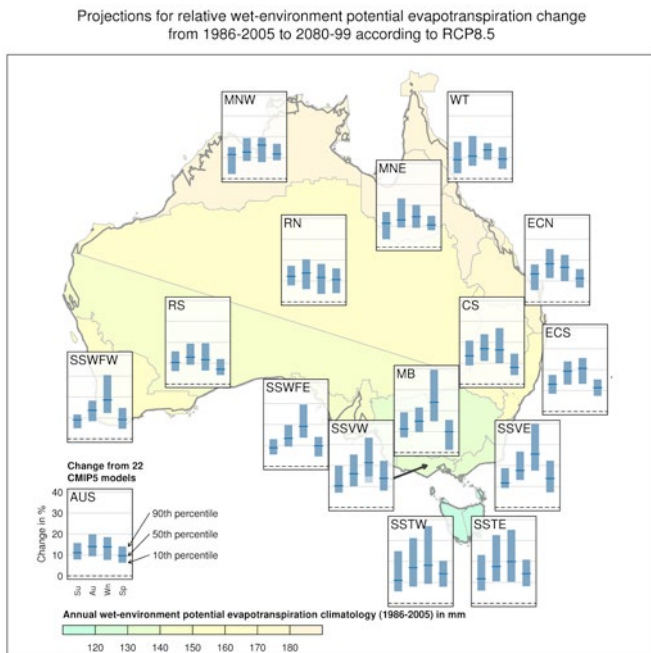


FIGURE 7.6.2 MEDIAN AND 10TH TO 90TH PERCENTILE RANGE OF PROJECTED CHANGE IN SEASONAL WET-ENVIRONMENTAL POTENTIAL EVAPOTRANSPIRATION FOR 2080–2099 RELATIVE TO 1986–2005 FOR RCP8.5 FOR 20-YEAR MEANS IN SUB-CLUSTERS. BLUE INDICATES INCREASE (SEE KEY) AND PALER PORTION OF THE BAR IS THE 10TH TO 90TH PERCENTILE RANGE EXPECTED FROM NATURAL VARIABILITY. THE POTENTIAL EVAPOTRANSPIRATION CLIMATOLOGY OVER THE 1986–2005 PERIOD IS INDICATED BY THE COLOUR OF THE SHADING ON THE MAP OF AUSTRALIA. THE AUSTRALIAN RESULT IS IN THE BOTTOM LEFT.

7.7 SOIL MOISTURE AND RUNOFF

SOIL MOISTURE IS PROJECTED TO DECREASE AND FUTURE RUNOFF WILL DECREASE.

There is *high confidence* in decreasing soil moisture in the southern regions (particularly in winter and spring) driven by the projected decrease in rainfall and higher evaporative demand. There is *medium confidence* in decreasing soil moisture elsewhere in Australia where evaporative demand is projected to increase but the direction of rainfall change is uncertain.

Decreases in runoff are projected with *high confidence* in south-western Western Australia and southern South Australia, and with *medium confidence* in far south-eastern Australia, where future rainfall is projected to decrease. The direction of change in future runoff in the northern half of Australia cannot be confidently projected because of the uncertainty in the direction of rainfall change.

Runoff is the water that flows into rivers and water bodies. Soil moisture is the water stored in the soil. Broadly, runoff follows the same pattern as rainfall over Australia, with the far north and parts of Tasmania having the highest runoff. Due to the high potential evapotranspiration, and modest or low rainfall (see Section 7.6), most of continental Australia has low mean annual runoff, with little to no runoff in most of interior Australia. Runoff can be highly seasonal, particularly to the north, with most regions having 95% or more of their runoff occurring during the wet season. These moisture variables are difficult to simulate in GCMs where, due to their relatively coarse resolution, the models cannot simulate much of the rainfall and land surface detail that is important to key hydrological processes. For such reasons, and for consistency with many previous studies, we do not present directly simulated GCM runoff and soil moisture, but rather examine results of hydrological models forced by rainfall and potential evapotranspiration from the same GCMs shown elsewhere in this Report.

7.7.1 PROJECTED CHANGES IN SOIL MOISTURE

Various studies project a wide range of significant changes in soil moisture, driven by changes in rainfall and higher evaporative demand (Chiew, 2006; Hennessy *et al.* 2008). Future soil moisture will decrease where rainfall decreases, and increase where rainfall increases significantly. Where there is a small increase in rainfall, the direction of soil moisture change will depend on the compensating effect of the higher rainfall and higher evaporative demand.

The soil moisture changes reported here are estimated using a dynamic hydrological model based on an extension of the Budyko framework (Zhang *et al.* 2008), forced by monthly rainfall and potential evaporation from the CMIP5 GCMs. Projected change in seasonal average soil-moisture

for 2020-39 and 2080-99 with respect to 1986-2005, under RCP4.5 and RCP8.5, are shown in Figure 7.7.1 (left hand column). Soil moisture, at the broad-scale as presented for Northern Australia, Eastern Australia, the Rangelands and the Southern Australia super-clusters, generally reflects the time lag of rainfall accumulated over several months. Different approaches should therefore generally show similar results, reflecting the changes in the seasonal rainfall inputs and higher potential evapotranspiration (from higher future temperatures). In all time frames, regions and emission scenarios in Figure 7.7.1 a decreasing tendency is evident. In 2030 this is mostly small compared to natural variability, but not in winter in Eastern Australia and the Rangelands, nor in winter and spring in Southern Australia. Changes are larger in 2090, with simulated decreases of up to 15 % in winter in Southern Australia. Figure 7.7.2 shows the projected changes in seasonal average soil moisture for 2080-2099 relative to 1986-2005 for RCP8.5 for each cluster region (detailed discussion can be found in respective Cluster Reports).

In summary, the simulated changes to soil moisture are influenced by the projected changes in rainfall (Section 7.2) and the higher evaporative demand (Section 7.6). There is *high confidence* in decreased soil moisture in the southern regions (particularly in winter and spring) driven by the projected decrease in rainfall and higher evaporative demand. There is *medium confidence* in decreased soil moisture elsewhere in Australia where evaporative demand will increase but the direction of rainfall change is uncertain.

7.7.2 PROJECTED CHANGES IN RUNOFF

Future runoff is strongly influenced by future rainfall, with the percentage change in annual rainfall in Australia generally amplified 2-3 times in the percentage change in annual runoff (Chiew, 2006). Runoff is also influenced by temperature, and the higher potential evaporation associated with each 1 °C increase in temperature will reduce annual runoff by 2–5 % (although some studies report bigger reductions) (Chiew, 2006, Cai and Cowan, 2008, Potter *et al.* 2008).

Reported here are projections of annual runoff estimated using the empirical Budyko energy and water balance relationship (Teng *et al.* 2012). The Budyko relationship is used here because it is simple and can provide estimates of changes in long-term average runoff resulting from changes in long-term average rainfall and potential evapotranspiration. As the Budyko relationship applies to long-term water and energy balances, the runoff projection plots show 30-year moving averages and the 20-year results presented here also come from these 30-year running means.

The projected range of change in annual runoff in the four broad regions across Australia are shown above in Figure 7.7.1 (right hand column), for 2020-39 and 2080-2099 relative to the present, under RCP4.5 and RCP8.5. The range of future runoff projections is large, mainly because of the uncertainty in the rainfall projections. The median runoff

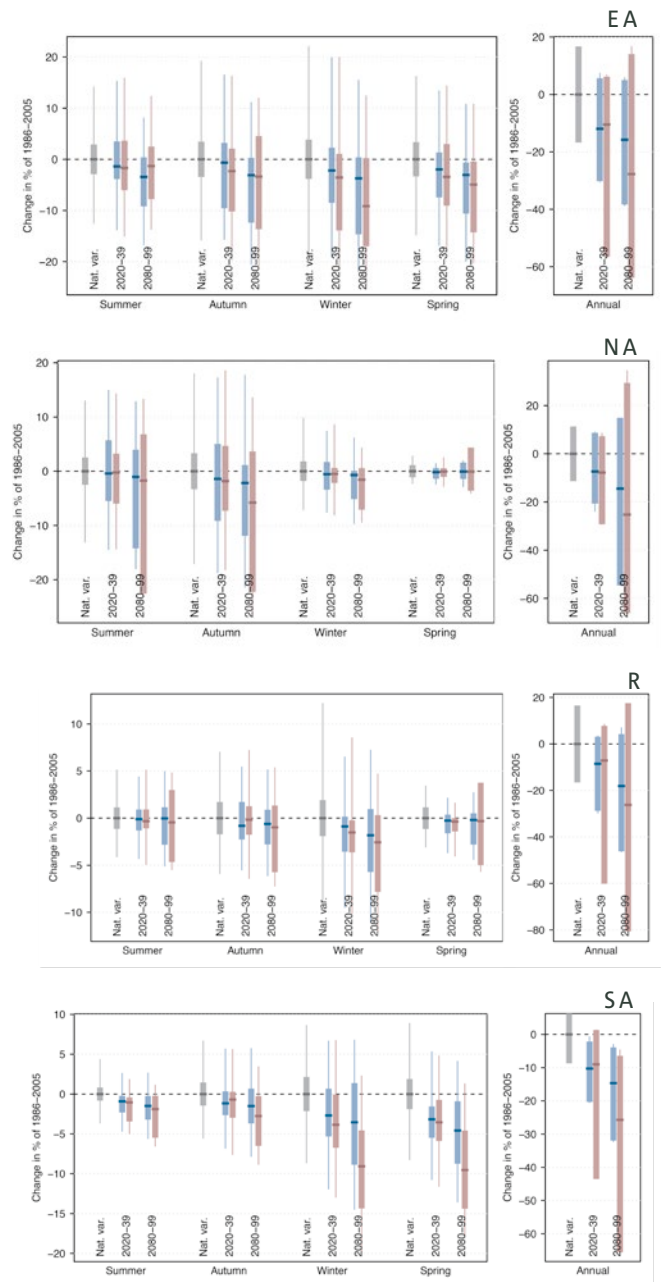


FIGURE 7.7.1: MEDIAN AND 10TH TO 90TH PERCENTILE RANGE OF PROJECTED CHANGE IN SEASONAL SOIL MOISTURE (LEFT COLUMN) AND ANNUAL RUNOFF (RIGHT COLUMN) FOR 2020-39 AND 2080-99 WITH RESPECT TO 1986-2005 ASSOCIATED WITH NATURAL VARIABILITY ONLY (GREY), RCP4.5 (BLUE) AND RCP8.5 (PURPLE). FINE LINES SHOW THE RANGE OF INDIVIDUAL YEARS AND SOLID BARS FOR TWENTY YEAR RUNNING MEANS.



projections show a general decrease. In Southern Australia practically all models show a decrease by 2090, ranging from around zero to -30 % and zero to -60 % under RCP4.5 and RCP8.5, respectively. Model median results are similar in the Rangelands, Eastern Australia, and Northern Australia although increase is evident in some models (a range of around +10 to -40 % for RCP4.5 and +30 to -70 % for RCP8.5). Results vary somewhat amongst individual cluster regions (Figure 7.7.2) with much stronger consistency for a decrease in south-west Western Australia.

It should be noted that the Budyko relationship does not take into account the influence of other climate factors on runoff, such as potential changes in seasonal rainfall and high intensity rainfall. The former is important in regions like south-east Australia where rainfall in many catchments is relatively uniform through the year while most of the runoff occurs in winter. The future annual runoff is therefore more dependent on changes in the cool season rainfall than the summer or annual rainfall. Future projections indicate a likely decline in winter rainfall (with less agreement in the direction of change in summer rainfall) in far southern Australia, and by not taking this into account, the Budyko relationship will overestimate future runoff (or underestimate the decline in future runoff).

By contrast, extreme high rainfall is likely to be more intense in the future (Section 7.2). As a significant amount of runoff is generated during high rainfall events and multi-day rainfall events, by not taking this into account, the Budyko relationship will underestimate future runoff (or underestimate the increase in regions where higher future runoff is projected, or overestimate the decline in regions where lower future runoff is projected). In addition, projections into the more distant future will need to also consider potential changes in the climate-runoff relationship and vegetation characteristics in a significantly warmer and higher CO₂ world. This explains why the runoff projections shown here may be different to those obtained from detailed hydrological modelling or directly from global climate models.

The range of potential change in long-term average runoff presented here is useful for broad-scale or initial assessment of climate change impacts on the many sectors affected by water. For more detailed impact assessment and adaptation studies, hydrological modelling with appropriate downscaled and regional climate scenarios can provide more reliable estimates of future average runoff and other runoff characteristics (Chiew *et al.* 2009b, CSIRO, 2012).

There are a number of larger regional hydrological modelling studies reporting projections of future runoff. These include the CSIRO Sustainable Yields projects (Chiew *et al.* 2009a for Murray-Darling Basin, Charles *et al.* 2010 for far south-west Australia, Petheram *et al.* 2009 for northern Australia, and Post *et al.* 2009 for Tasmania), South Eastern Australian Climate Initiative (Post *et al.* 2012) and Vaze and Teng (2011) for New South Wales. These studies differ in the choice of hydrological models, method used to construct future climate scenarios and the range of global climate models used (typically CMIP3), but the broad projections in long-term average annual runoff are consistent to those presented here.

In summary, the simulated changes in runoff are strongly influenced by the projected changes in rainfall and their uncertainties (Section 7.2). Decreases in runoff are projected with *high confidence* in the Southern and South-western Flatlands region (Southern Australia and south-western Western Australia), where the decrease in rainfall is most strongly indicated, and with *medium confidence* in far south-eastern Australian, where rainfall is also projected to decrease. The direction of change in runoff in the northern half of Australia is less certain because of the uncertainty in the direction of rainfall change.

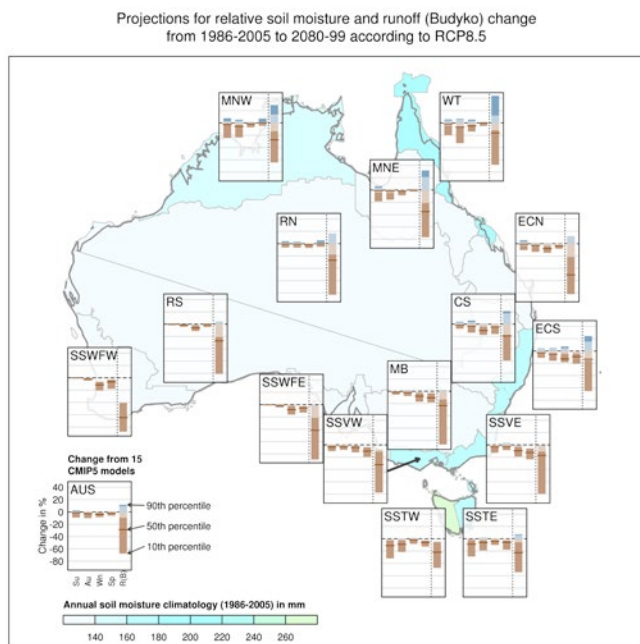


FIGURE 7.7.2: MEDIAN AND 10TH TO 90TH PERCENTILE RANGE OF PROJECTED CHANGES IN SEASONAL AVERAGE SOIL-MOISTURE (LEFT PANEL) AND ANNUAL RUNOFF (R(B): RIGHT PANEL) FOR 2080–2099 RELATIVE TO 1986–2005 FOR RCP8.5 (IN PERCENT) FOR SUB-CLUSTERS. BLUE INDICATES INCREASE AND BROWN DECREASE (SEE KEY) AND PALER PORTION OF THE BAR IS THE 10TH TO 90TH PERCENTILE RANGE EXPECTED FROM NATURAL VARIABILITY. IN THE BACKGROUND IS CLIMATOLOGICAL ANNUAL AVERAGE SOIL-MOISTURE SIMULATED FROM OBSERVED RAINFALL AND POTENTIAL EVAPORATION (SILO GRIDDED DATASETS).



7.8 FIRE WEATHER

SOUTHERN AND EASTERN AUSTRALIA ARE PROJECTED TO EXPERIENCE HARSHER FIRE WEATHER; CHANGES ELSEWHERE ARE LESS CERTAIN

Projected warming and drying in southern and eastern Australia will lead to fuels that are drier and more ready-to-burn, with increases in the average forest fire danger index and a greater number of days with severe fire danger (*high confidence*).

There is *medium confidence* that there will be little change in fire frequency in tropical and monsoonal northern Australia. There is *low confidence* in projections of fire risk in the arid inland areas where fire risk is dependent on availability of fuel, which is driven by episodic rainfall.

Bushfire occurrence at a given place depends on four ‘switches’: 1.) ignition, either human-caused or from natural sources like lightning; 2.) fuel abundance or load – a sufficient amount of fuel must be present; 3.) fuel dryness, where lower moisture contents are required for fire, and; 4.) suitable weather conditions for fire spread, generally hot, dry and windy (Bradstock, 2010). The settings of the switches depend on meteorological conditions across a variety of time scales, particularly the fuel conditions. Given this strong dependency on the weather, climate change will have a significant impact on future fire weather (e.g. Hennessy *et al.* 2005, Lucas *et al.* 2007, Williams *et al.* 2009, Clarke *et al.* 2011a, Grose *et al.* 2014b).

Fire weather is estimated here using the McArthur Forest Fire Danger Index (FFDI; McArthur, 1967), which captures two of the four switches. The fuel dryness is summarised by the drought factor (DF) component of FFDI, a metric ranging from 0 to 10, that indicates the fuel’s readiness to burn. The DF varies in response to both long-term and short-term rainfall. See Lucas (2010b) for an example of these dependencies. The FFDI also captures the ability of a fire to spread, as the temperature, relative humidity and wind speed are direct inputs into the calculation. Fuel abundance is not measured by FFDI, but does depend on rainfall to first order. Higher rainfall totals generally result in a larger fuel load, particularly in regions dominated by grasslands. The FFDI does not consider ignitions.

A set of eight CMIP5 models were selected for the provision of application-ready data, based on current climate performance, data availability and adequate representation of the span of projected climate change in CMIP5 (See Box 9.2 in Chapter 9). Due to the specific data format requirements of the fire weather assessment, and project resource limitations, it was only possible to use a sample of three of these eight CMIP5 GCMs (GFDL-ESM2M, MIROC5 and CESM-CAM5). Despite the use of a small sample and regional variation, representation of the range of future climates is reasonable, with MIROC5 and CESM-CAM5

generally in the middle to the wetter end of the range of rainfall projections and GFDL-ESM2M toward or at the dry end (see the model distribution of projected rainfall changes in Figures 9.9 and 9.10 in Chapter 9).

From these models, monthly-mean changes to maximum temperature, rainfall, relative humidity and wind speed were calculated for each sub-cluster over 30 year time-slices centred on 2030, 2050, 2070 and 2090. Following Hennessy *et al.* (2005) and Lucas *et al.* (2007), the mean changes from these models were applied to observation-based high-quality historical fire weather records (Lucas, 2010b). Generally, these stations are the same as those selected for the study of Clarke *et al.* (2013). A period centred on 1995 (*i.e.* 1981–2010) was chosen as the baseline. The observed station records of maximum temperature, relative humidity, rainfall and wind speed were modified using the model-derived changes for each time-slice and emission scenario. From these adjusted records, future fire weather was estimated using the FFDI. Severe fire weather occurs when the FFDI exceeds 50, the level where the human impacts of bushfire rapidly increase (e.g. Bianchi *et al.* 2010). Being based on observed records, this methodology maintains the observed variability of past fire weather, preserving the relationship between the variables and avoiding potential issues of model bias. However, by fixing this variability, any future changes that may be important to future fire weather, such as a change in the frequency of El Niño events, will not be captured; the observed interannual and decadal variability is not changed. This approach is good at capturing the mean changes to FFDI, while approaches based on direct use of climate model output (Clarke *et al.* 2011a) or dynamical downscaling (Grose *et al.* 2014b) may better capture changes to the extremes and overall variability of fire weather.

In southern and eastern Australia, significant fire activity occurs primarily in areas characterised by forests and woodlands; fuel is abundant and the ‘weather switch’, well-characterised by FFDI, is key to fire occurrence. The results show the future as having a harsher annual-mean fire weather climate in these areas (Table 7.8.1). In both super-clusters, the simulations suggest progressively warmer and drier future climates. In Southern Australia, the results from the models used suggest a 15–25 % reduction in rainfall on average, particularly focused on the Murray Basin. The average decline is 10–15 % in Eastern Australia, with large declines in south-east Queensland in particular (see further discussion of projected rainfall change in Section 7.2). The simulated reduction in rainfall leads to higher drought factors (DF), which implies drier, more ready-to-burn fuels. Simulations also indicate a greater number of ‘severe’ fire danger days. Across both super-clusters, these number of severe days increases by up 160–190 % in the worst case 2090 scenario (driest model, RCP8.5), nearly a threefold increase. Increases of 30–35 % in annual total FFDI (Σ FFDI from July to June) are also simulated by 2090 in the worst case, indicating a broad increase in fire weather conditions.



Many stations in these two super-clusters overlap with those used by Lucas *et al.* (2007). The 2050 RCP8.5 estimates from this study (not shown) are similar to the high global warming results shown in Lucas *et al.* (2007), although individual stations may be different.

There is also sub-regional uncertainty in the projections, largely driven by the spread in rainfall projections amongst the models. For instance, the considerably drier GFDL-ESM2M model results in a harsher fire weather climate than what is reflected by the average values shown here. As shown in the Cluster Reports, changes to Σ FFDI are upwards of 50 % at many stations in the worst case, indicating higher trends than the average. However, it should also be noted that Section 7.2, based on a range of evidence additional to the full range of GCM results, concluded that a decrease in rainfall in eastern Australia could only be confidently projected in winter (although confidence in southern Australian decreases was much higher). Nevertheless, models projecting greater rainfall may reduce the size of the change in FFDI, but probably not its direction. Hence, there is *high confidence* placed in the

direction of change (i.e. harsher fire weather climates) in southern and eastern Australia, but less on the magnitude of the future change.

In Northern Australia and the Rangelands, the weather conditions are often conducive to fire activity, and the limiting switch in these regions is fuel availability (*e.g.* Williams *et al.* 2009). In this case FFDI is not as relevant to understanding future fire activity. In Northern Australia, bushfire is frequent, occurring on an annual basis in some areas, as abundant wet season rainfall drives vegetation growth that dries and eventually burns during the following dry season. Moving southward into the Rangelands, the average rainfall amount declines, vegetation becomes sparser and bushfire is correspondingly rarer. In more arid regions, the rainfall is subject to higher interannual variability, driven by tropical cyclones, the position of the monsoon trough and large-scale factors like the El Niño-Southern Oscillation. If there are more extended wet periods, then fuel becomes more abundant and fire risk increases, while more dry periods would lower fuel loads and reduce fire risk.

TABLE 7.8.1: MEAN ANNUAL VALUES OF MAXIMUM TEMPERATURE (T; °C), RAINFALL (R; MM), DROUGHT FACTOR (DF; NO UNITS), THE NUMBER OF SEVERE FIRE DANGER DAYS (SEV; FFDI GREATER THAN 50; DAYS PER YEAR) AND CUMULATIVE ANNUAL FFDI (CUM. FFDI; NO UNITS) FOR THE 1995 BASELINE AND PROJECTIONS FOR 2030 AND 2090 RCP4.5 AND RCP8.5 SCENARIOS. RESULTS ARE ORGANISED BY SUPER-CLUSTER; ALL STATIONS AND THE RESULTS FOR THE THREE MODELS USED WITHIN THE SUPER-CLUSTER ARE AVERAGED FOR EACH TIME-SLICE AND SCENARIO.

SUPER CLUSTER	VARIABLE	1995 BASELINE	2030 RCP4.5	2030 RCP8.5	2090 RCP4.5	2090 RCP8.5
SOUTHERN AUSTRALIA	T	21.1	22.3	22.2	23.2	24.8
	R	614	507	521	509	468
	DF	6.4	6.7	6.6	6.8	7.3
	SEV	2.8	3.6	3.4	3.8	5.3
	cum. FFDI	2772	3043	2978	3132	3638
EASTERN AUSTRALIA	T	25.0	26.1	26.4	27.3	29.0
	R	968	856	830	828	809
	DF	6.4	6.6	6.7	6.8	7.1
	SEV	1.2	1.5	1.8	1.9	3.2
	cum. FFDI	2692	2859	3037	3103	3584
NORTHERN AUSTRALIA	T	30.3	31.2	31.5	32.3	33.8
	R	1235	1193	1194	1256	1217
	DF	7.2	7.3	7.3	7.2	7.3
	SEV	2.5	3.1	3.4	3.6	5.3
	cum. FFDI	3568	3726	3762	3829	4168
RANGELANDS	T	28.4	29.8	29.9	30.8	32.7
	R	318	273	293	293	285
	DF	8.6	8.8	8.7	8.8	8.9
	SEV	12.7	18.6	17.1	18.8	27.6
	cum. FFDI	6949	7784	7530	7763	8709



Section 7.2 and the Cluster Reports for the Wet Tropics and the Monsoonal North indicate *low confidence* in the direction of rainfall change, although rainfall declines are more likely in the inland and southern parts of these clusters. In the Rangelands, the spread of model results is quite large, and reductions are greater in the southern sub-cluster of the Rangelands.

In both Northern Australia and the Rangelands, when and where fire occurs there is *high confidence* that fire behaviour will be more extreme, the result of higher temperatures and a relatively greater number of 'severe' fire danger days. However, projecting specific changes in future fire frequency from the information used in this evaluation is difficult and the projections are limited to general tendencies. In areas where copious amounts of rain already fall, the projected changes in the rainfall are unlikely to have a significant impact on fire frequency; even in the drier GFDL model simulations, there is still a 'wet season' that results in significant rain and the growth of vegetation, leading to bushfire. Thus there is *medium confidence* that there will be comparatively little change in fire frequency in these regions (Top End, Kimberley, Wet Tropics). In southern and inland regions of Monsoon North, the future fire frequency is less clear. If rainfall-producing weather events occur more often (i.e. a change in the frequency of wet years), then more frequent fire activity could be expected. This uncertainty in the future is even larger in the Rangelands, where sufficient rainfall to drive adequate fuel growth for bushfire is very episodic and even more sensitive to the interannual variability that is not suitably accounted for in this analysis. Consequently, there is *low confidence* for fire projections in the Rangelands. Additionally, changes to the vegetation type from the introduction of exotic species and the higher CO₂ background should also be considered. More detailed modelling efforts encompassing these effects are required to address future fire activity.